



IFM-GEOMAR

Leibniz-Institut für Meereswissenschaften
an der Universität Kiel

RV CELTIC EXPLORER
Fahrtbericht / Cruise Report CE0913

Fluid and gas seepage in the North Sea

Bremerhaven - Bremerhaven
26.07. - 14.08.2009



Berichte aus dem Leibniz-Institut
für Meereswissenschaften an der
Christian-Albrechts-Universität zu Kiel

Nr. 36
Januar 2010



IFM-GEOMAR

Leibniz-Institut für Meereswissenschaften
an der Universität Kiel

RV CELTIC EXPLORER

Fahrtbericht / Cruise Report CE0913

Fluid and gas seepage in the North Sea

Bremerhaven - Bremerhaven
26.07. - 14.08.2009



Berichte aus dem Leibniz-Institut
für Meereswissenschaften an der
Christian-Albrechts-Universität zu Kiel

Nr. 36

Januar 2010

ISSN Nr.: 1614-6298



IFM-GEOMAR

Leibniz-Institut für Meereswissenschaften
an der Universität Kiel

Das Leibniz-Institut für Meereswissenschaften
ist ein Institut der Wissenschaftsgemeinschaft
Gottfried Wilhelm Leibniz (WGL)

The Leibniz-Institute of Marine Sciences is a
member of the Leibniz Association
(Wissenschaftsgemeinschaft Gottfried
Wilhelm Leibniz).

Herausgeber / Editor:

Peter Linke, Mark Schmidt, CE0913 cruise participants

IFM-GEOMAR Report

ISSN Nr.: 1614-6298

Leibniz-Institut für Meereswissenschaften / Leibniz Institute of Marine Sciences

IFM-GEOMAR
Dienstgebäude Westufer / West Shore Building
Düsternbrooker Weg 20
D-24105 Kiel
Germany

Leibniz-Institut für Meereswissenschaften / Leibniz Institute of Marine Sciences

IFM-GEOMAR
Dienstgebäude Ostufer / East Shore Building
Wischhofstr. 1-3
D-24148 Kiel
Germany

Tel.: ++49 431 600-0
Fax: ++49 431 600-2805
www.ifm-geomar.de

Table of Contents

1. Introduction	
1.1. Objectives of the cruise.....	2
1.2. List of participants.....	3
1.3. Cruise narrative	4
2. Water column physical data acquisition and sensor measurements	
2.1. Introduction.....	8
2.1.1. Overview of instrumentation and data.....	8
2.2. ADCP measurements	
2.2.1. Methodology	9
2.2.2. Ship-mounted ADCP acquisition.....	9
2.2.3. POZ-Lander ADCP	10
2.2.4. Profiler-Lander ADCP	11
2.3. CTD measurements	
2.3.1. Introduction.....	12
2.3.2. Ship CTD	12
2.3.3. ROV CTD	14
2.3.4. POZ-Lander CTD.....	15
2.4. HydroC-CH ₄ /CO ₂ /PAH sensors	
2.4.1. Introduction and methodology.....	15
2.4.2. Preliminary results	20
2.5. Microstructures Profiler	
2.5.1. Introduction and methodology.....	18
2.5.2. Preliminary results	18
3. Water column gas geochemistry	
3.1. Introduction.....	21
3.2. Methods.....	21
3.3. Preliminary results	24
4. Water column and pore water geochemistry	
4.1. Introduction and methods	32
4.2. Preliminary results	35
5. Sea floor observations and <i>in situ</i> sampling operations	
5.1. ROV 6000 operations	41
5.2. Lander deployments	
5.2.1. Methodology	46
5.2.2. Preliminary results	48
5.3. Eddy correlation measurements	
5.3.1. Introduction and methodology.....	50
5.3.2. Preliminary results	51
6. Geophysical data acquisition	
6.1. Methods.....	54
6.2. Preliminary results	55
7. Sedimentology	
7.1. Methodology	60
7.2. First results	61

Appendix

- I Station list
- II Detailed station maps
- III Gas concentration data measured by gas chromatography

1. Introduction (P. Linke, M. Schmidt)

1.1. Objectives of the cruise

The aim of the SDNS project is to detect sites of active fluid and gas seepage in the North Sea, to decipher and map possible migration pathways in the Pleistocene and Holocene deposits, to quantify gas fluxes in the water column related to tides and currents, and to analyze the chemical compositions of emitted fluids and gases, in order to investigate relationship of fluid/gas seepage to subsurface reservoir geochemistry, sediment deposits and migration structures.

Diffuse venting of CO₂-rich fluids was observed during a research cruise in the Southern German North Sea in October 2008 with RV Alkor (Linke et al., 2008). The highest CO₂ (low pH) values were measured in the water column above subsurface salt diapiric structures and fractured neogene sediments ("Salt Dome Juist"). The venting could mainly be addressed as diffuse venting, however few gas bubbles venting from the seafloor were also observed in this area.

The actual cruise with RV Celtic Explorer aimed to reinvestigate the venting area, to determine seasonal changes in CO₂-activity, and comparing it to normal "background" area (i.e. Borkum Reef Ground), and areas with strong gas bubble venting fields in the North Sea (i.e. Tommeliten, Ekofisk).

Furthermore, a main goal was to test the recently developed seagoing combination of video-guided CTD/Water sampler rosette and online membrane inlet mass spectrometry. The system was designed to determine gas concentrations (i.e. N₂, O₂, CO₂, CH₄, etc.) in the water column near the seafloor.

Conventional echosounder, ADCP, and multi beam techniques were applied to get background information about sea surface morphology (e.g. pockmarks), shallow sediment characteristics and physical oceanography.

To identify and quantify endmember fluid composition (e.g. originated from deep reservoirs), and secondary degradation of gases and fluids (e.g. by benthic filter processes), sediment and porewater studies were performed during the cruise. A newly designed *in situ* porewater sampler was tested to avoid oxidation processes

New techniques (Benthic chambers, eddy flux correlation) were applied to record the variability of the gas and fluid fluxes across the sediment seawater interface and the important environmental control parameters (currents, tides) during *in situ* time series measurements.

1.2. List of cruise participants and contributors to the report

1	Peter Linke	IFM-GEOMAR	Chief scientist
2	Fritz Abegg	IFM-GEOMAR	Chief ROV team
3	Mark Schmidt	IFM-GEOMAR	Gas geochemist
4	Klaus Schwarzer	IFG, Universität Kiel	Geologist
5	Sören Themann	IFG, Universität Kiel	Geologist
6	Stefan Sommer	IFM-GEOMAR	Biogeochemist
7	Anja Reitz	IFM-GEOMAR	Inorganic Geochemist
8	Christian Dos Santos Ferreira	IFM-GEOMAR	Geophysical technician
9	Sergiy Cherednichenko	IFM-GEOMAR	Lander technician
10	Ralf Schwarz	IFM-GEOMAR	Lander technician
11	Bettina Domeyer	IFM-GEOMAR	Lab technician
12	Markus Faulhaber	IFM-GEOMAR	Lab technician
13	Meike Dibbern	IFM-GEOMAR	Lab technician
14	Peggy Wefers	IFM-GEOMAR	Lab technician
15	Daniel McGinnis	IFM-GEOMAR	Oceanographer
16	Lorenzo Rovelli	IFM-GEOMAR	Oceanographer
17	Andreas Doennebrink	BSH	Core technician
18	Reimund Ludwig	BSH	Core technician
19	Claus Hinz	IFM-GEOMAR	ROV team
20	Hannes Huusmann	IFM-GEOMAR	ROV team
21	Arne Meier	IFM-GEOMAR	ROV team
22	Martin Pieper	IFM-GEOMAR	ROV team
23	Inken Suck	IFM-GEOMAR	ROV team

1.3. Cruise narrative

The Irish RV *CELTIC EXPLORER* arrived in Bremerhaven in the afternoon of July 26 and made fast at the Labradorkai, a remote harbor basin of the fishery harbor next to the construction site of the off-shore wind power plants. Already in the evening a group of 8 persons received a familiarization course of the ship's safety, rescue and housekeeping procedures. Seven containers arrived in the next morning, which were unpacked in the next 2 days and their content was installed at deck or in the labs of the vessel together with the rest of scientists. On July 28 the vibro corer from the BSH arrived on a truck and was rigged up on shore. In the evening all scientific equipment and crew was on board. In the morning of July 29 a first meeting of the principal investigators and ship's officers was conducted to discuss the launch and recovery procedures of the various scientific instruments. After lunch oil was pumped into the hydraulic system of the ROV and in the afternoon of this 3rd harbor day the successful harbor test of the ROV finalized the mobilization of the substantial equipment. After this the pilot was called and cruise CE0913 started (Fig. 1.1).

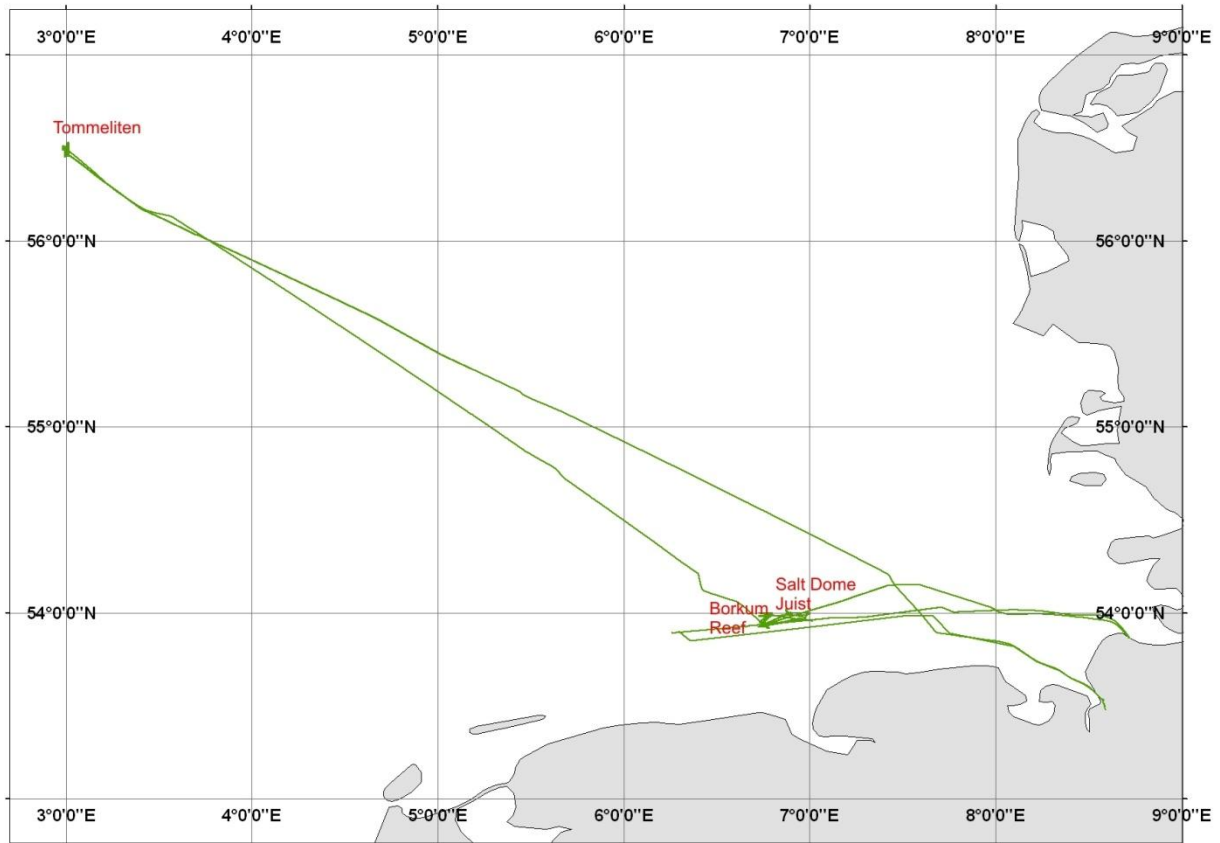


Fig. 1.1: CE0913 cruise track and working areas in the North Sea.

While the weather was nice and calm during our departure, wind peaked up with heavy gales and thunderstorms at the first day and enabled us only to deploy a video-guided CTD and a vibro corer in the “Borkum Reef” working area. As the wind slowed down on July 31, we were able to conduct a full working program with vibro corer, CTD and the first ROV dive in the working area “Salt Dome

Juist". Unfortunately, strong currents and high particle load diminished the visibility substantially. On the other side the shallow water navigation system installed in the drop keel proved to work at once and allowed for navigation under these difficult conditions.

During the second dive on August 1 in the western part of the working area the visibility was so bad that the pilots could not see the hydraulic arms in front of the cameras. On the following day the visibility improved in the eastern part that much that we were able to deploy the new pore water sampler (PWS) successfully. The sampling program was completed by push corer, water samplers and samples obtained by the Kiel *in situ* pump system (KIPS); at the same time the pH, concentrations of methane, CO₂ and poly aromatic hydrocarbons were measured with a sensor package. After the ROV recovery the POZ lander was deployed. This deployment was inspected on the next day by ROV. The 3rd August was completed by the lander recovery and by an intensive CTD program, which demonstrated the excellent manoeuvrability of the CELTIC EXPLORER. In the morning of August 4 the vessel stopped in Cuxhaven for exchange of personal and the exchange of the BSH vibrocorer for an almost identical instrument belonging to the Geological Survey of Ireland. The short stay in the harbor was used to review the data collected so far and to discuss the sampling strategy for the following working days.

At 18.00 h the RV CELTIC EXPLORER departed during clear skies from Cuxhaven and headed back towards the Salt Dome Juist working area. After arrival in the working area we succeeded in deploying a new submersible pump on the CTD rosette to pump water from depth in a towed profile across the salt dome into the lab attached to a mass spectrometer. The eagerly awaited results demonstrated the capabilities of this new measurement technique and showed a clear increase in CO₂ concentration in the bottom waters. The next 3 days were occupied with an intensive sampling program involving all instruments on board, which demanded all cruise participants and pushed lab personal to their limits. Beside the CTD with pump, the POZ-lander and for the first time with a ROV, a novel benthic chamber was deployed). All instruments were deployed successfully and obtained samples and data.

After this intense program all cruise participants were cheerful for the 20 h transit to the working area Tommeliten in Norwegian waters, where a comparable investigation of fluid and gas discharge was planned. After arrival at lunchtime of August 8 the vibrocorer and the POZ-lander were deployed. The following ROV dive in approx. 70 m water depth showed pilots and scientists at clear visibility spectacular pictures of bacteria mats, gas ebullition and chemoherm carbonates, which were densely colonized and serve as a shelter and feeding ground for various fish species. Again we deployed a benthic chamber with the ROV at a bacteria mat and obtained gas flux measurements and samples. Inspired by this experience and the fantastic weather conditions an intensive deployment schedule was planned for the following day. It involved the deployment of the Profiler Lander, the 2 Eddy Correlation Systems and the second benthic chamber in a row perpendicular to the tidally changing currents. This work was performed with great enthusiasm and

eagerness by all contributors and was completed around midnight by the recovery of the first benthic chamber. During the night an intense acoustic survey for gas flare detection was performed, which was accompanied by physical microstructure measurements in the water column.

On August 10 the vibrocorer of the Geological Survey of Ireland was deployed again. Excellent sediment samples were recovered, which will be studied with respect to their sedimentology and geochemistry to characterize the origin and migration pathways of the ascending fluids and gases. Afterwards a ROV dive was conducted where a self-made bubble measurement tool and a gas sampler for quantification and characterization of the discharged gasses as well as push cores for sediment sampling were deployed. After the successful sampling the ROV did a 500m long transit in parallel to the vessel to reach the instruments which had been deployed on the previous day in a line perpendicular to the currents. The first of the 4 instruments to be recovered was the benthic chamber which arrived on deck without damage. After this the Profiler-Lander was released acoustically and recovered. The major component this lander carries, beside two acoustic current profilers, is a profiler which moves microsensors in x, y, and z direction at the seafloor to measure high-resolution oxygen profiles. The measured sediment microprofiles were of excellent quality. As a night program measurements with the microstructure CTD were obtained as well as an intensive acoustic survey and sampling of gas flares in the water column by the video-guided CTD.

During this deployment the submersible pump was deployed down to 70 m water depth to obtain on-line measurements of gas composition with the mass spectrometer. After various failures with 3 different pumps this one, which was exchanged in Cuxhaven and is designed for 20 m water depth, has proven to be a good investment.

During the last day at the Tommeliten working area a change of weather became apparent with increasing winds from the northwest and swell from the Atlantic. Therefore, after sampling with the vibrocorer we had to cancel the deployment of the pore water sampler and had to conduct two rapid, sequential ROV dives to recover the 2 sensitive eddy correlation systems. Both instruments were recovered without damage by the excellent handling capabilities of the ROV pilots. Both instruments recorded high-resolution data for the measurement of the dynamics of oxygen fluxes in the benthic boundary layer. By this the ROV conducted a total of 14 dives with almost 50 h of bottom time during this cruise.

At last, the POZ-lander, which had been deployed during the whole duration of our work at Tommeliten, was released by acoustic command and recovered. The end of scientific work was the acoustic survey of the whole working area until the vessel lifted its drop keel around mid-night and headed for Bremerhaven. The vessel arrived at the locks at 7.00 h on August 13 and made fast at the J.H.K. pier at 8.00 h. Here, the 5 containers had been left behind and were packed in the remaining time. In the morning of August 14 all containers were loaded on trucks and transported back to Kiel.

Altogether we can look back at a very successful program with many new instruments which was favoured by calm summer weather and a fantastic crew.



Fig. 1.2: Top: RV CELTIC EXPLORER in Bremerhaven loading equipment. Bottom: Scientific crew members of the second leg of cruise CE0913.

On behalf of the crew members we like to thank Captain Anthony Hobin and his crew for the excellent and professional cooperation as well as the friendly and warm atmosphere on board of the Irish vessel Celtic Explorer.

2. Water column physical data acquisition and sensor measurements

(L. Rovelli, D. F. McGinnis, S. Cherednichenko)

2.1. Introduction

Physical measurements in the water column define the hydrodynamic and constituent boundaries for benthic measurements. These measurements include water velocity and direction, scalars (temperature, dissolved constituents measured with *in situ* sensors, etc.), and turbidity (particles, bubbles). These measurements are crucial as they define conditions both in the benthic boundary layer (BBL – bottom meters of water column above the sediment-water interface), and at the sediment-water interface.

2.1.1. Overview of instrumentation and data

Water column measurements were conducted with a high-resolution CTD (Conductivity-Temperature-Depth) profiler, hydroacoustic equipment such as ADCPs (Acoustic Doppler Current Profilers) and single/multibeam, and fine-scale microstructure profilers.

Three CTDs (SBE9: Sea-Bird Electronics, Inc., Washington, USA; NXIC CTD: Falmouth Scientific Inc., Cataumet, USA; RBR Ltd., Ottawa, CAN) were used for both stationary measurements on Landers and dynamic measurements on ship and on the ROV (remotely operated vehicle) Kiel 6000. Three ADCPs (Acoustic Doppler Current Profiler: Workhorse Monitor, Teledyne RDI Instruments, Poway, USA) and three lander-mounted ADCPs (2x Workhorse Sentinel: Teledyne RDI Instruments, Poway, USA; Aquadopp, Nortek As, Rud, NOR) were deployed from either the ship and obtained both water current information and acoustic backscatter, i.e. from particulate matter (e.g. algae, suspended sediment, gas bubbles). A turbulence profiler (MSS90, Sea & Sun Technology, Trappenkamp, GER) was used to obtain the water column fine-structure (mm-scale) vertical profiles as well as the required turbulence measurements to determine water column fluxes. Figure 2.1.1 gives an overview of the collected physical data from water column measurements during CE0913 research cruise.

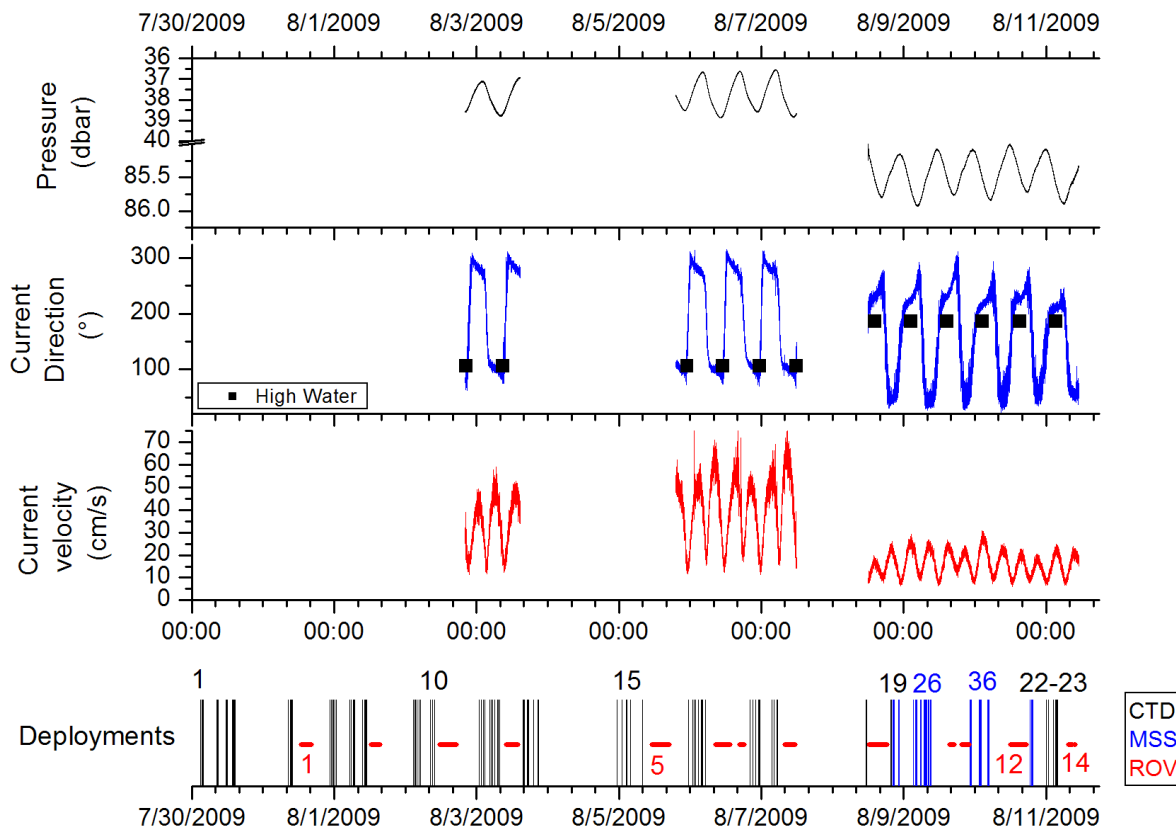


Fig. 2.1.1: Overview of the physical measurements with *in situ* recorded tidal regimes. Pressure (dbar \approx water depth), current direction ($^{\circ}$) and velocity (cm/s) were collected by ADCP/sensors mounted at the POZ-Lander. The bottom plot shows a timeline of the deployment for the ship CTD, the microstructure profiler (MSS CTD) and the ROV-mounted CTD with the respective cast numbers.

2.2. ADCP measurements

2.2.1. Methodology

Acoustic Doppler current profilers, ADCPs, are hydroacoustic instruments which measure 3-dimensional current velocity by recording the Doppler shift of acoustic pulses reflected from particles that are assumed to move with the current. Depending on the settings, deployment mode, and acoustic frequency, ADCPs can resolve current velocities from 10s to 100s of meters with bin sizes of cms to meters. As a useful by-product of the measurement principles, ADCPs also record the acoustic backscatter strength reflected by particles, fish and bubbles. Backscatter results allow us to locate possible outgassing events and sites, since higher values are expected due to the large density difference between bubbles and water. Flare observations and locations were correlated with the ship echosounder and the multibeam (Chapter 6) to confirm observations and rule out artifacts.

2.2.2. Ship-mounted ADCP acquisition

A downward looking 600 kHz ADCP (RD Instruments Workhorse Monitor) was mounted with custom constructed metal mounting bracket on the ship drop keel (Fig. 2.2.2.1, left). Details on the ADCP beam positions relative to the ship are on Figure 2.2.2.1 (right).

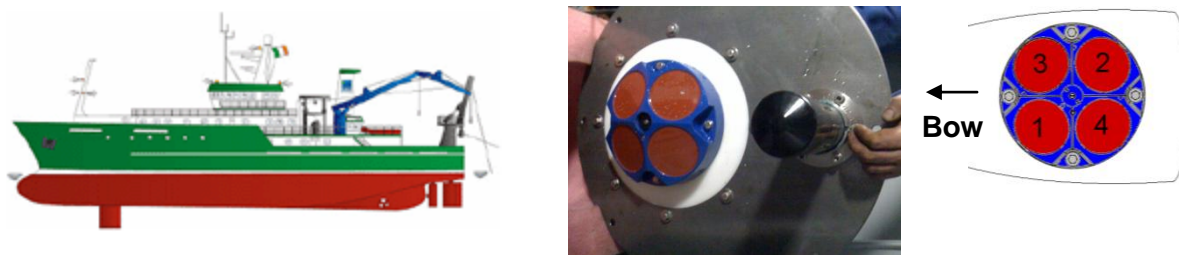


Fig. 2.2.2.1: ADCP Beam position relative to the ship and its orientation. Left: The relative position of the drop keel of the RV Celtic Explorer. Center: Mounting plate with ADCP next to the ORE Track Point transducer of the shallow water navigation system. Right: beam orientation with regards to the ship main axis.

Real-time ADCP data were collected with WinRiver™ software. The software simultaneously recorded ship navigation data (coordinates, ship heading and ship speed).

As an example, Figure 2.3.2 shows a particularly strong flare recorded at the Tommeliten site; the flare presumably reached the water surface. The acoustic signal was partially blanked underneath the flare due to the gas absorbing the energy of the sound pulse. A further example of acoustic backscatter anomalies detected with the shipboard ADCP is shown with Figure 2.8.

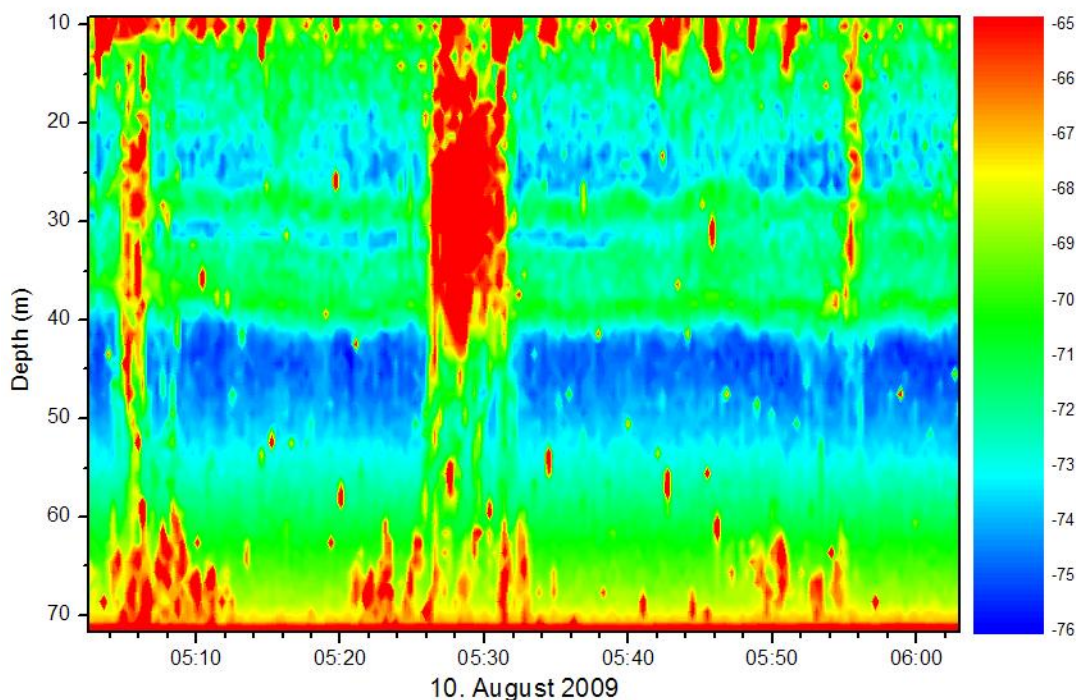


Fig. 2.2.2: ADCP recorded flare at the Tommeliten site.

2.2.3 POZ-Lander ADCP

The POZ-Lander (Fig. 2.2.3.1, left) is a low-profile lander equipped with a 300 kHz ADCP (and a RBR CTD, discussed below). The POZ ADCP was deployed with Mode 12 which subpings at faster rates than standard ADCPs and therefore allows higher temporal resolution, with much more accuracy (low noise). Figure 2.2.3.1 (right) shows the data recorded at Salt Dome Juist and

demonstrates the tidal changes based on the current velocity magnitude for the whole water column (water velocities approach 80 cm/s). The changes in the water level are also distinctively visible as the lower-most black line. The blanking at 20 hours was the ship positioned above the lander. Figure 2.1.1 shows a summary of the bottom water current velocities and directions collected by all three POZ-Lander deployments

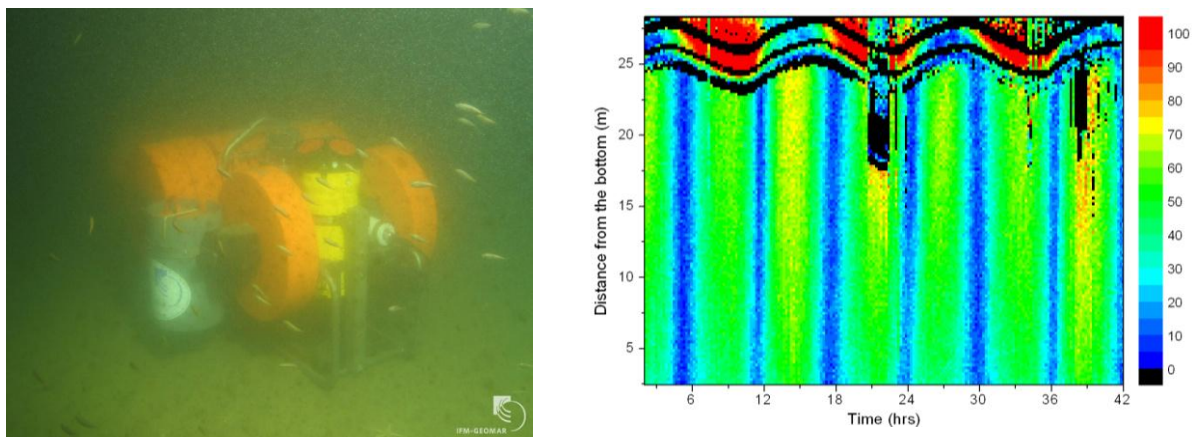


Fig. 2.2.3.1: Left: POZ-lander with Workhorse ADCP. Right: Current velocity magnitude (cm/s) as well as the tidal driven water level changes as record by the ADCP on the POZ-Lander at the Saltdome Juist site. Note that the black spots are due to the ship cruising over the POZ-Lander location.

2.2.4 Profiler-Lander ADCP

Both an ADCP (upwards looking) and an ADP (Acoustic Doppler profiler, downward looking) were deployed on the Profiler-Lander. The upward looking ADCP was an RDI Sentinel 300 kHz (Fig. 2.2.4.1 – top white circle), working with a standard water column profiling mode 5 (data not shown). The downward looking ADP was the newly acquired 2 mHz ADP (Nortek Aquadopp; Fig 2.2.4.1 – bottom white circle). While the RDI collects simple background current speed, the Nortek ADP using high-resolution pulse-to-pulse coherent mode.

Aquadopp High-resolution ADP

The Aquadopp ADP (herein ADP) is a specialized high-resolution velocity profiler designed for fine-structure and turbulence resolution. The high frequency (2 mHz) provides very accurate data, but at very short ranges. The ADP was deployed in burst mode on the Profiler lander (Fig. 2.2.4.1 right – bottom white circle), and collected data at 8 Hz for 900 seconds. The total profiling range was to the bottom (1.6 meter) with remarkably fine vertical resolution (bin sizes were 30 mm). This fine resolution allows us to resolve the velocity profiles to the sediment water interface and scale them to the theoretical law of the wall (Fig. 2.2.4.1 – right). Future analyses will involve resolving the dissipation within each bin using the inertial dissipation technique. These data will then provide the highly accurate vertical diffusion coefficient in the BBL, which in turn, allows us to very accurately estimate the bottom fluxes of all measured constituents.

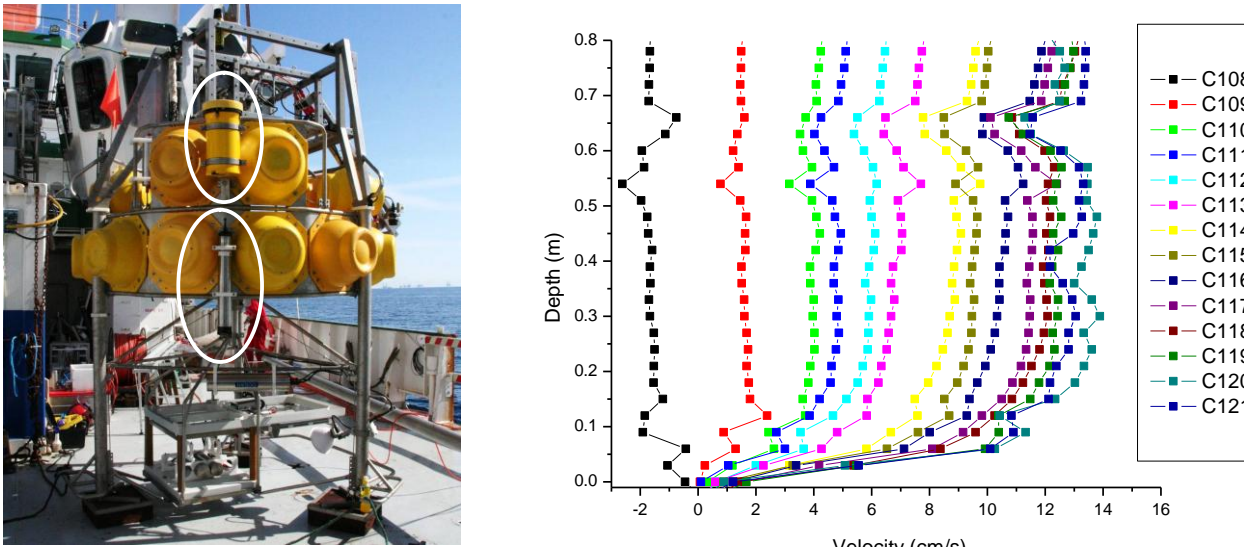


Fig. 2.2.4.1: Left: Profiler lander showing positions of the RDI ADCP (top white circle) and the Nortek High-Resolution ADP (bottom circle). Right: Current profile time series in the BBL with a 30-mm spatial resolution. Bottom is estimated slightly to be a few mm below 0.0. The profiles show the temporal evolution (starting with the black) of the increasing current direction with a 15-minute resolution. Developed flow field follows law-of-the-wall velocity distribution.

2.3. CTD measurements

2.3.1. Introduction

CTD (Conductivity-Temperature-Depth) measurements provide the background information on water column stratification with depth, and other scalar parameters (O_2 , pH, light transmission, etc.). CTD data are used to help detect gas seepage, particularly salinity, O_2 , Temperature and pH anomalies. Additionally, CO_2 and methane sensors (Contros HydroC sensors, see next section) were mounted for some of the CTD casts as well as on the ROV deployments.

2.3.2 Ship CTD

The ship SBE9 Seabird CTD was the main instrument we used for water column measurements. The SBE9 samples at 24Hz and was equipped with the default sensors (temperature, conductivity, pressure), standard additions (oxygen, light transmission) and a pH sensor. Furthermore, a 24-carousel Rosette system was installed for discrete water sampling (though only 12 bottles were mounted). The ship navigation data were recorded by the CTD software, which allowed the recording of the sampled Niskin-bottles coordinates. The CTD was generally deployed for benthic surveys in the towed mode. The georeferenced data were imported into ArcGIS to display spatial changes in the water chemistry and physical properties. Additionally, the CTD frame was furnished with the same underwater video system used on the Lander launcher (Chapter 5.2; Fig. 5.2.2.1). It was thus possible to see the sea floor (Fig. 2.3.2.1) as with the OFOS (Alkor 328), but with far more sampling and sensor capability.



Fig. 2.3.2.1: Bacterial mats at the Tommeliten site as seen with the CTD camera (CTD23).

Water column profiles:

The water column almost fully mixed on Borkum Riff and Saltdome Juist (Figure 2.3.2.2 left). Those study sites also showed lower salinity due to the relative proximity to the River Elbe and North Sea confluence.

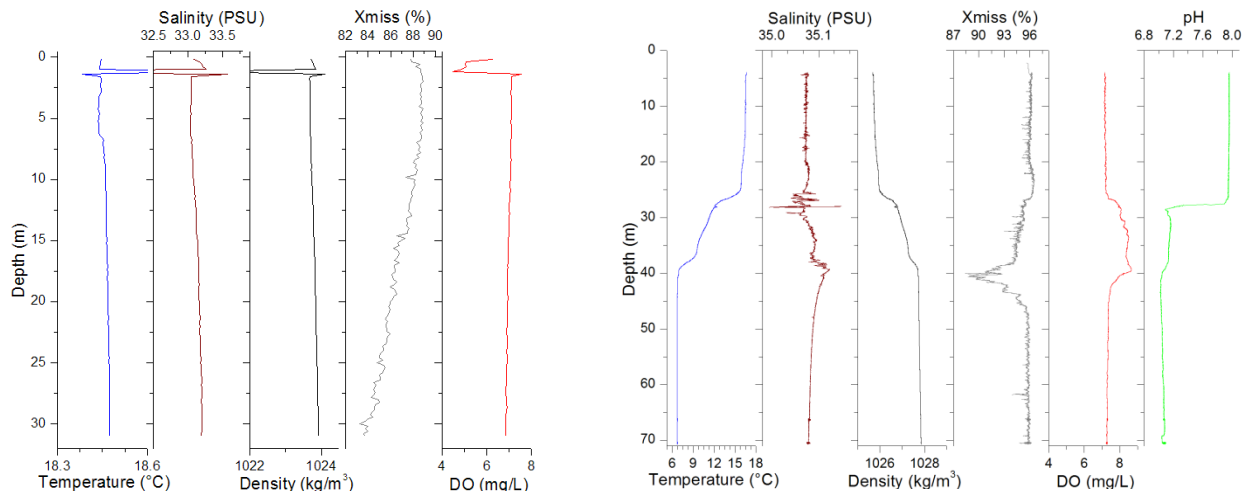


Fig. 2.3.2.2: Examples of water column characteristics from working areas (left: Borkum Riff; Right; Tommeliten). Displayed are temperature, salinity, density, light transmission in percentage (Xmiss), dissolved oxygen (DO) and pH. Comparison of the two sites show the very weakly stratified conditions at Borkum Riff (very similar to Salt Dome Juist) and two-layer structure at Tommeliten.

At the Tommeliten site, the 70 m deep water column displayed three well defined zones; very weakly stratified surface and bottom layers (20 m and 30 m thick respectively (Fig. 2.3.2.2 right) separated by a strongly stratified ~15 m thick interior layer ($2^{\circ}\text{C}/\text{m}$). The water was found to be relatively clear (light transmission was consistently around 96%).

Towed CTDs:

Using the RV Celtic Explorer's dynamic positioning system, we were able to set search patterns to search for flares and CH_4 concentrations. Figure 2.3.2.2 shows the search pattern performed on CTD casts 22 and 23 at Tommeliten (Stations 66, 67; Tab. 1.5).

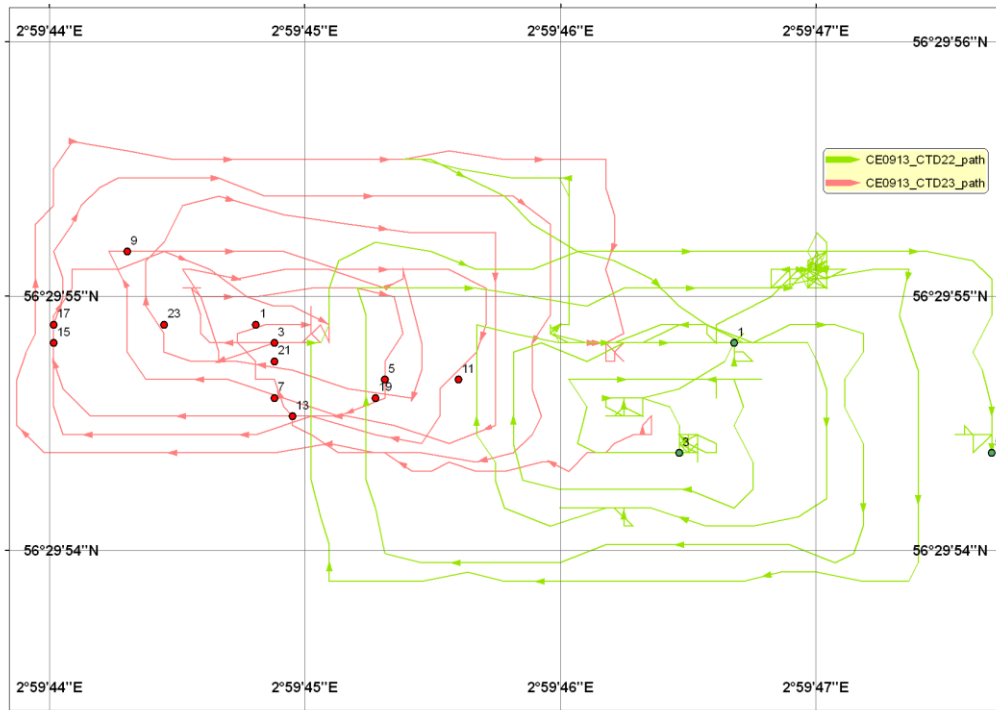


Figure 2.3.2.2: Search patterns and fired Niskin bottles on CTD tracks 22 and 23 at Tommeliten.

ADCP and CTD coupled results:

During CTD tows, shipboard ADCP real-time data were simultaneously recorded. At the Saltdome Juist site we discovered what are presumed to be fresh water ‘flares’ that were caused by low backscatter ADCP signals. This phenomenon occurred concurrently with lower salinity readings, noted in our ship CTD (Fig. 2.3.2.3). These results suggest that these ‘flares’ are freshwater intrusions with low associated backscatter signals.

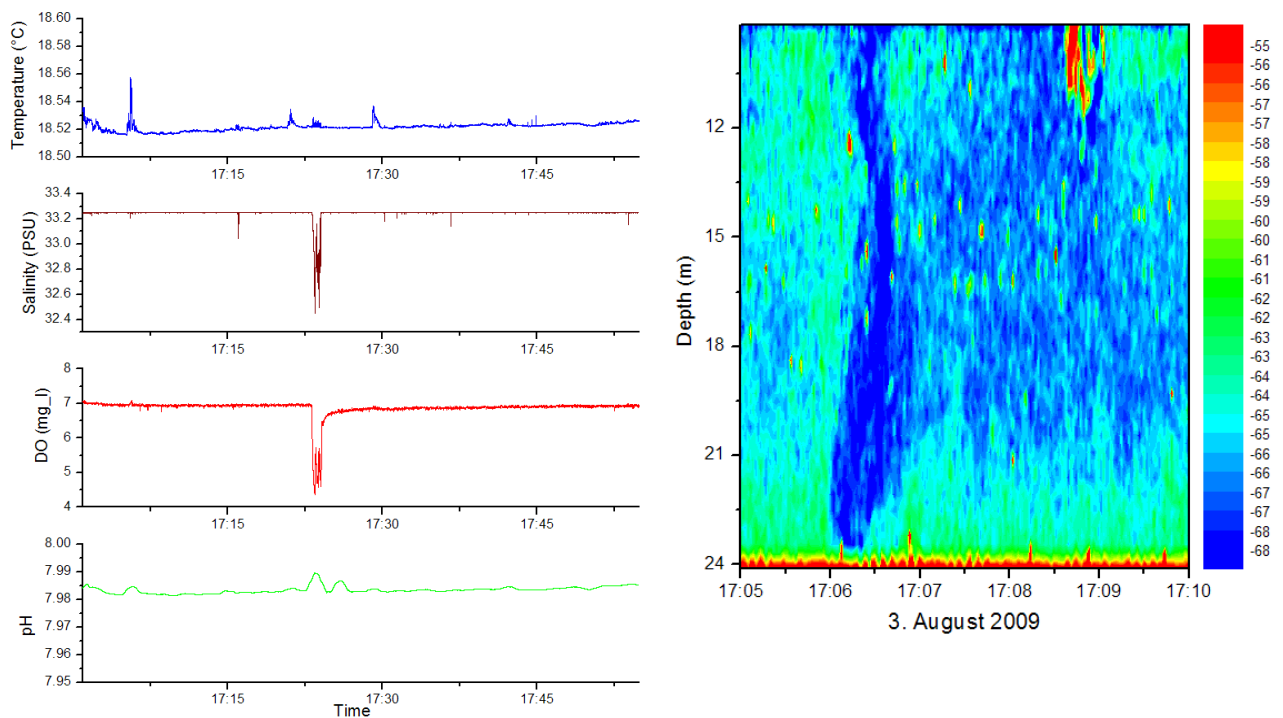


Fig. 2.3.2.3: Freshwater flare at Salt Dome Juist. Evidence from the ship CTD (left) and ADCP backscatter (right).

2.3.3. ROV CTD

The primary advantage of the ROV mounted CTD is the ability to more thoroughly investigate seafloor anomalies (e.g. the previously discussed freshwater intrusion). The FSI CTD on board the ROV was equipped with the sensors temperature, conductivity, pressure and a pH sensor. At the Saltdome Juist site, the ROV CTD measured the same salinity drops (Figure 2.3.3.1) detected by the ship CTD (Figure 2.3.2.3).

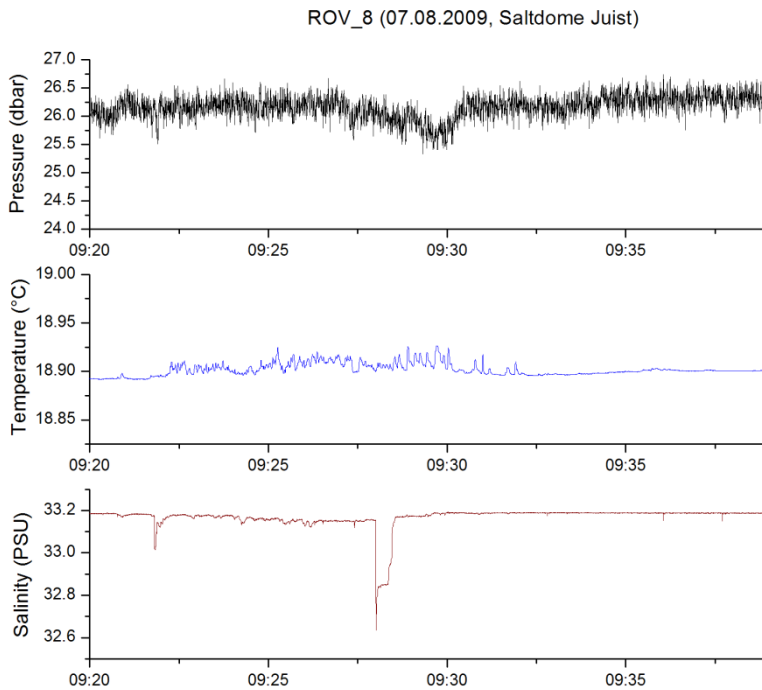


Fig. 2.3.3.1: Salinity drops at the Saltdome Juist site, as seen on the ship CTD and ADCP (Figure 2.3.2.3).

2.3.4 POZ-Lander CTD

The POZ RBR CTD was equipped with temperature, conductivity, and pressure sensor to monitor and log tidal-driven hydrographic changes (Fig. 2.1.1). Tidal induced changes in the water level are important to be considered while performing bathymetric surveys, i.e. with multibeam systems. The POZ-Lander pressure data were used to calculate the tide amplitudes and thus correct the bathymetric results.

2.4 HydroC-CH₄/CO₂/PAH sensors

2.4.1. Introduction and methodology

Instruments capable of measuring CO₂ and methane directly were deployed on the CTD and ROV. During the CE0913 cruise, a Contros HydroC/CO₂ membrane sensor was added to the previously used Contros measurement suite (Alkor 328 cruise), which consisted of a HydroC/CH₄ membrane methane sensor, the HydroC/PAH (polyaromatic hydrocarbon) fluorometer, the data storage unit as well as a battery pack.

Since the last deployment in 2008 (Alkor 328 cruise) both the methane and carbon dioxide sensors went through major enhancements. The sensors were attached to the ships SBE9 to enable online, low resolution analog readings during CTD casts. High resolution digital signals from the sensor were also recorded at 1Hz in data storage unit. To allow the sensors internal temperature to reach the thermal stabilisation point, the methane and CO₂ sensors were powered-up around half-hour before the CTD casts beginning. An overview of the Contros HydroC sensors and their features is shown on Table 2.4.1.1. The CONTROS sensors were deployed on both the ship CTD (casts 1-7, 22-23) and the ROV (dives 3-10).

Table 2.4.1.1: HydroC sensor specifications given by CONTROS.

	HydroC TM / CH ₄	HydroC TM / PAH	HydroC TM / CO ₂
Measuring range	10/100 nM – 50µM	0-500 ppm	0-5000 ppm
Resolution	1nM	0.1 ppm	5 ppm
Response time	30s	500 msec	
Warm-up time	up to 30 min (until thermal stabilisation)	Less than 10 s	Up to 30 min
Operational depth	4000 m	500 m	2000

2.4.2. Preliminary results

Figure 2.4.2.1 provides an overview of the analog readings of both the HydroC/CH₄ and HydroC/CO₂ during CTD cast 23 at Tommeliten.

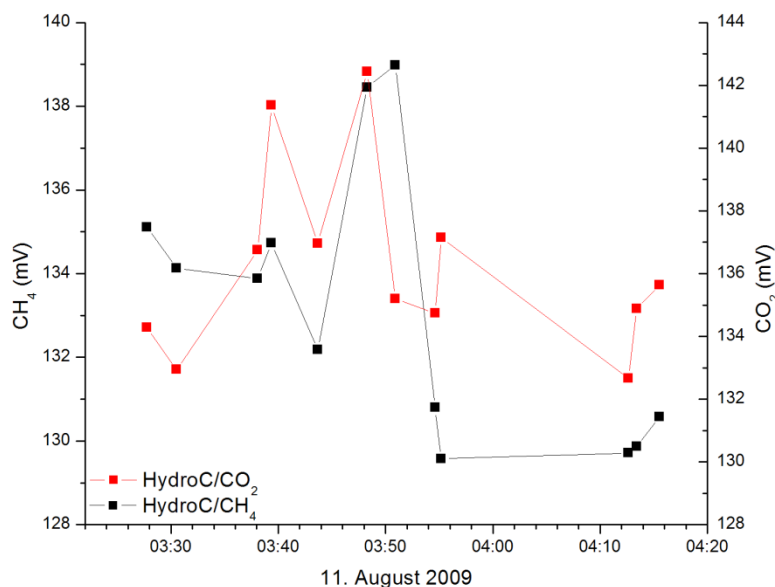


Fig. 2.4.2.1: Analog Contros HydroC recorded at the same time of the fired Niskin-bottles at the Tommeliten site (CTD 23).

HydroC/CH₄:

Figure 2.4.2.1 shows evidence for methane concentration changes (expressed in millivolts). Those changes were cross-checked with the gas analysis carried out on the discrete water samples (Chapter 3, Fig. 3.3.4).

HydroC/CO2:

In general CO₂ readings with HydroC/CO2 were noisy and only small changes of pCO₂ were indicated during each deployment (e.g. blue line is the calculated mean value for CTD 23; Fig. 2.4.2.2). This is in accordance to pCO₂ measurements performed with the MIMS (Chapter 3). The noisy fluctuations were probably artefacts caused by an internal pressure sensor.

Figure 2.4.2.3 shows calculated CO₂ partial pressures (pCO₂) recorded on CTD 5 track at Saltdome Juist and Tommeliten CTD 23 track, respectively. Again no significant CO₂ concentration changes were detected within one run (i.e. only small spatial pCO₂ variability). However, a comparison of the reading from Saltdome Juist and Tommeliten revealed that the pCO₂ (527 µatm) in bottom waters at Tommeliten (70 mbsl) was higher than the one at Saltdome Juist at about 25 mbsl (450 µatm).

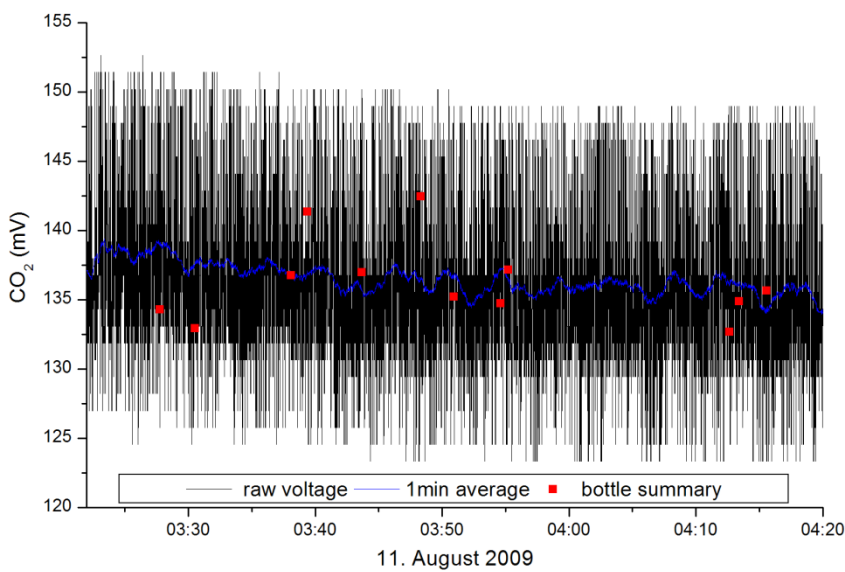


Fig. 2.4.2.2: Analog Contros HydroC/CO2 signals (CTD 23). Large noise was recorded due to malfunction of an internal pressure sensor.

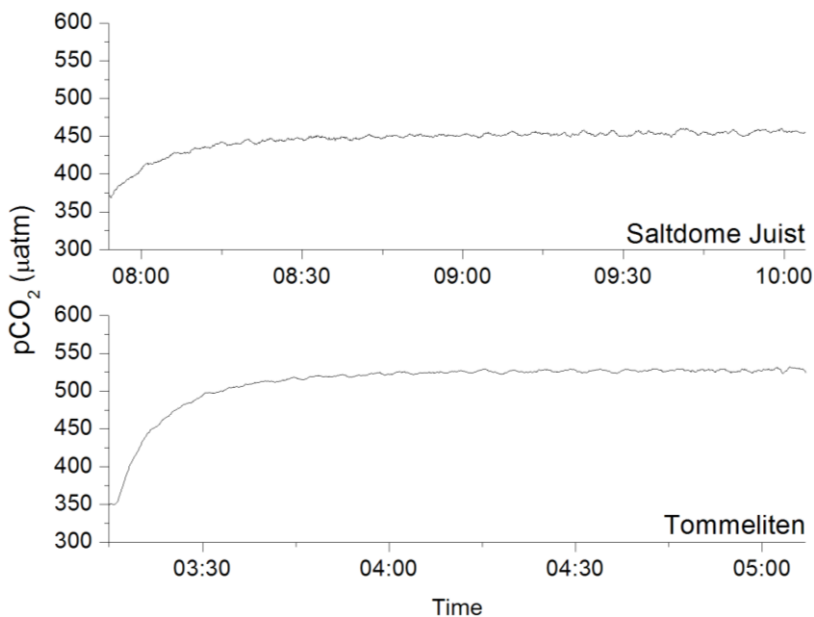


Fig. 2.4.2.3: Digital HydroC/CO2 data for Saltdome Juist (top, CTD5) and Tommeliten (bottom, CTD23).

HydroC/PAH:

The HydroC/PAH sensor recorded strong fluorescence signals (i.e. at Salt Dome Juist), when it was operated during ROV dives. The strong signals were recorded only near the seafloor and were not correlated to any changes in physical oceanographic parameters (CTD measurements). As reported in the Alkor 328 cruise, those peaks were found to be genuine, but particles cannot be ruled out as a possible reason for this.

2.5. Microstructures Profiler

2.5.1 Introduction and methodology

Microstructure profilers are well established oceanographic instruments capable of profiling the water column with a very high resolution (mm scale) and collect turbulence information necessary for determining constituent fluxes in the water column. For this cruise we used a MSS90 probe (Sea & Sun Technology, Trappenkamp, GER).

Capabilities: The MSS90 is deployed as a free-falling probe, in which the winch cable is used only for data transfer and probe recovery (Fig. 2.5.2.1, left). The probe was equipped with 2x shear probes (to collect turbulence data), an accelerometer (to correct the readings according to the probe pitch/roll/yaw and vibration), a fast temperature sensor (FP07, 7ms response time) and standard CTD sensors (Temperature, Pressure, Conductivity, membrane DO). In addition, we tested a fast (0.2 s response time) galvanic oxygen sensor (AMT Analysen-Messtechnik GmbH, Rostock, GER).

Deployments: A total of 39 profiles were obtained at the Tommeliten site. As the profile locations were maintained for each casts, data for different tidal regimes were collected.

2.5.2. Preliminary results

Preliminary results on the turbulence level showed the presence of a three layer structure, with highly turbulent surface and bottom layers divided by a relatively calm interior, which is well described in the theory and ubiquitous in natural water with wind and /or tidal driven dynamics (Fig. 2.5.2.1).

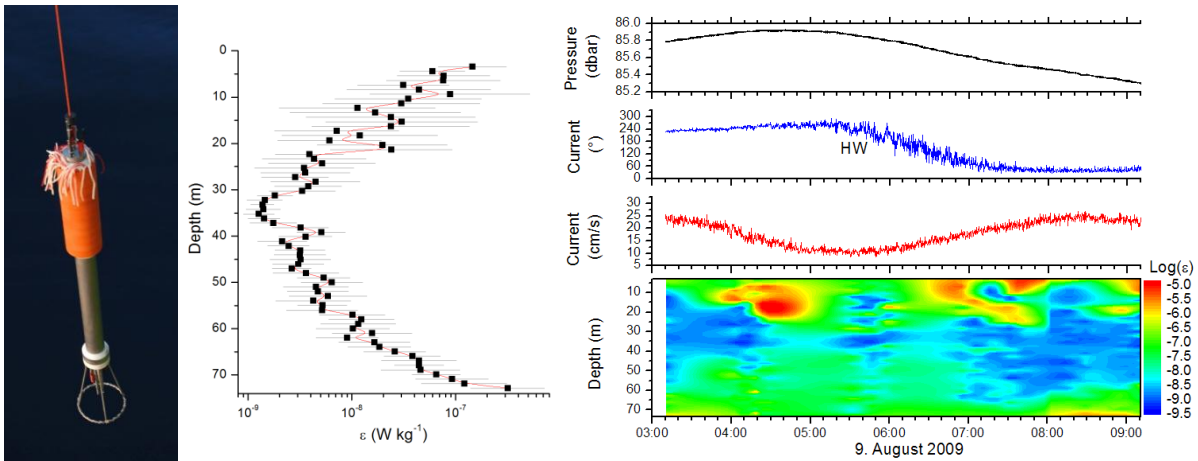


Fig. 2.5.2.1: MSS Probe and results overview. Left: the MSS90 profiler being retrieved. Center: Averaged turbulence level profile calculated from the shear probe sensor readings. Right: turbulence level contour plot (bottom) with the consequent tidal information from the POZ-Lander (see Section 2.1.1).

A comparison of bottom velocity, from the POZ-Lander ADCP, and turbulence level showed a correlation between currents and turbulence (Fig. 2.5.2.1). Such correlation is consistent with the theory and characteristics of the BBL. From temperature microstructures (Figure 2.5.2.2) we were able to fully resolve the stratified interior, where the thermocline lays. The fast galvanic AMT DO sensor revealed small changes in the water column DO concentration that are not detected by typical membrane DO sensors (Fig. 2.5.2.2).

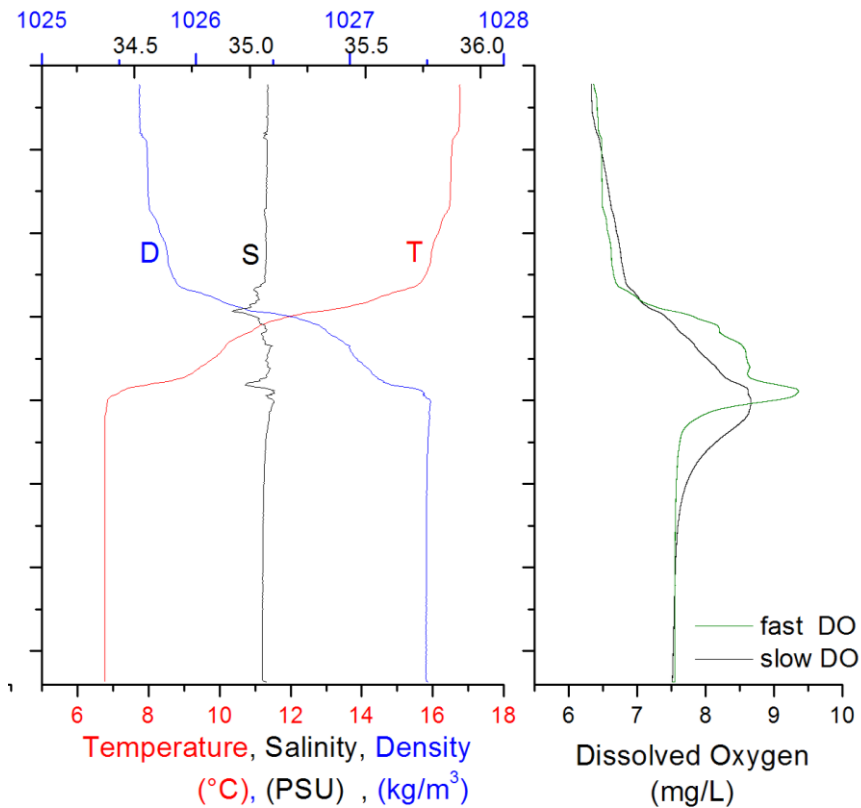


Fig. 2.5.2.2: MSS90 CTD and oxygen profiles. Left: Temperature, salinity and density profiles. Right: Oxygen profiles based on the standard oxyguard sensor (black line) and the high-resolution AMT sensor (green line).

Applications and future perspective:

From the turbulence data and the density profile we can calculate the vertical eddy diffusion coefficient, K_z , as $K_z = \gamma \cdot \varepsilon / N^2$ (Osborn 1980); it is possible to calculate fluxes throughout the water column (e.g. DO fluxes (J_{DO}) based K_z and a concentration gradient with Fick's Law

$$J_{DO} = K_z \cdot dC_{DO} / dz).$$

Reference

Osborn, T. R. (1980). Estimates of the local rate of vertical diffusion from dissipation measurements. *Journal of Physical Oceanography*, 10: 83-89.

3. Water column gas geochemistry (Stefan Sommer, Mark Schmidt, Markus Faulhaber)

3.1. Introduction

Major aim of this cruise was to measure bottom water gas concentrations of N_2 , Ar, CH_4 , and pCO_2 at Borkum Reef, Juist Salt Dome as well as around methane seeps in the Tommeliten area. Borkum Reef serves as a background station, where no fluids or gases were released from the seafloor. At the Juist Salt Dome diffusive gas release has been observed and at Tommeliten fluids and gas bubbles emanate from the sea bed. Gas measurements were conducted using the following water samples; Borkum Reef (CTD 1), Salt Dome Juist (CTD 2, 5, 6, 7, 8, 11, 12, 13, 14, 15, 16, 17) and Tommeliten (CTD 20, 21, 22). For details of deployments see station list. Presently, data analysis is ongoing, hence only preliminary results for selected areas will be shown.

3.2. Methods

Membrane Inlet Mass Spectrometry

During the first cruise leg gas measurements were conducted using discrete water samples which were obtained using a video-guided CTD water sampling rosette (Fig. 3.2.1.), which was towed in about 1m distance to the seafloor. During the second leg continuous gas measurements were conducted using an immersion pump that continuously pumped bottom water into the laboratory, where it was connected to a Membrane Inlet Mass Spectrometer (MIMS, IPI GAM 200), Fig. 3.2.2.

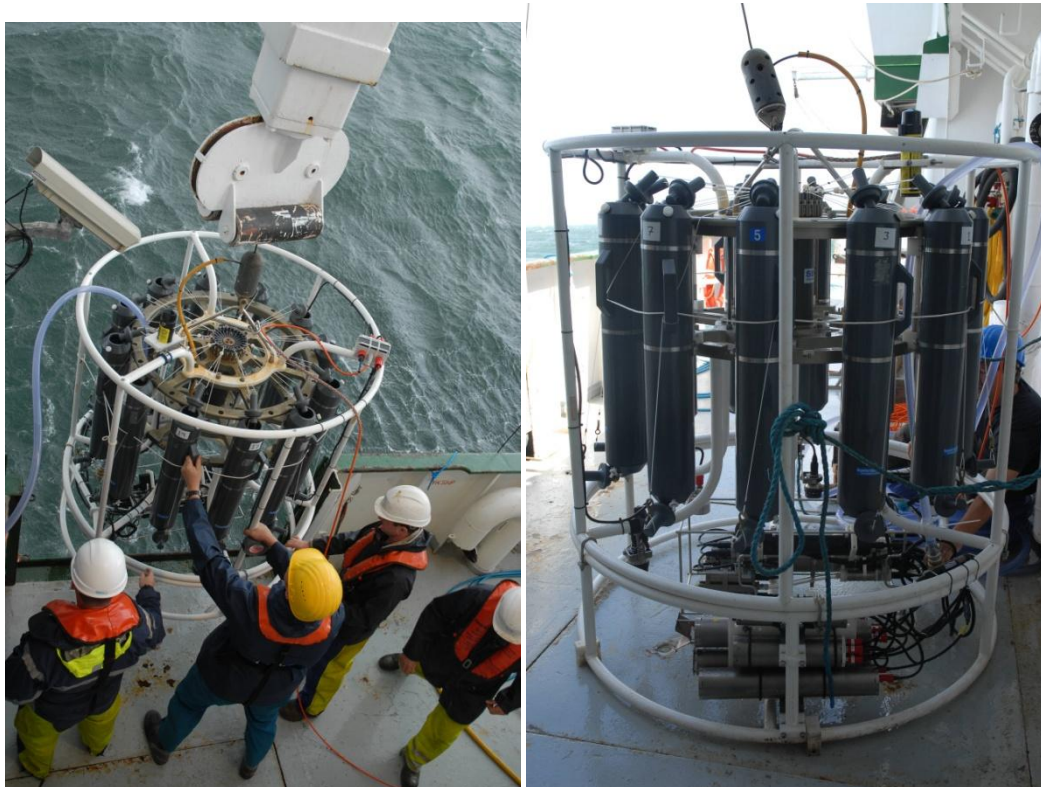


Fig. 3.2.1: Video-guided water sampling rosette, equipped with Seabird CTD, 10 L Niskin bottles, pH sensor, and Contros HydroC/CO₂/CH₄/PAH.

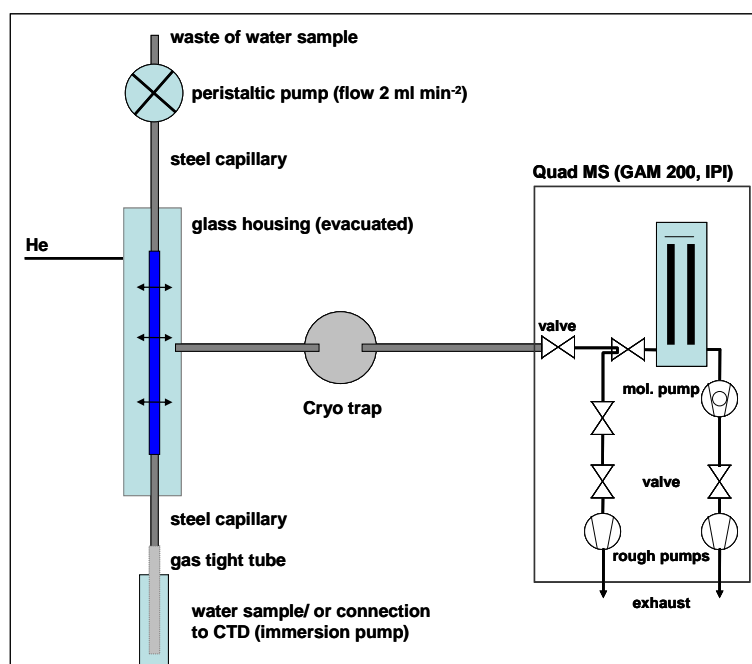


Fig. 3.2.2: Scheme of the set up of the Membrane Inlet Mass Spectrometer. For details see text.

From the pump tubing (i.d.: ~ 3 cm) we continuously sub-sampled water at a flow rate of 2 ml min^{-1} using a thermally insulated stainless steel capillary and a peristaltic pump (Ismatec). This water flow was directed through a membrane inlet that was connected to the mass spectrometer. Gas flow from the inlet to the mass spectrometer was supported with Helium that was supplied through a fused silica capillary (i.d. $100 \mu\text{m}$). A cryo trap (ethanol at -35°C) inline between the inlet and the mass spectrometer was used to reduce water vapour. In order to reduce temperature induced permeability changes of the silicone tubing inside the glass inlet, it was kept in a cooler close to *in situ* temperature. Temperature equilibration of water samples was achieved by forming the steel capillary as a heat exchanger (length ~ 3 – 4m) that was also kept in the cooler. Concentration of N_2 , Ar, CO_2 and CH_4 were sequentially obtained from ion currents at mass to charge (m/e) ratios 28, 40, 44, and 15 respectively. Gases were detected using a Secondary Electron Multiplier (SEM). Instrument response time was typically less than 3 min, hence only “smeared” gas concentrations alongside the towed transects were obtained. Instrumental CO_2 ion current (44) was calibrated using equilibrated sea water standards. Standards were prepared by bubbling CO_2 standards (100.6 ± 2 , 994 ± 20 , 9500 ± 190 ppm) balanced with N_2 through filtered ($0.2 \mu\text{m}$) seawater kept in septum stoppered glass vials (Labco Exetainers). Ion currents of N_2 (28), Ar (40), and O_2 (32) were calibrated using air equilibrated water samples at different salinities (0, 20, 35 psu) following the method of Kana et al. (1994). These standards consisted of 500 ml glass bottles containing filtered water ($0.2 \mu\text{m}$) gently bubbled with air through a diffusing stone. Whilst bubbling they were kept close to *in situ* temperature. The bottles were capped to reduce evaporation losses. The dissolved gas concentrations in the standards were calculated using the solubility equations of Hamme & Emerson (2004) and Garcia & Gordon (1992) for appropriate temperature and salinity. Before

calculating the gas concentrations the ion currents were corrected for instrument drift and temperature fluctuations inside the cooler.

Gas chromatography

Dissolved gas sampling in the North Sea was conducted mainly during near-seafloor CTD-tracks. Water samples were collected during CTD-tracks in 10 L Niskin bottles. Dissolved gases were released from the seawater samples by directly transferring 1.8 L of seawater into a pre-evacuated gas-tight glass bottle after recovery. This procedure leads to almost quantitative degassing of physically dissolved gases (~93%, Keir et al., 2008). The gas phase was then recompressed into 20 ml headspace vials at atmospheric pressure. The gas tight headspace vials were stored with 4 ml of NaCl-saturated sealing liquid. Parallel gas samples were stored in dry headspace vials without sealing liquid. The head space vials are stored for further stable isotope analyses at room temperatures. 3.5 ml of the extracted gas sample was analysed onboard by gas chromatography (CE8000top). 1 ml headspace gas was injected for hydrocarbon analyses (Porapak QS, 12 feet, 1/8"; FID; T-programmed; He-carrier gas). 2.5 ml sample gas was injected for atmospheric gas determination (Porapak Q - MS5A combination, He-carrier gas, 50°C isotherm, HCD). Gas bubbles were sampled by ROV using a funnel-type metal bottle (Fig. 3.2.3). The metal bottle is gas-tight, and pressure-proven and is closed after filling the cylinder totally with gas. The gas flux of the sampled bubble streams are calculated by known volume and measured sampling time. The gas bottles are attached to a high vacuum line with pressure control and known volume. The gas is subsampled into preevacuated glass containers and head space vials. The gas composition is measured onboard (see above) and subsamples are stored for further isotope geochemical analyses.

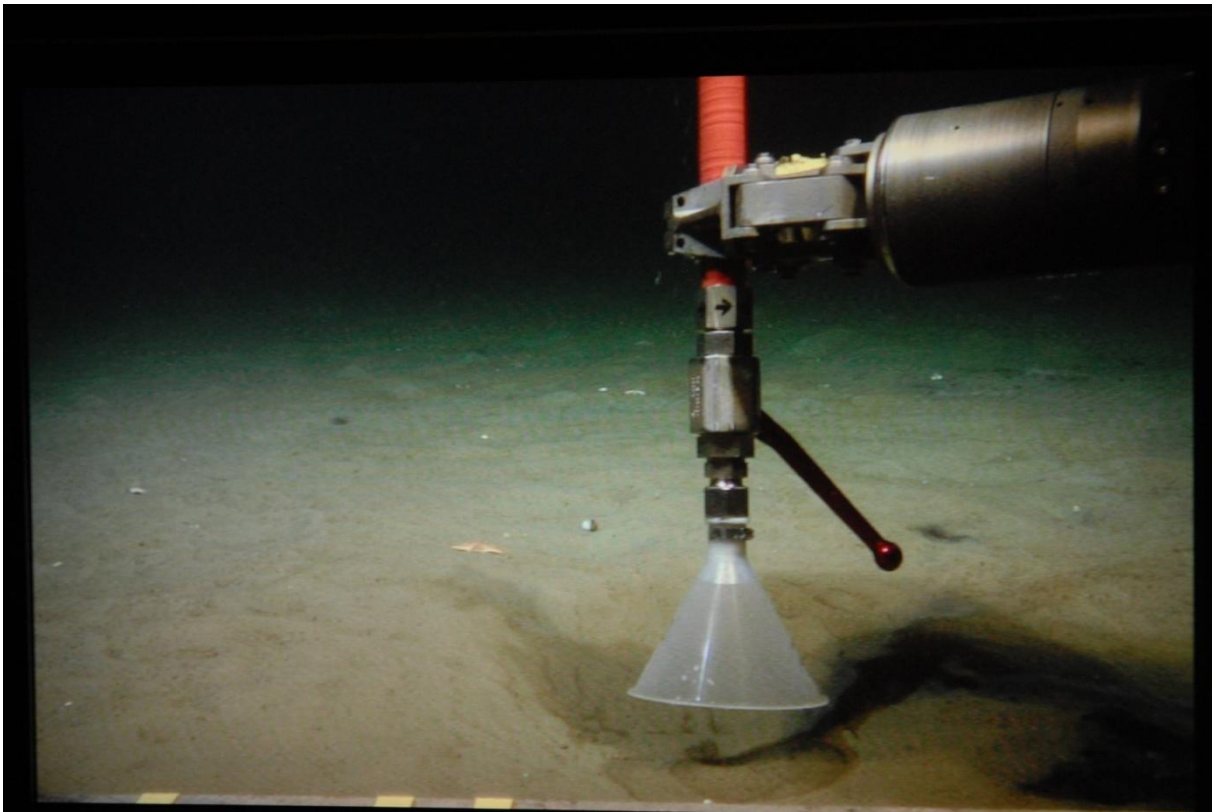


Fig. 3.2.3: Sampling of a gas bubble stream at the hydrocarbon seepage area "Tommeliten".

3.3. Preliminary results

Salt Dome Juist

During Alkor cruise 328 in 2008 elevated CO₂ concentrations were measured at the Juist Salt Dome area (McGinnis et al., submitted), to further constrain this enhanced CO₂ release a series of towed pump CTD's (15, 16, & 17) during three subsequent nights was conducted in this area (Fig. 3.3.1). Differences of pCO₂ between these CTD casts are mainly related to differences in water depth, average pH, and total alkalinity which were 2.35, 2.38 and 2.42 meq l⁻¹ respectively. The pCO₂ variability during each CTD tow, except CTD 16, was moderate with standard deviations of 10 ppm. However, during CTD 16 the fluctuation of pCO₂ was substantial and range between 575 and 732 ppm.

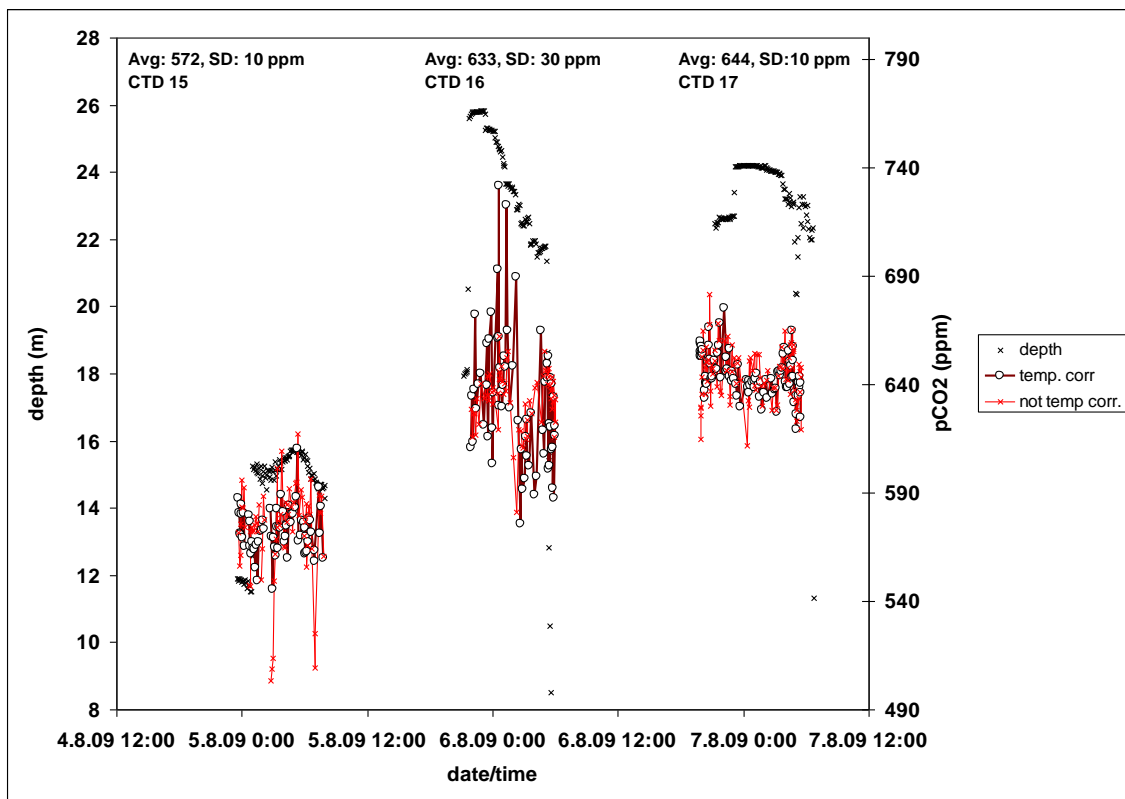


Fig. 3.3.1: pCO₂ recorded in the Salt Dome Juist area during 3 different towed CTD deployments (15, 16, 17) using a Membrane Inlet Mass Spectrometer. The circles represent pCO₂ values that were corrected for temperature fluctuations at the membrane inlet, the red lines show not corrected values. The crosses represent the depth of the CTD water sampling rosette.

It appears that during the deployment of CTD 16, pCO₂ accumulated in the bottom water until a distinct drop occurred at 242 min (6.8.09 02:00 UTC) followed by a phase of accumulation again, Figure 3.3.2, upper panel. The reasons explaining this pattern is presently not clear.

Bottom water N₂ ($447 \pm 8 \mu\text{M}$) was oversaturated (sat. N₂: $435 \mu\text{M}$) which is indicative for microbial dinitrogen release caused by denitrification and/or anammox in the anoxic sediments, figure 3.3.2, upper panel. During deployment of CTD 16 pronounced maxima of N₂ levels were detected. The extent to what the nitrogen levels deviate from the solubility equilibrium with the atmosphere is expressed in the saturation normalized N₂/Ar ratio, where $(\text{N}_2/\text{Ar})_{\text{sat}} = (\text{N}_2/\text{Ar})_{\text{molar ratio}} / (\text{N}_2/\text{Ar})_{\text{saturation equilibrium ratio}}$ (Emerson et al. 1991), Figure 3.3.2, lower panel. Equilibrium values are equal to 1, oversaturated and undersaturated are > 1 and < 1, respectively. To what extent, if at all, N₂ which possibly is released from deeper reservoirs contribute to the oversaturated bottom water N₂ levels and local N₂ maxima presently remains speculative.

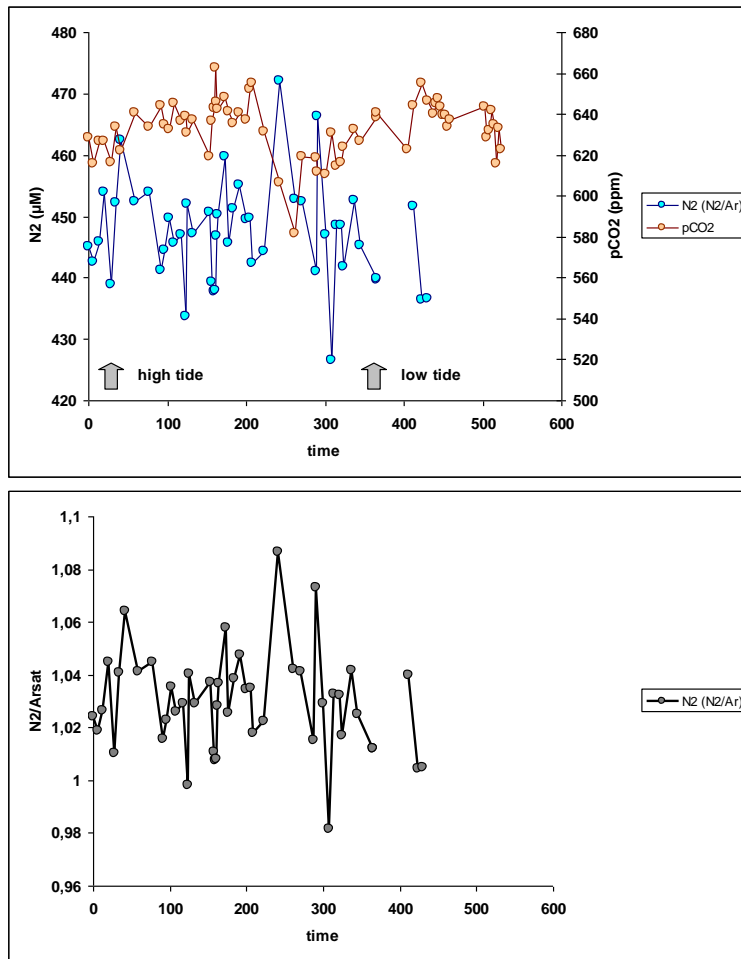


Fig. 3.3.2: Upper panel; Bottom water N_2 concentrations in the Salt Dome Juist area in comparison to the respective $p\text{CO}_2$ values. Concentrations were obtained using the measured N_2/Ar ratio multiplied by the saturated Ar ($11.45 \mu\text{M}$) concentration which was assumed to be constant. Lower panel; saturation-normalized N_2/Ar ratio (the molar N_2/Ar ratio divided by the N_2/Ar ratio at equilibrium with the atmosphere for a given temperature and salinity).

N_2 determined by gas chromatography (CTD 15, 16, 17; Tab. 3.1) is plotted in a contour map showing the western Salt Dome Juist area (Fig. 3.3.3). The measured data shows little variation above the Salt Dome and is generally comparable to the N_2 -concentration data measured by membrane inlet mass spectrometry (Fig. 3.3.2 upper panel). The Contour plot indicates a drop in N_2 in the southwest which is an area where salt doming is absent. This effect can be coincident, as the samples from the southeast were taken during low tide. However, reduced pressure would result in enhanced gas seepage from sediment. Nevertheless, different water masses could have also caused this drop, and further data evaluation (current, salinity, temperature) will give further insights into the local nitrogen distribution pattern.

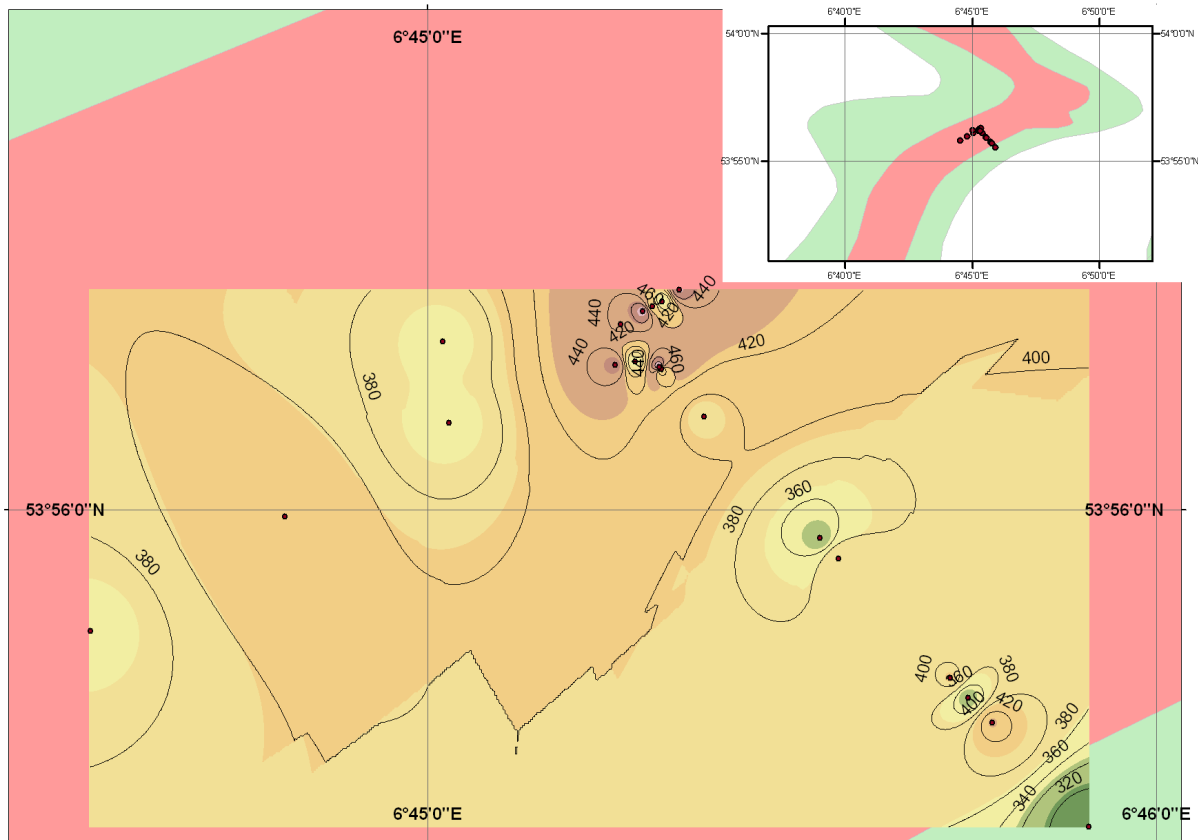


Fig. 3.3.3: N₂-contour plot of Salt Dome Juist near bottom waters (CTD 15-17). Gas concentrations were determined by gas chromatography (Tab. 3.1). Only little N₂-variation is indicated above the salt dome area and a sharp decrease in N₂ is shown in the southeast where salt doming is absent.

Methane concentrations determined by gas chromatography during CE0913 cruise (~2-4 nmol/l, Tab. 3.1, stations 1-42), are slightly higher than values measured during Alkor 328 cruise in October 2008. However, they are still in the range of normal background concentrations known for well mixed water masses in equilibrium with the atmosphere.

Tommeliten methane seep area, N₂/CH₄

Major goal in this area was to determine seabed methane release and bottom water N₂ levels around seep structures using the towed CTD's (20, 21, 22) which as described above were connected to the MIMS allowing continuous gas measurements. Preliminary results of CTD cast 22 are depicted in Figure 3.3.3 A-D. The time period from 0 to ~ 160 min represents the descent of the CTD through the water column to the seafloor. Beyond 160 min the CTD was towed across seeps where gas bubble release from the sediment was observed. The surface water was separated from the bottom water by a thermocline at about 25 to 40 m water depth, Fig. 3.3.3 A/B. This thermocline was associated with a maximum of dissolved oxygen. Below the thermocline we measured elevated pCO₂ levels (data not yet temperature corrected). When towed above the seafloor oxygen, pCO₂, temperature and salinity remained constant.

Dinitrogen levels increased during the lowering of the CTD which is related to an increased solubility by lower water temperatures. Below the thermocline, when the temperature was constant at ~ 6.8°C the N₂ levels were fluctuating around 500 µM, Fig 3.3.3 C.

The atomic mass unit (amu) 15 was used as indicator for methane, Fig. 3.3.3 D. However, it appears that this mass alone can be used only to a limited extent. The ion current strength for this mass would indicate strongly elevated methane levels at the sea surface that decline exponentially with depth, which is not realistic. Hence, the mass 15 has to be interpreted in combination with the presence of other gases which after ionisation could contribute to the overall ion current of mass 15. We assume that during the descent of the CTD changes of N₂ concentration and resulting mass fragments are contributing to the measured signal strength of amu 15. Nitrogen possesses two naturally stable isotopes ¹⁴N and ¹⁵N with a relative abundance of 99.632 and 0.368 % respectively. Dinitrogen predominantly occurs as ²⁸N and to a minor extent as ²⁹N. At depth where changes of gas solubility are almost negligible, we expect that the ratio of the major nitrogen fragments (28/29) remains constant as is shown by our measurements, Fig. 3.3.3 E. Under these conditions nitrogen fragments do not contribute to the fluctuations measured for the amu 15 and might be exclusively due to different bottom water methane levels. Under these conditions the ratio between the masses 28 (dinitrogen) and 15 (methane) appears to represent a very suitable indicator to detect methane. We are convinced that the above described method of gas analysis has a high potential for continuous online gas measurements which allows high resolution mapping of wider areas.

Methane concentrations measured at the Tommeliten (Ekofisk) area are reaching much higher values than normal background concentrations in seawater (up to 346 nmol/l, Appendix III, stations 48-67). Methane concentrations of the upper water mass (0-25m) vary between 1.7 and 5.3 nmol/l which indicates near equilibrium conditions there. Below the thermocline, which is well established at the Tommeliten site the methane concentration sharply increases to about 40-60 nmol/l and the highest concentrations are measured near the seafloor at about 70 mbsl (Appendix III). CTD23 methane concentration data, measured by gas chromatography, is presented in detail in Fig. 3.3.4. The GC-data is compared with *in situ* methane sensor signals (HydroC/CH₄) recorded when the Niskin bottles were fired. A general comparable trend in concentration variation is indicated in Fig. 3.3.4. However, inconsistent trends and a decreasing offset with time of sensor signal strength is also obvious. Distances of 0.5-1 m between sensor and Niskin bottles could possibly explain these inconsistencies. Equilibration times of several minutes could also explain the delay between sensor and GC data and the offset of the sensor. The sensor calibration for calculating concentrations by signal strength data (V) will be performed. The sensors detection limit of about 30-50 nmol/L is estimated based on the data comparison in figure 3.3.4. The onshore calibration of the sensor under controlled T-conditions and longer equilibration time will probably show a better detection limit.

The water samples showing the highest methane concentrations were sampled directly at active gas bubble seeps. Gas bubbles were also directly sampled by ROV in pressure tight metal bottles (Fig. 3.1.1). The gas composition and bubble flux was detected at two vents (Tab. 3.3.2). The dominant gas at the seafloor is methane, and the bubble flux ranges between 2.5 and 13.4 ml/min (Tab. 3.3.2; calculated for insitu pressure). The measured data is comparable to gas fluxes determined at this site in 2006 (AL290) by Schneider v. Deimling et al., submitted.

Tab. 3.3.2: Preliminary gas composition and bubble flux of seeping gas bubbles at Tommeliten.

Date	UTC Time	Station	ROV position		ROV Depth	Bubble Flux	CH ₄	N ₂	O ₂	CO ₂
		No.	Lat. N	Lon. E	mbsl	ml/min	Vol.%	Vol.%	Vol.%	Vol.%
08.08.09	16:43	49	56.497883	2.9966333	71	2.45	98,7	5.9	1.5	1.0
10.08.09	15:00	63	56.4985519	2.9960216	71	13.4	99.5	5.6	1.5	0.9

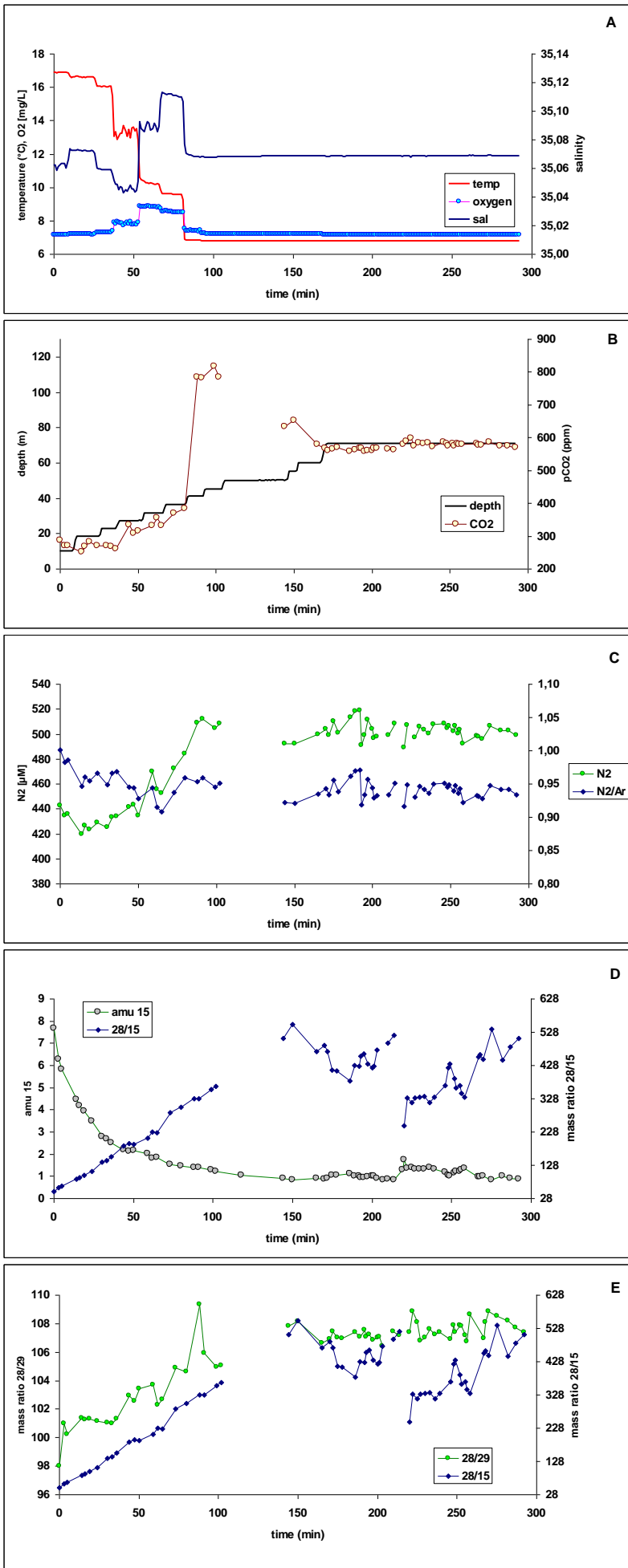


Fig. 3.3.3: Gas measurements during CTD cast 22 at the Tommeliten methane seep area. The different parameters are plotted against time rather than depth. A, temperature, salinity and oxygen; B, depth and pCO₂; C, dinitrogen levels and the saturation-normalized N₂/Ar ratio; D, raw signal (ion current) for the mass 15 and the ratio 28/15; E ratios 28/29 and 28/15 (raw signal).

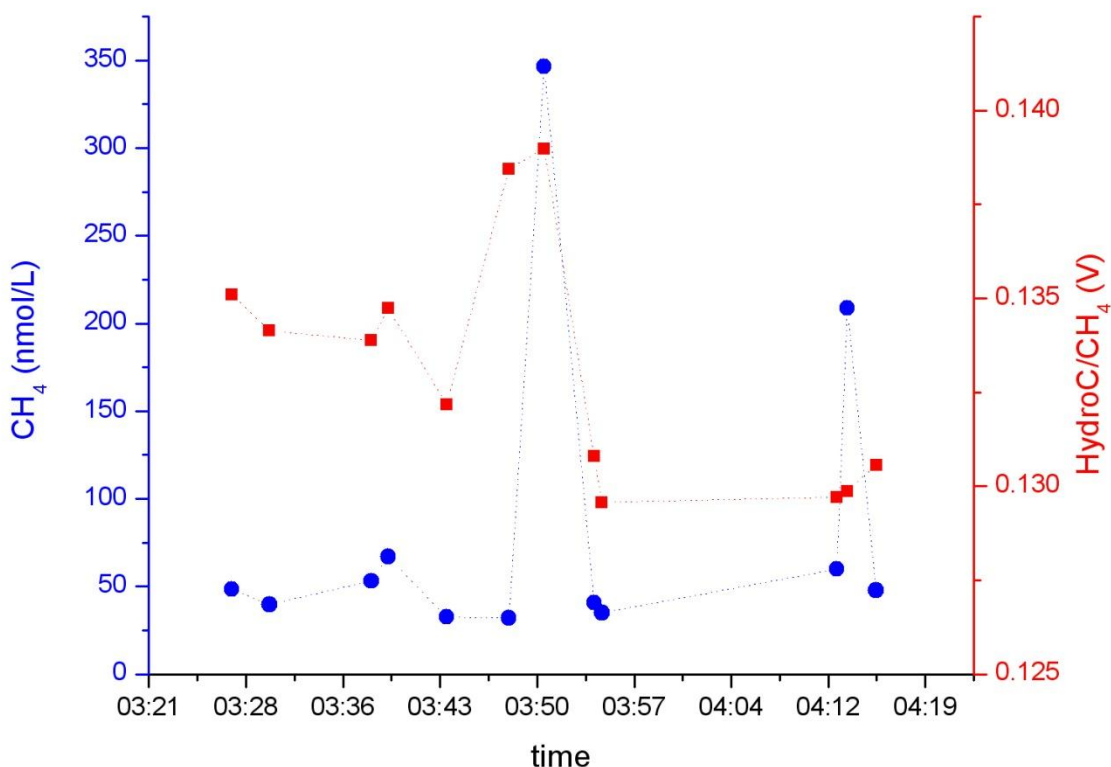


Fig. 3.3.4: Methane concentrations along CTD 23 profile (St. 67, Tommeliten), determined by gas chromatography from Niskin bottle samples (blue symbols) compared to methane signals (V) measured in the water column with HydroC/CH₄ sensor (red symbols).

References

- Emerson S, Quay P, Stump C, Wilbur D, Knox M (1991) O₂, Ar, N₂, and ²²²Rn in surface waters of the subarctic Pacific Ocean: net biological O₂ production. *Global Biogeochem. Cycles*, 5, 49-69
- Garcia HE, Gordon LI (1992) Oxygen solubility in seawater: Better fitting equations. *Limnol. & Oceanogr.*, 37, 1307-1312.
- Hamme RC, Emerson SR (2004) The solubility of neon, nitrogen and argon in distilled water and seawater. *Deep-Sea Res. I*, 51, 1517-1528.
- Kana TM, Darkangelo C, Hunt MD, Oldham JB, Bennett GE, Cornwell JC (1994) Membrane inlet mass Spectrometer for rapid high-precision determination of N₂, O₂, and Ar in environmental water samples. *Anal. Chem.*, 66, 4166-4170.
- Keir R. S., Schmale O., Walter, M., Sültenfuß J., Seifert R., Rhein M. (2008). Flux and dispersion of gases from the "Drachenschlund" hydrothermal vent at 8°18'S, 13°30'W. *Earth and Planetary Science Letters*, 270: 338-348.
- McGinnis D.F., Schmidt M., Themann S., DelSontro T.S., Rovelli L., Reitz A., Linke P.. Discovery of a natural CO₂ seep in the German North Sea: Implications for shallow dissolved gas and seep detection. Submitted.
- Schneider von Deimling, J.; Rehder, G.; McGinnis, D.F.; Greinert, J.; Linke, P.: A multidisciplinary approach to quantify methane gas seepage at Tommeliten (North Sea). In preparation.

4. Water column and pore water geochemistry

(A. Reitz, B. Domeyer, M. Dibbern, P. Wefers, R. Schwarz)

4.1. Introduction and methods

The geochemical investigation of various solvents in subsurface pore waters comprises valuable information for an improved comprehension of fluid advection and diagenetic processes. During CE0913 pore water geochemistry was conducted to identify CO₂ discharge, changes in pCO₂, fluid advection and the source of fluids. It is well known that conservative solvents like Cl and Li amongst others do indicate fluid advection and deep burial diagenetic processes exquisite. In the following section procedures of sediment, pore water, and water column water retrieval and processing and geochemical laboratory methods are described. Furthermore, a selection of major results is utilized to explain the geochemical characteristics obtained during CE0913.

Sampling, processing, and on-board geochemical analysis

Surface and subsurface sediment samples for pore water extraction and solid phase sampling were taken with a vibro corer (VC) and a push corer by means of a ROV; furthermore pore water was also taken *in situ* by an *in situ*-Pore Water Sampler (PWS) by means of a ROV. Water column and bottom water samples were taken with a CTD-rosette, with Niskin bottles mounted to a ROV, by the Kiel *In situ* Pump System (KIPS) by means of a ROV, and by time-controlled syringe-sampling in a benthic chamber system (Table 4.1.1). Direct cooling of samples after retrieval was not required because the bottom water temperature of the southern North Sea was about 18°C during summer; however the bottom water temperature of the northern part was about 7°C. Water samples from the CTD-rosette were filtered (0.2 µm cellulose-acetate filters) for subsequent analyses. Vibro cores were cut in 1 meter sections directly after recovery and perforated in about 25 cm resolution to enable immediate pore water sampling by the use of Rhizons. Plastic syringes were used to apply under-pressure to the Rhizons; the first 0.5 ml of pore water was discarded. If Rhizon-sampling was unsuccessful, which was mainly within very dry, dense, and organic rich layers, pore water was extracted by a pressure filtration system (0.2 cellulose-acetate filters) at pressures up to 7 bars. Subsequently, the core sections were opened lengthwise and each pore water sample depth was supplementary sampled for physical properties (porosity), selected solid phase concentrations (carbon, nitrogen, sulfur), and volatile hydrocarbon gas concentrations. About 5 ml sediment was filled into pre-weighed plastic vials and stored at about 6-8°C for subsequent analyses in the shore-based laboratory. For volatile hydrocarbon gas analyses 3 (6) cm³ of sediment were extruded and disaggregated in a sealed 20 ml headspace vial filled with 9 (4) ml saturated NaCl solution. The obtained pore waters were as followed subsampled for subsequent on board, shore-based, and specific isotope analyses: 3 ml of water were taken for on-board analysis, for shore-based analysis 1.7 ml were taken into plastic vials for IC analysis (Cl, SO₄, I, Br), 3 ml were taken into acid-cleaned plastic vials and acidified with 30 µl 65% s.p. HNO₃

for ICP-AES analysis (B, Mn, Ca, Fe, Na, Mg, Sr, Si, Ba, Li, K), 1 ml was sampled into a glass vial for selective isotope analyses e.g. $\delta^{18}\text{O}$, $\delta^2\text{H}$, $\delta^{37}\text{Cl}$, and 3 ml and 1.9 ml were sampled into gas-tight glass vials and poisoned with 12 μl and 8 μl HgCl_2 , respectively for $\delta^{13}\text{C}$ and DIC analyses. Regarding the CTD-water samples 20 ml and 8 ml were sampled in gas-tight glass vials and poisoned with 80 μl and 40 μl HgCl_2 , respectively for $\delta^{13}\text{C}$ and DIC analyses. All subsamples for shore-based analyses were stored at about 6-8°C, except of the IC subsamples that were stored frozen at -20°C. Selected samples for potential acetate analyses were taken at station 48 (ROV9), 63 (ROV12), and 68 (VC14) 2 ml pore water were filled in pre-cindered vials and stored at -20°C. Furthermore, selected samples for potential Nitrate analyses were taken at station 57 (ROV11), 63 (ROV12, PC1-3) 2 ml were filled in glass vials and stored at -20°C. On board pore water analyzes were started immediate after sample retrieval. The pH was determined with a glass electrode in the pore water. It was planned to measure the pH within the sediment but the pore water was draining to quickly out of the sandy sediment precluding any pH measurement within the sediment. The temperature was as well recorded parallel to the pH measurement and the electrode was calibrated with 2 solutions of defined pH values, 2-Aminopyridine and N,N-Dimethyl-1,4-phenylenediamine-monohydrochloride (Dickson, 1993). It has to be admitted that the ex situ pH values do not reflect the true pH of the sediment, because, the dominating carbonate and calcium carbonate equilibrium show considerable pressure dependence. Pore water and water samples were analyzed for total alkalinity (TA) by titration with 0.02N HCl using the Tashiro indicator, any CO_2 and H_2S produced during the titration was stripped by bubbling with argon (Ivanenkov, 1987). Dissolved chloride (Cl) was determined in the pore water by titration after Mohr (Grasshoff et al., 1999). The IAPSO (International Agency of the Physical Science of the Oceans) seawater standard was use to calibrate both titration procedures as well as to perform the accuracy and precision monitoring. Sulfide (TH_2S), ammonium (NH_4), and phosphate (TPO_4) concentration were retrieved by standard photometric procedures described in Grasshoff et al. (1999). In total samples of 14 vibro corers, 16 CTDs, 12 KIPS, 6 Niskin (mounted to ROV), 12 PCs, 2 PWS, and 2 benthic chamber syringe sets (Table 4.1.1)

Table 4.1.1: List of stations sampled for geochemical analysis; the number of pore water or water column samples taken at each station is indicated

Station	Gear	No.	Area	Latitude N	Longitude E	depth	Remarks/ Samples
2	VC	1	Borkum Reef	53.893917	6.259000	30.0	25 samples
7	VC	2	Salt Dome Juist	53.936883	6.755220	24.0	25 samples
17	VC	4	Salt Dome Juist	53.966028	6.971697	25.0	26 samples
21	VC	5	Salt Dome Juist	53.927697	6.747760	22.0	23 samples
24	VC	6	Salt Dome Juist	53.924848	6.726510	22.0	24 samples
35	VC	8	Salt Dome Juist	53.926863	6.742665	22.0	25 samples
39	VC	9	Salt Dome Juist	53.925592	6.720870	22.0	29 samples
43	VC	10	Salt Dome Juist	53.988840	6.757380	25.0	26 samples
46	VC	11	Tommeliten	56.501817	2.995950	70.0	20 samples
54	VC	12	Tommeliten	56.497883	2.996633	71.0	11 samples
61	VC	13	Tommeliten	56.498625	2.995835	71.0	24 samples
68	VC	14	Tommeliten	56.497592	2.996063	73.0	14 samples
9	ROV	1	Salt Dome Juist	53.935367	6.758150		2 samples (2 KIPS)
16	ROV	2	Salt Dome Juist	53.956100	6.974867		5 (2 Niskin, 3 KIPS)
	Niskin bottle	1		53.966	6.9715333	26.0	
	Niskin bottle	2		53.965633	6.9718165	26.0	
	KIPS	1		53.965935	6.97175026	25.0	
	KIPS	2		53.965984	6.97149992	26.0	
	KIPS	3		53.965649	6.97183323	26.0	
23	ROV	3	Salt Dome Juist				17 (10 PWS, 1 KIPS, 1 Niskin, 1 PC)
	Niskin bottle	1		53.936966	6.7542167	24.0	
	PC	1		53.936966	6.7542334	24.0	
	KIPS	1		53.937	6.75421667	24.0	
	PWS			53.936985	6.7542167	24.0	
30	ROV	4	Salt Dome Juist	53.937067	6.756250	25.0	14 (9 PC, 3 KIPS, 2 Niskin)
	Niskin bottle	1		53.936798	6.7551498	24.0	
	Niskin bottle	1		53.936798	6.7551498	23.0	
	PC	1		53.936798	6.7551332	23.0	
	PC	2		53.936783	6.7551332	23.0	
	PC	3		53.936817	6.7551332	23.0	
	KIPS	1		53.936817	6.75461674	23.0	
	KIPS	2		53.936783	6.75466681	23.0	
	KIPS	3		53.936798	6.75514984	23.0	
36	ROV	5	Salt Dome Juist	53.937500	6.754300	25.0	20 (10 PWS, 8 PC, 1 KIPS, 1 Niskin)
	PWS			53.936749	6.7550168	24.0	
	KIPS	1		53.936768	6.7554169	24.0	
	PC	1		53.936832	6.7553668	23.0	
	PC	2		53.936852	6.7554002	23.0	
	PC	3		53.936832	6.7554002	23.0	
40	ROV	6	Salt Dome Juist	53.963883	6.972433	26.0	1 sample (KIPS)
44	ROV	8	Salt Dome Juist	53.937150	6.758333	26.0	10 (5 PC, 5 syringe)
	PC			53.936783	6.7554331	26.0	
49	ROV	9	Tommeliten	56.498583	2.995250		14 (12 PC, 2 KIPS)
	PC	1		56.498299	2.9955332	71.0	
	PC	2		56.498085	2.9965501	71.0	
	KIPS	1		56.498051	2.99655008	71.0	
	KIPS	2		56.497784	2.99616671	71.0	
58	ROV	11	Tommeliten	56.501400	3.001367	70.0	7 (syringe)
63	ROV	12	Tommeliten	56.498617	2.995900		23 (16 PC, 7 syringe)
	PC	1		56.498855	2.9959837		
	PC	2		56.498868	2.996009		

Station	Gear	No.	Area	Latitude N	Longitude E	depth	Remarks/ Samples
1	CTD	1	Borkum Reef	53.900433	6.296367		12 samples
3	CTD	2	Salt Dome Juist	53.936050	6.759633	26.0	9 samples
4	CTD	3	Salt Dome Juist	53.935390	6.758153	26.0	4 samples
8	CTD	5	Salt Dome Juist	53.935367	6.758100	26.0	12 samples
13	CTD	7	Salt Dome Juist	53.969233	6.971033	28.0	12 samples
15	CTD	8	Salt Dome Juist	53.965017	6.972717	27.0	7 samples
19	CTD	9	Salt Dome Juist	53.924982	6.726162	25.0	6 samples
22	CTD	10	Salt Dome Juist	53.935390	6.758135	27.0	6 samples
28	CTD	12	Salt Dome Juist	53.931667	6.742333	25.0	8 samples
32	CTD	13	Salt Dome Juist	53.936817	6.755283		10 samples
33	CTD	14	Salt Dome Juist	53.936687	6.754925		4 samples
34	CTD	15	Salt Dome Juist	53.936782	6.755143		4 samples
38	CTD	16	Salt Dome Juist	53.945820	6.745720	24.0	4 samples
42	CTD	17	Salt Dome Juist	53.930493	6.742118	26.0	6 samples
50	CTD	19	Tommeliten	56.498593	2.996320		10 samples
67	CTD	23	Tommeliten	56.498517	2.995800		3 samples

4.2. Preliminary results

Salt Dome Juist

Subsurface geochemistry

Pore waters from subsurface sediments at the Salt Dome Juist area show about bottom water concentrations with respect to TA, except of core VC10 and the Cl profiles of all cores except core VC9 do show about bottom water concentrations. VC10 shows higher nutrient concentrations (NH_4 , TPO_4) with depth (Fig. 4.2.1). pH measurement were some sort of troublesome to problematic, which will be discussed later.

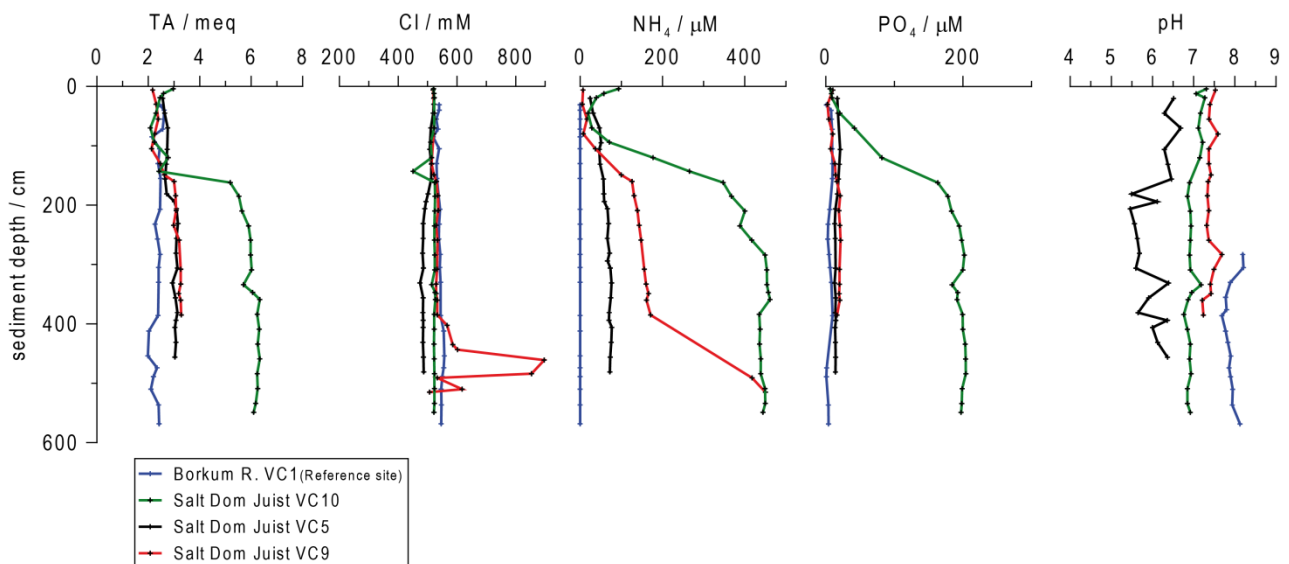


Fig. 4.2.1: Concentration vs. depth profiles of dissolved TA, Cl, NH_4 , TPO_4 , and pH values obtained in subsurface pore waters at the Salt Dome Juist area.

The total alkalinity (TA) value is a measure of the dissolved bicarbonate (HCO_3^-) concentration because bicarbonate is the major anion taking up and neutralizes protons to buffer the pH. Bicarbonate is mainly produced by three different processes (i) anaerobic degradation of organic matter, (ii) dissolution of carbonate, and (iii) weathering of silicates. Between 1.42 and 1.47 m sediment depth in core VC-10 an oxidation horizon (reddish layer) with a clay or silt layer at the bottom was observed. Below this horizon organic matter particles seems to be dispersed. This is also indicated by the increase in NH_4 and TPO_4 below that depth. Seeing that, this disperse organic particles are forming a considerable potential for organic matter degradation post-burial it seems most likely that bicarbonate and thus TA are mainly produced by anaerobic degradation of organic matter. However, hydrogen sulfide was not measured in this core as no H_2S smell was observed. TPO_4 is release du to the microbial degradation of phosphate-bearing organic matter; released values show a maximum concentration of about 200 μM at about 200 cm sediment depth. Unfortunately, we do not have the results for sulfate concentrations; they will be measured in the shore-base laboratory.

Core VC9, that displays Cl enrichment between about 400 and 500 cm core depth with a maximum concentration of about 900 mM, was taken above a salt dome structure. It seems that this horizon of Cl enrichment comprises a conduit or layer of higher porosity. The NH_4 depth profile that shows increasing concentrations down to the bottom of the core may be a further indication for the same explanation as NH_4 from depth might be delivered by this conduit as well. pH measurements were rather problematic; unfortunately, they could not be accomplished directly within the sediment as pore water drained to quickly out of the sediment causing several errors and delays during measurements. The alternative method of measuring the pH in the pore water directly after recovery comprised other obstacles from which the sensitivity of the electrode to other charges (e.g. other instruments) was most relevant next to the fact that the laboratory was not temperature controlled. However, even though the pH values might not indicate the true values, because of this analytical problems and the fact the dominating carbonate and calcium carbonate equilibrium show considerable pressure dependence shifts within the profiles seem to be real. This can be demonstrated e.g. by core VC5 that shows a shift in pH were clay layers occur (Fig. 4.2.2).

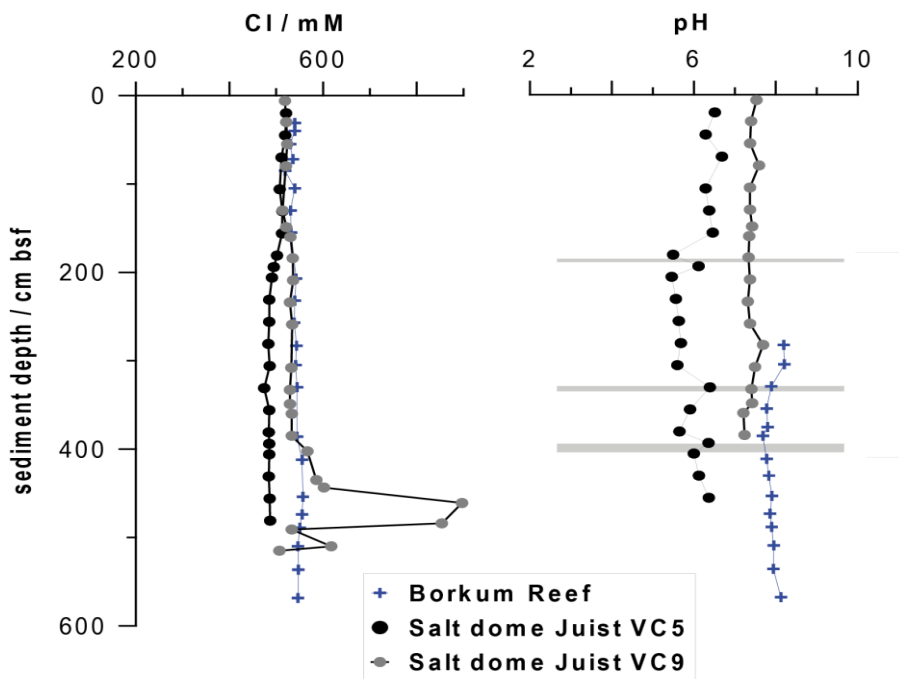


Fig. 4.2.2: Cl concentration and pH value depth profiles of selected cores. The grey layers indicate the clay layers observed in VC5.

The new *in situ* pore water sampler (PWS) that was for the first time successfully applied by means of ROV produced some very nice pore water profiles that correlate convincingly with the profiles obtained by a push core next to the PWS (Fig. 4.2.3). The depth concentration profiles show constant TA and increased NH_4 and PO_4 concentrations between about 6 and 15 cm core depth.

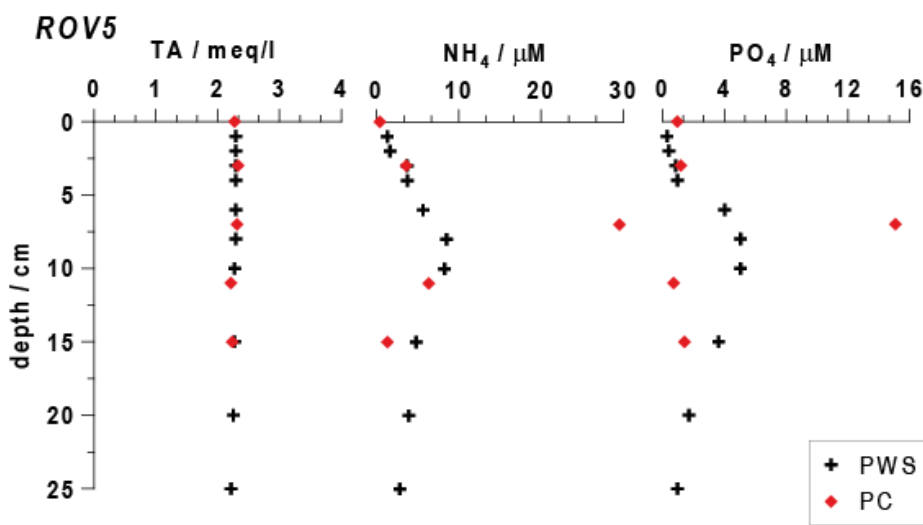


Fig. 4.2.3: TA, NH_4 , and PO_4 concentration profiles of pore water samples (PWS) taken during ROV dive number 5 with the *in situ* pore water sampler and ex situ from a push core taken next to the PWS at a pock mark structure at the Salt Dome Juist area.

Bottom water geochemistry

The contour maps that were calculated applying the minimum curvation method for interpolation of chlorine and total alkalinity distribution in bottom waters within the Juist Salt Dome area (Fig. 4.2.4), show a general trend of increasing Cl values from South to North the same trend seem to be displayed for TA. However, it has to be pointed out that the differences in TA are rather small and should not be overstated. Nevertheless, looking at the small-scale map of the Salt Dome Juist-West site an area of fluid discharge carrying a less saline signature was identified. Further investigations are needed to identify the processes behind this discharge. Potential processes that

would lead to the escape of less saline fluids are (i) fluid advection caused by a convection cell releasing less saline fluids of Holocene age or (ii) fluid and gas seepage from depth due to hydrostatic pressure increase. This area of fluid discharge seems also be shown by the TA contour map of the western area.

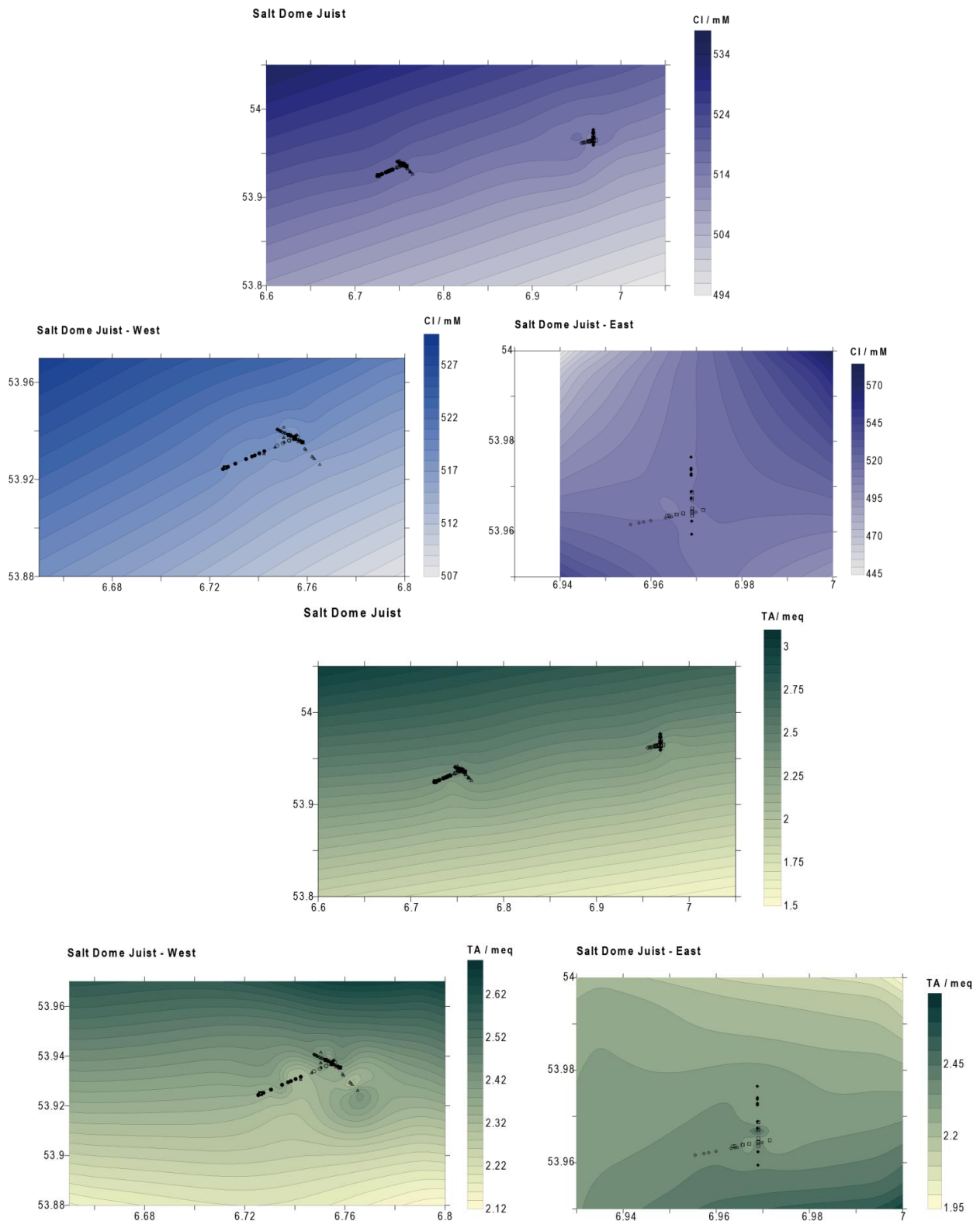


Fig. 4.2.4: Chlorine and TA concentration distribution in bottom water maps of the Salt Dome Juist area; The upper Cl and TA panel shows the east and west site on one map and the lower Cl and TA panel shows the east and west part separately.

Tommeliten

Subsurface geochemistry

The Tommeliten site is an area where methane gas is released through cracks in the buried clay horizon at several venting spots (see description of ROV observation at section 5; Niemann et al., 2005). Even though, methane gas is obviously actively transported through the sediments conservative elements like Cl do not indicate fluid advection along with gas ascent. The geochemical profiles at the Tommeliten site are characteristic for sites dominated by anaerobic oxidation of methane (AOM). The process of AOM increases total alkalinity by the production of HCO_3^- and HS^- (Fig. 4.2.5). Furthermore, thermogenic degradation of organic matter producing methane (Niemann et al., 2005) and NH_4 seems to occur at depth, which is reflected by the increase in NH_4 . Both processes, oxidation of organic matter and AOM seem to occur well below the depth of core penetration as TA and NH_4 have not reached maximum value at the bottom of the cores. pH is varying between 7 and 8, thus typical for normal seawater.

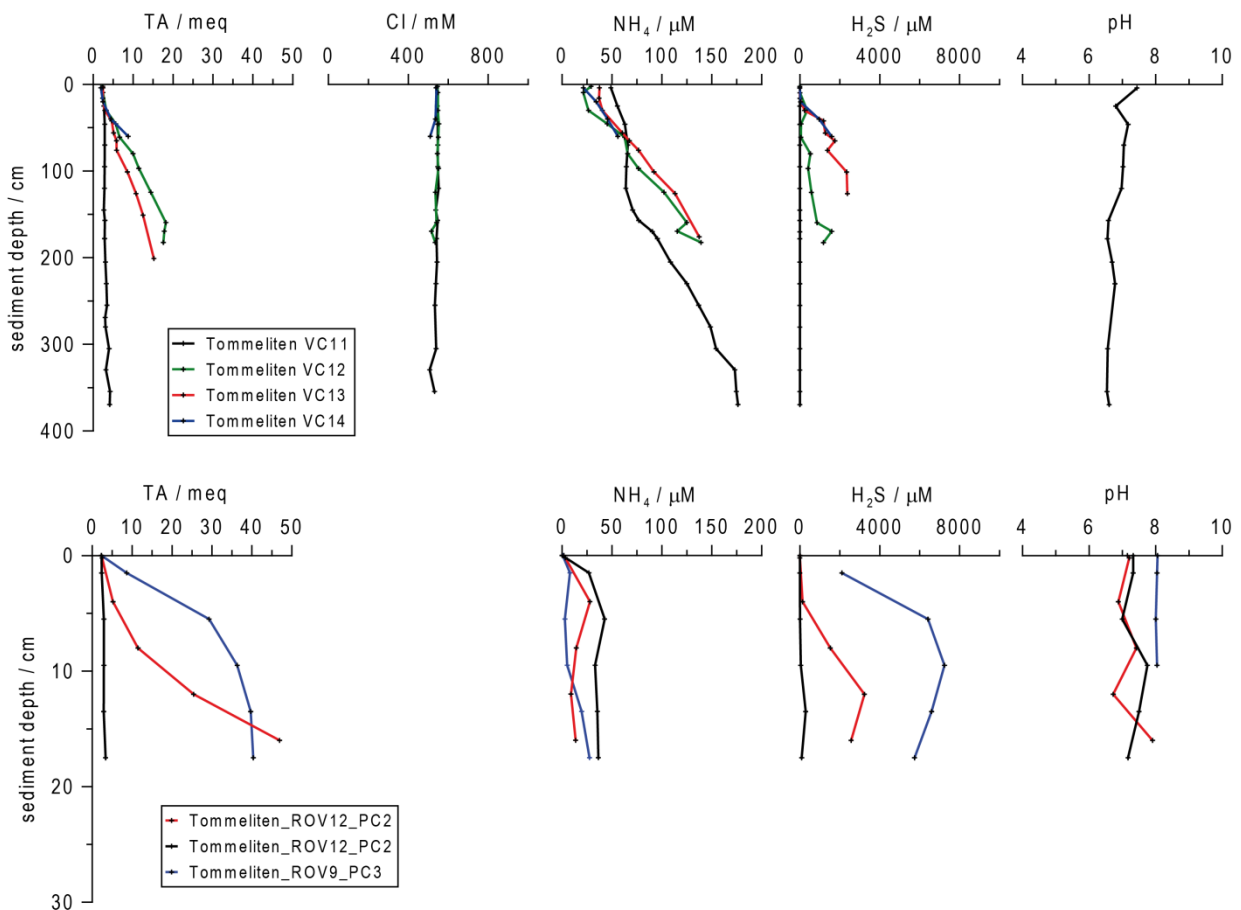


Fig. 4.2.5: Concentration vs. depth profiles of dissolved TA, Cl, NH_4 , TH_2S , and pH values obtained in subsurface pore waters at the Tommeliten area.

Some of the cores were rather stiff and clayey hampering pore water sampling with Rhizons, for this cores we performed pore water sampling with Rhizons as far as possible and parallel sampling by pore water squeezer. The results of this parallel sampling procedure show that there are distinct

differences regarding the result of the parameters that are not stable after core retrieval i.e. TA, TH₂S, and NH₄ (Fig. 4.2.6) The fast pore water sampling method with Rhizons produce higher TA and lower NH₄ values than the Squeezer method and the TH₂S results obtained on squeezed pore waters show that obviously TH₂S is quickly lost after core recovery. Rhizon samples show increase values at around 50 cm, but the squeezed pore waters show a steep increase at 100 cm. This comparison confirms once more that a very fast procedure from core retrieval over pore water sampling to parameter analyzes is essential to obtain reliable results.

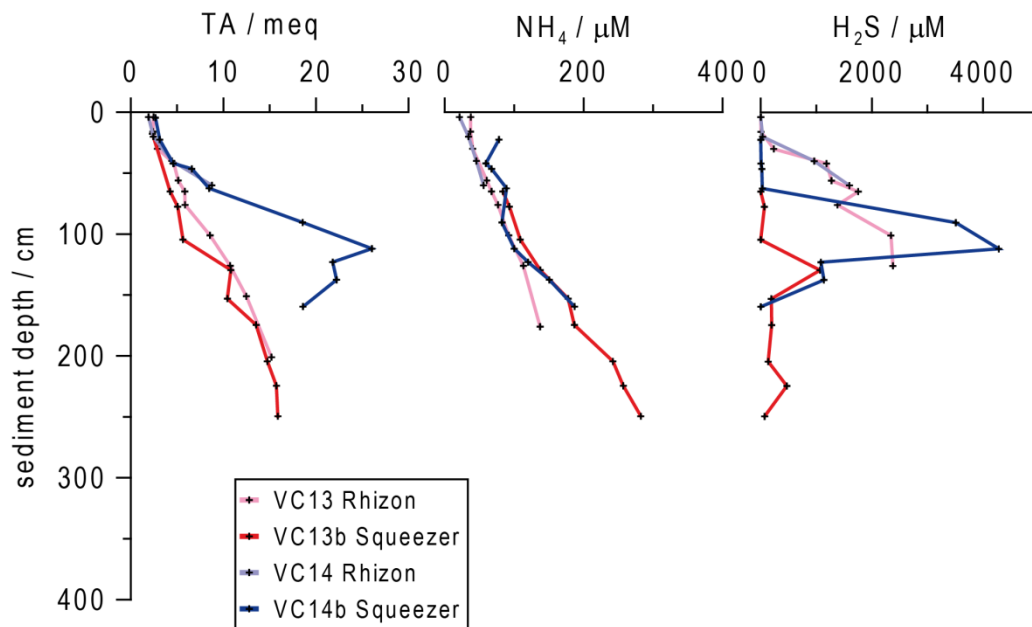


Fig. 4.2.6: TA, NH₄ and TH₂S concentration profiles from pore waters of the Tommeliten site obtained by Rhizons and by squeezing sediments in cores VC13 and VC14.

References

- Dickson, A.G., 1993. pH buffers for sea water media based on the total hydrogen ion concentration scale. *Deep-Sea Research I* 40, 107-118.
- Grasshoff, K., Ehrhardt, M. and Kremling, K., 1999. *Methods of Seawater Analysis*. Wiley-VCH, Weinheim, 600 pp.
- Niemann, H., Elvert, M., Hovland, M., Orcutt, B., Judd, A., Suck, I., Gutt, J., Joye, S., Damm, E., Finster, K., Boetius, A., 2005. Methane emission and consumption at a North Sea gas seep (Tommeliten area). *Biogeosciences* 2, 335-351.

5. Seafloor observations and *in situ* sampling operations

(P. Linke, F. Abegg, S. Sommer, D. McGinnis, C. Hinz, H. Huusmann, A. Meier, M. Pieper, I. Suck, S. Cherednichenko, R. Schwarz)

5.1. ROV 6000 operations

The ROV (remotely operated vehicle) KIEL 6000 is a 6000 m rated deep diving platform manufactured by Schilling Robotics LLC. As an electric work class ROV from the type QUEST, this is build no. seven, and is based at the Leibniz Institute for Marine Sciences IFM-GEOMAR in Kiel, Germany. The UHD vehicle is equipped with 7 brushless thrusters, with 210 kgf peak thrust each. Power is supplied through the umbilical with up to 4160VAS/460 Hz. The data transfer between the vehicle and the topside control van is managed by the digital telemetry system (DTS™) which consists of two surface and four sub-sea nodes, each representing a 16-port module. Each port may be individually configured for serial, video or ethernet purposes. The vehicle was linked to the topside control unit via a 22 mm diameter aramid enforced tether. No tether management system (TMS) is used. To unlink the vehicle from ship's movements, floats are attached to the umbilical. For more details, please visit www.ifm-geomar/kiel6000.

The decision to use a 6000 m rated vehicle in the shallow North Sea was based on the thrust power and manipulating capabilities of the vehicle. This was necessary to withstand the high current speed of more than one knot and allowed diving operations independent from the tidal cycle. Tools standardly installed on the vehicle include a HDTV camera, two high-resolution colour zoom cameras and one digital still camera as well as four black and white observation cameras. Besides the video capabilities, the two manipulator arms are the major tools used on this platform. One is a seven-function position controlled manipulator of the type ORION and the other one is a five-function rate controlled manipulator, type RIGMASTER. Further tools include a DIGIQUARTZ depth sensor, a SIMRAD sonar system, a PNI TCM2-50 compass, a motion reference unit (MRU) containing a gyro compass, and an RDI doppler velocity log (DVL). For navigation a shallow water positioning ORE Trackpoint system was used – the transducer was attached to the drop keel of the vessel (Fig. 2.2.2.1). Additionally, a SONARDYNE HOMER™ system is available as a tool for finding devices equipped with HOMER beacons (Figs. 5.1.5 C, 5.1.7).



Fig. 5.1.1: Views of ROV Kiel 6000; left: front with cameras, manipulators and tool sled for storage of the push corers; right: starboard side with KIPS water sampler, CONTROS sensor package and FSI CTD.



Fig. 5.1.2: View of the aft deck of Celtic Explorer, with winch in front and ROV KIEL 6000 in the background..



Fig. 5.1.3: View of KIEL 6000 front, ECS and BC (background) on porch.

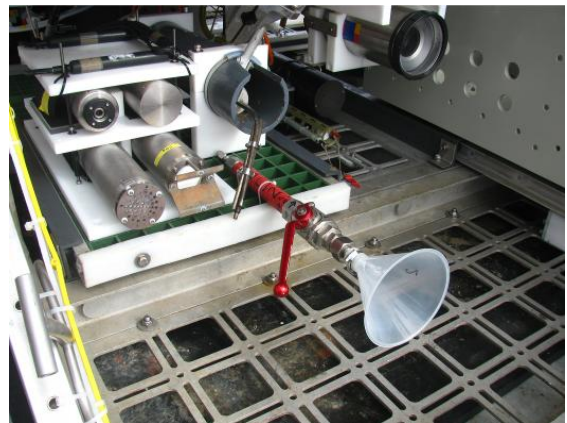


Fig. 5.1.4: View of starboard drawer with CONTROS probes, gas sampler, KIPS nozzle and HDTV camera.

The tool sled in the lower-most part of the vehicle is especially dedicated to take up the scientific payload. A SBE 49 FastCAT CTD is permanently mounted. Located on portside front of the tool sled is a sample tray which hydraulically operated. On starboard front there is a drawer likewise hydraulically driven, which can take up probes continuously mounted or used by the manipulator. Port aft and starboard aft are reserved for additional scientific payload which differ from mission to mission.

During the CE 0913 cruise, the starboard aft side was occupied by the KIPS fluid sampling system with its sampling nozzle and temperature probe on the starboard drawer (Fig. 5.1.1). Additional tools used for scientific samples during this cruise were Push Cores, Niskin Bottles, a Gas Sampler, a self-made bubble measure tool and a pH/ORP sensor (SBE 27) connected to a CTD (FSI). PAH, methane and CO₂ probes, manufactured by CONTROS, were occasionally mounted (Figs. 5.1.1, 5.1.4). Besides these built-in probes, the ROV was used for deployment and recovery of various other tools: a Pore Water Sampler (PWS, Fig. 5.1.5), two Benthic Chambers (BC, Fig.

5.1.6) and two Eddy Correlation Systems (ECS, Fig. 5.1.7). Many of these ROV tools were deployed for the first time and due to the perfect weather conditions, we were able to conduct 14 scientific dives, 8 at the Salt Dome Juist area and 6 at the Tommeliten Seep area, summing up to more than 49 hours of bottom time (Table 5.1.1). The PWS was used for the first time at the Salt Dome Juist area for high-resolution extraction of pore water within a depth range of up to 40 cm below the sediment surface. The advantage of this method is to separate pore water and sediment before sample retrieval, which prevents artifacts by decompression and temperature changes. The device basically consists of a lance with small filtering elements (Rhizones) and a syringe carrier. After penetration of the lance into the seafloor the Rhizones can be moved laterally out into the sediment. Pore water will be ingested by applying a vacuum through pressure-resistant syringes (Fig. 5.1.5). Results from the deployment are shown in Fig. 4.2.3.

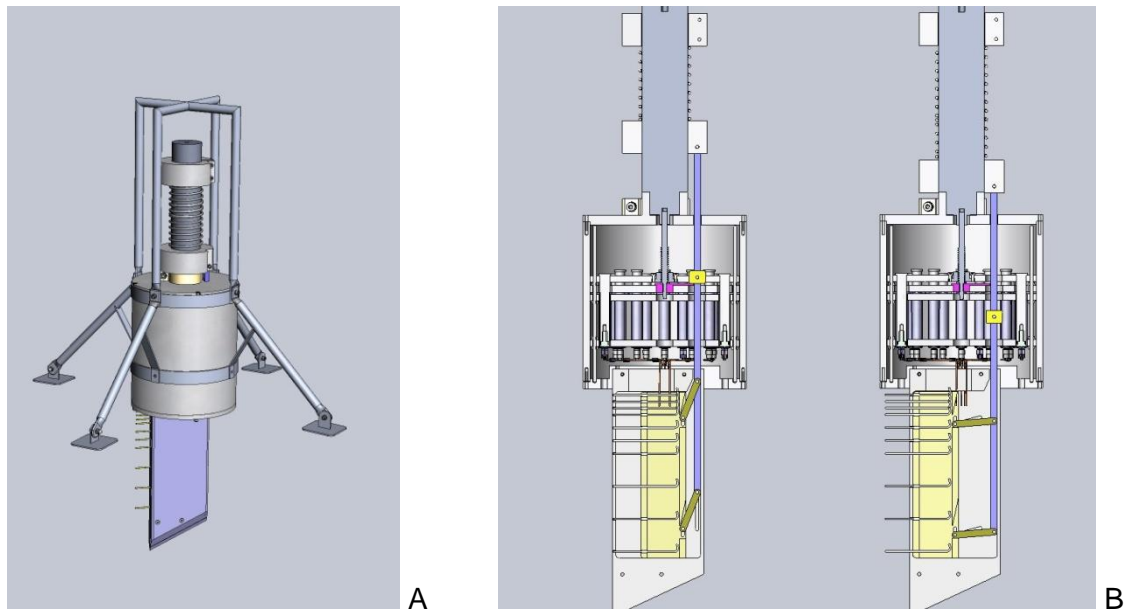


Fig. 5.1.5: Schematic drawings of the Pore Water Sampler (PWS). **A:** Overall setup with frame, **B:** Cross-section showing Rhizon lance and syringe carrier in penetration and operation modes, **C:** PWS with HOMER beacon deployed by ROV in the sandy sediments of the Southern German North Sea during CE0913.



The Benthic Chambers (BC) are designed to measure benthic fluxes of dissolved chemical species over time at the sediment-water interface. They contain a cylindrical chamber (20 cm diameter)

which is pushed by the ROV into the sediment (Fig. 5.1.6). The displaced water in the chamber is pushed through a non-return valve and any resuspended matter is extruded by flushing the overlying water with a small submersible pump (SBE 5) and a small stirrer. After starting the incubation of the enclosed sediment, a time series of 8 water samples is obtained by motor-driven glass syringes from the overlying water. Furthermore, each BC carries 2 oxygen optodes, one inside and one outside of the chamber (Fig. 5.1.7). After incubation a motor-driven shutter closes the bottom of the chamber for retrieval of the incubated sediment. Each chamber is self-contained with its own power supply and control unit for the timing of the sampling cycle and storage of the obtained data. The two BCs were deployed for the first time during cruise CE0913 in a seep (material mat) and off-seep location in the Tommeliten working area (Fig. 5.1.7).



Fig. 5.1.6: View on the ROV console with the computer screens showing the different camera views, sonar and navigation data in the control van during deployment of the BC.

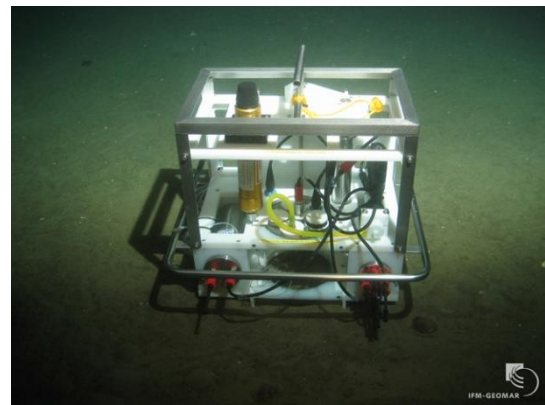


Fig. 5.1.7: Benthic Chamber (BC) equipped with syringe water sampler, oxygen optodes, stirrer, power and control unit, and HOMER beacon deployed at Tommeliten.

The experiment in the off-seep location involved the deployment of the Profiler Lander (Fig. 5.1.8), the 2 Eddy Correlation Systems (Fig. 5.1.9) and the second benthic chamber in a row, each 10 m apart and perpendicular to the tidally changing currents. Both chambers worked correctly; however, the closing device responsible for retrieval of surface sediments did not work properly due the sandy type of sediments. Accordingly, some adjustments are required, if it should again be applied to this type of sediments.



Fig. 5.1.8: View on the Profiler Lander deployed at an off-seep site at Tommeliten (for detailed description see chapter 5.2).

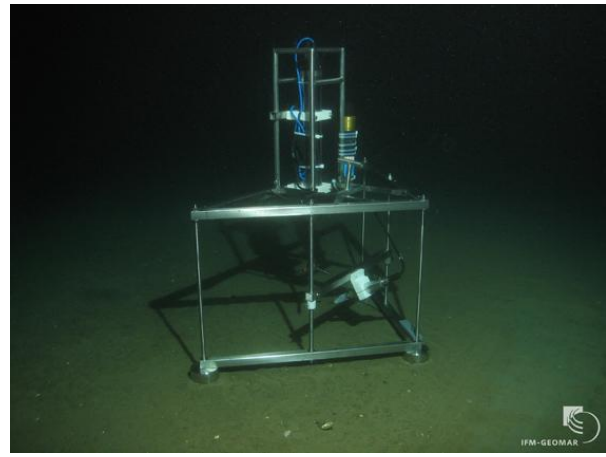


Fig. 5.1.9: One of two Eddy Correlation Systems (ECS) deployed by ROV at Tommeliten (for detailed description see chapter 5.3).

Tab. 5.1.1: Summary of dives during the CE 0913 Expedition.

Station No. CE 0913-	Dive No.	Date	Time Start (UTC)	At Bottom (UTC)	Off Bottom (UTC)	Time End (surface) (UTC)	ROV Bottom Time	% Bottom Time	Location
	64	29.07.2009							Harbour Test
09-ROV 1	65	31.07.2009	12:11	12:25	16:21	16:32	03:56	90.4	Salt Dome Juist
16-ROV 2	66	01.08.2009	12:10	12:20	15:33	17:30	03:13	60.3	Salt Dome Juist
23-ROV 3	67	02.08.2009	11:15	11:30	16:40	16:55	05:10	91.2	Salt Dome Juist
30-ROV 4	68	03.08.2009	10:00	10:00	13:49	14:00	03:49	95.4	Salt Dome Juist
36-ROV 5	69	05.08.2009	11:00	11:15	16:50	17:05	05:35	91.8	Salt Dome Juist
40-ROV 6	70	06.08.2009	08:18	08:30	13:28	13:49	04:58	90.0	Salt Dome Juist
41-ROV 7	71	06.08.2009	15:30	15:40	18:20	18:30	02:40	88.9	Salt Dome Juist
44-ROV 8	72	07.08.2009	07:48	08:00	11:20	11:31	03:20	89.7	Salt Dome Juist
49-ROV 9	73	08.08.2009	12:08	12:21	18:25	18:41	06:04	92.6	Tommeliten
57-ROV 10	74	09.08.2009	15:00	15:10	17:00	17:12	01:50	83.3	Tommeliten
58-ROV 11	75	09.08.2009	19:16	19:30	21:49	22:00	02:19	84.8	Tommeliten
63-ROV 12	76	10.08.2009	11:29	11:40	17:02	17:22	05:22	91.2	Tommeliten
69-ROV 13	77	11.08.2009	07:29	07:43	08:37	08:47	00:54	69.2	Tommeliten
70-ROV 14	78	11.08.2009	09:14	09:31	09:55	10:03	00:24	49.0	Tommeliten
Total: 14 scientific dives							49:34	86.37	

5.2. Lander deployments

5.2.1. Methodology

During CE0913 two different lander systems were used to study the physical and biogeochemical properties of the benthic boundary layer: the profiler lander (PRF-Lander) and the POZ-Lander. The PRF-Lander belongs to the series of the GEOMAR Lander System (GML), which is based on a tripod-shaped universal platform, capable of supporting different scientific payloads (Pfannkuche & Linke, 2003). The profiler lander was equipped with two acoustic current profilers (uplooking 300KHz ADCP, downlooking 2 MHz Nortek), a storage CTD (RBR) with 2 optodes, a digital still camera system (Ocean Imaging Systems) and as the major component a profiler, which moves microelectrodes in x, y and z direction at the seafloor to resolve high-resolution oxygen profiles in the sediment (Fig. 5.2.1.1).

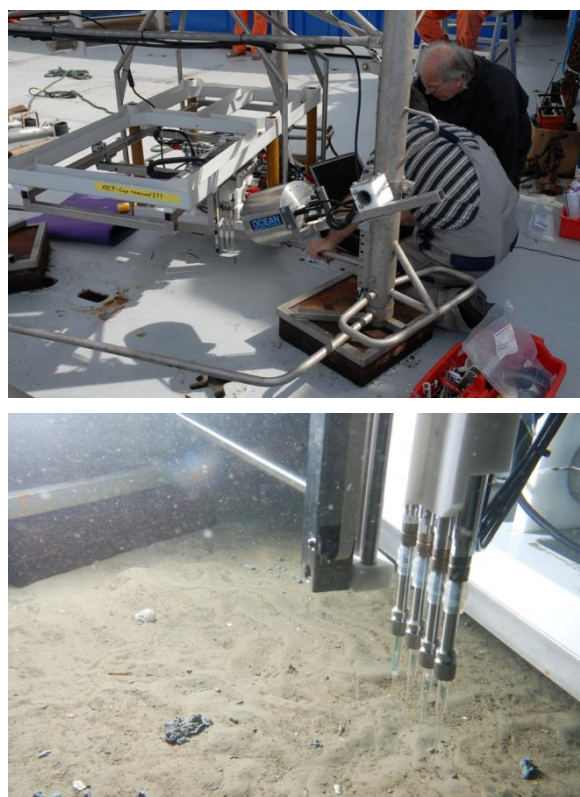


Fig. 5.2.1.1: Video-guided deployment of the Profiler Lander (PRF-L) is equipped with the microprofiler, a digital still camera system and 2 acoustic current profilers.

Top: Programming of the microprofiler and the optodes.
Bottom: Picture of the microelectrodes.

The profiling unit consists of a lower and upper glass fibre frame, which are connected by four glass fibre poles. The upper frame extends about 50 cm towards the front defining an area across which sensors can be moved in mm increments along the x and the y axis. Along the vertical z axis, the sensors can be moved at freely selectable increments. The rear part of the profiler houses four battery packs, the data logging- and the control unit steering the movements of the micro sensors. For the deployment the profiling unit was mounted into a lander.

Commercially available oxygen and pH micro sensors (tip diameters: ~ 100 μm . Unisense, DK) were used to measure *in situ* pH and oxygen concentration profiles. The sensors (A) were connected to miniaturized amplifier units (C) which were jointly developed with Unisense DK. The connecting steel tube (B) was filled with silicone oil, pressure compensation of the sensor was allowed by the transparent flexible tubing shown in Figure 5.2.1.2.

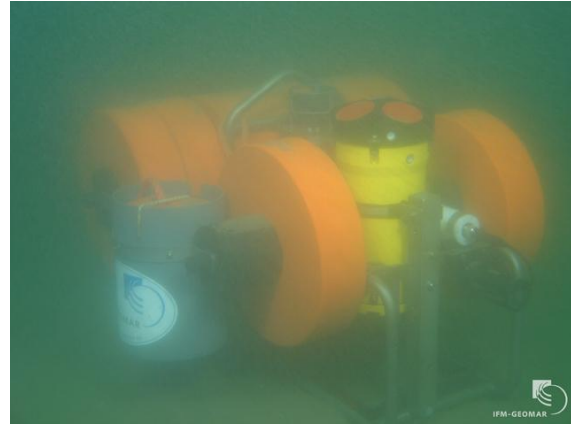


Fig. 5.2.1.2: upper panel, *in situ* micro-sensors connected to the data logging unit; lower panel, detail of *in situ* O₂ micro-sensor (A) connected to the amplifier (C) via an oil filled steel tube (B).

Recently, a novel type of lander (POZ-Lander) was developed following the revised design of the Ocean Bottom Seismometers (OBS). Aim of the redesign was to decrease the size of the instrument in settings with high bottom water current velocities. Additionally, the design put all sensors close to the sediment at ~50 cm above the seafloor. The floatation is provided by modular syntactic foam cylinders. The lander carries an ADCP and a small storage CTD with a Digiquartz pressure sensor. The anchor weight underneath the lander keeps the system in a horizontal plane during free-fall descent and deployment at the sea floor (Fig. 5.2.1.3). Upon recovery the lander rises to the sea surface with the floatation first while the heavy ADCP and CTD are oriented vertical below and are protected during recovery.



Fig. 5.2.1.3: Left: Video-guided deployment of the POZ-Lander with the launcher on top. The side view on the lander shows the ADCP (yellow) and the recovery items (flash, radio beacon and flag) in horizontal position.



Right: The low profile lander deployed in the high bottom water current regime of the Southern German North Sea. Visible are the casings of the ADCP (yellow), the pressure sensor (white) and the recovery line (grey).

Both types of landers can be either deployed in free-fall or targeted mode. The launcher enables accurate positioning for soft deployments and rapid disconnection from the lander by electric release. Bi-directional video and data telemetry provide online video transmission, power supply and surface control of various relay functions. During cruise CE0913 no telemetry was used due to the lack of a coaxial cable and the shallow water depth. A cable was attached to the launching rope connecting the cameras and lights of launcher directly to a small deck unit and the video monitors in the dry lab. The electric release to disconnect the lander from the launcher was triggered from this deck unit.

5.2.2. Preliminary results

The data measured by the POZ lander system is mainly presented in chapter 2 (pressure, current velocity, current direction). Whereas ADCP data of the profiler lander (PRF-L) are presented in chapter 2.2.4., preliminary O_2 microprofile data are shown in figure 5.2.2.1. A total of 129 O_2 and 43 pH microprofiles were measured during this deployment. This allows the reconstruction of spatial as well as temporal variability of oxygen. Although fluctuations of bottom water oxygen levels are very low the temporal variability of the diffusive oxygen uptake (DOU) of the sediments is very high, figure 5.2.2.1. Beside organic carbon availability in the sediment, this might be related to the hydrodynamic regime of the bottom water and the thickness of the diffusive benthic boundary layer. Moreover, O_2 represents a major control parameter for early diagenetic processes and the redox-balance of marine sediments, e.g. aerobic bacterial methane oxidation, affecting Mn- and Fe-turnover, or releasing redox-sensitive compounds such as phosphorus, ammonium or sulfide from sediments. Summarized, the consequences of the monitored O_2 fluctuations for the overall geochemical turnover of these sediments are hardly understood and will be subject of further investigations.

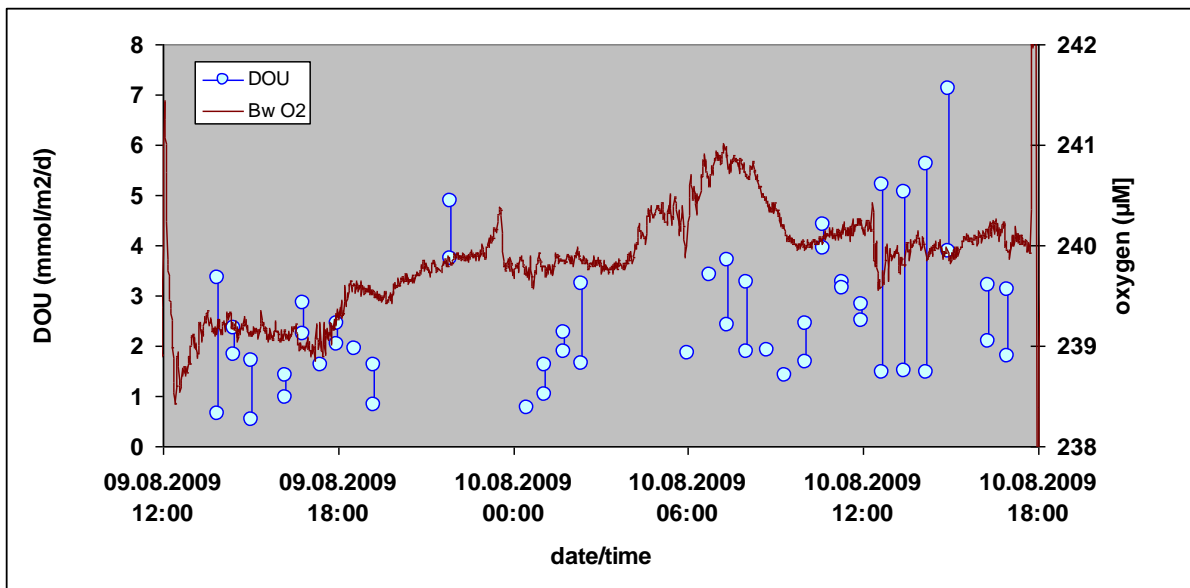


Fig. 5.2.2.1: Temporal variability of diffusive oxygen uptake (DOU) calculated from O₂ microprofiles in comparison to fluctuations of bottom water O₂ levels.

References

Pfannkuche O, Linke P (2003) GEOMAR landers as long-term deep-sea observatories. *Sea Technol.* 44 (9): 50-55.

5.3. Eddy correlation measurements

5.3.1. Introduction and methodology

The Eddy Correlation technique is a well established technique to measure constituent fluxes in the atmosphere (Lee *et al.* 2004). Its use to measure fluxes at the sediment-water interface in the BBL of lakes and oceans, however, is still a relatively new. So far Berg *et al.* (2003, 2007, 2008, 2009) and Kuwae *et al.* (2006) used the EC technique to determine DO fluxes in coastal marine systems, over various marine sediments. McGinnis *et al.* (2008) and Brand *et al.* (2008) studied DO flux dynamics in a riverine reservoir and a freshwater seiche-driven lake, respectively.

Technique description:

The general idea of the eddy correlation is that by correlating the vertical velocity fluctuations w' , with the fluctuations of the constituents (DO, T) C' , the instantaneous exchange flux $w'C'(t)$ can be calculated in a straight-forward manner. Its average $\overline{w'C'}$ yields the net flux directed towards (consumption) or away from (production) the sediment.

Since Berg *et al.* (2003) first tested the EC technique, by combining oxygen micro-sensor and acoustic velocimeter (ADV) measurements, the experience and confidence have increased with respect to instrumentation, deployment and data analysis. An extensive method paper is now being published by Lorrai *et al.* (*subm.*)

Main advantages:

The outstanding advantage of the EC technique over i.e. benthic chambers and *in situ* microprofilers, is the potential to record undisturbed fluxes with high temporal resolution. The EC techniques will not disrupt the hydrodynamics of the system and is less affected by localized bioturbation.

The IFM-GEOMAR system:

Using the IFM-GEOMAR facilities and technical skills, we have developed the next generation of EC for oxygen measurements. Two complete System was developed based on knowledge and experience gained from Eawag system (McGinnis *et al.*, 2008), together with experience from an internationally recognized experts (P.Berg, R.Glud, V.Meyer).

Our system consists of a Nortek ADV coupled with a Clark-type oxygen microsensors (Fig. 5.3.1.1 left). The sensor amplifiers as well as the ROV deployable (Fig 5.3.1.1 right) light inox steel EC frame were completely designed at the IFM-GEOMAR.



Fig. 5.3.1.1: Eddy Correlation (EC) Technique. Our EC system on the North Sea bottom (left) and on the ROV Kiel 6000 during the pre-deployment.

State of research:

Our system was successfully tested in shallow freshwaters. This cruise, however, represented our first saltwater deployment.

5.3.2. Preliminary results

We deployed both our systems at the Tommeliten site, in relative proximity to the Profiler-Lander (see section 5.2). As our systems were designed to collect undisturbed data (no frame interference) we first had to rule out the measurements that occurred while the tidal driven current was reaching the EC system from unsuitable directions. This is generally done by analyzing the particles track. The particle track describes the path of single hypothetical particle moving along with the current without rising or falling into the sediment. Figure 5.3.2.1 shows the results of our particle track analysis.

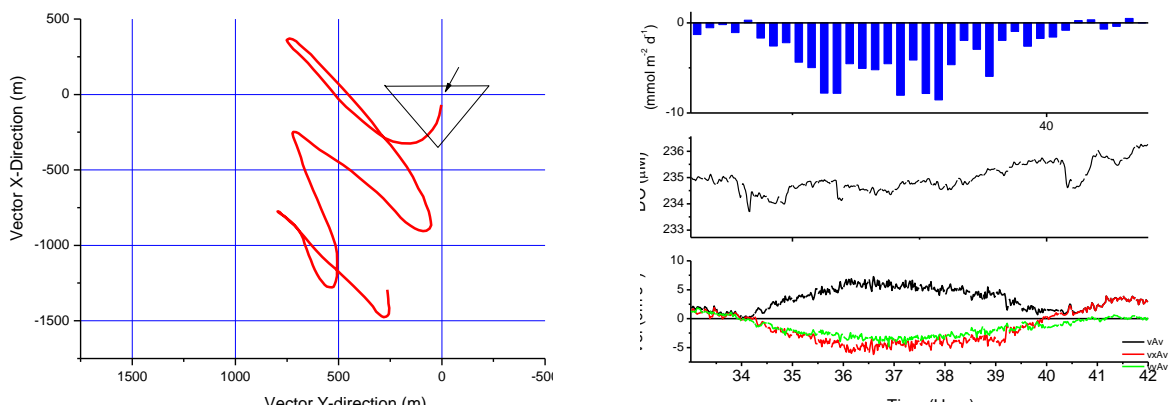


Fig. 5.3.2.1 : Eddy Correlation Technique. Graphical visualization of the path, with respect to the EC device, of a single water parcel moved around by the current over the whole deployment time (left); preliminary results from one of our system (right), velocity components (bottom), DO concentration (center) and the calculated DO fluxes into the sediment (top).

Figure 5.3.2.1 shows the EC techniques results over half of a tidal cycle in which the frame was found not to interfere with the measurements current. It shows time series of the oxygen

concentration measured by the microsensor, all velocity components (x,y,z) from the ADV and the resulting calculated oxygen fluxes into the sediment.

It can be clearly seen how strong the bottom current changes are enhancing or limiting the oxygen fluxes.

Future perspective:

We plan to extend the EC system for testing of new DO sensors e.g. galvanic DO, optodes and any other promising constituents sensors with reasonable response times (<2 s).

References

- Lee, X., W. J. Massman and B. E. Law. (2004). Handbook of micrometeorology: A guide for surface flux measurement and analysis. Kluwer Academic, 250 pp.
- Berg, P., H. Røy, F. Janssen, V. Meyer, B. B. Jørgensen, M. Hüttl, and D. de Beer (2003). Oxygen uptake by aquatic sediments measured with a novel non-invasive eddy-correlation technique. *Marine Ecology Progress Series*, 261: 75-83.
- Berg, P., H. Røy, and P. L. Wiberg (2007). Eddy correlation flux measurements: The sediment surface area that contributes to the flux. *Limnology and Oceanography*, 52: 1672-1684.
- Berg, P. and M. Hüttl (2008). Monitoring the seafloor using the noninvasive eddy correlation technique: Integrated benthic exchange dynamics. *Oceanography*, 21: 164-167.
- Berg, P., R. N. Glud, A. Hume, H. Stahl, K. Oguri, V. Meyer and H. Kitazato (2009). Eddy correlation measurements of oxygen uptake in deep ocean sediments. *Limnology and Oceanography-Methods*, 7: 576-584.
- Brand, A., D. F. McGinnis, B. Wehrli, and A. Wüest (2008) Intermittent oxygen flux from the interior into the bottom boundary of lakes as observed by eddy correlation. *Limnology and Oceanography*, 53: 1997-2006.
- Kuwae, T., K. Kamio, T. Inoue, E. Miyoshi, and Y. Uchiyama (2006). Oxygen exchange flux between sediment and water in an intertidal sandflat, measured *in situ* by the eddy-correlation method. *Marine Ecology Progress Series*, 307: 59-68.
- Lorrai, C., D. F. McGinnis, P. Berg, A. Brand and A. Wüest. Application of Oxygen Eddy Correlation in Aquatic Systems. *Journal of Atmospheric and Oceanic Technology*. *Subm.*
- McGinnis, D. F., P. Berg, A. Brand, C. Lorrai, T. J. Edmonds, and A. Wüest (2008). Measurements of eddy correlation oxygen fluxes in shallow freshwaters: Towards routine applications and analysis. *Geophysical Research Letters*, 35: L04403.

6. Geophysical data acquisition

(S. Themann, K. Schwarzer, C. dos Santos Ferreira)

6.1. Methods

For sub-bottom profiling and seafloor mapping, three different systems have been used during the cruise:

- A hull mounted shallow-water multibeam echosounder EM1002 by KONGSBERG MARITIME, operating with 111 beams at 95 kHz.
- A single-beam echosounder EA600 by KONGSBERG MARITIME, operating with two transducers at 38 and 200kHz.
- A hull mounted Sub-bottom profiler SES Probe 5000 with a 4x4 array by GeoPulse, operating at 10 kHz with 5 kW output.

The multi-beam, as well as the single-beam echosounder were operating only occasionally during the first leg but 24 hours a day during the second leg. The sub-bottom profiler was only used at Tommeliten. Survey lines for the Sub-bottom profiler for Tommeliten are given in Fig. 6.1.1. An overview of the bathymetry in this area is given in Fig. 6.1.2.

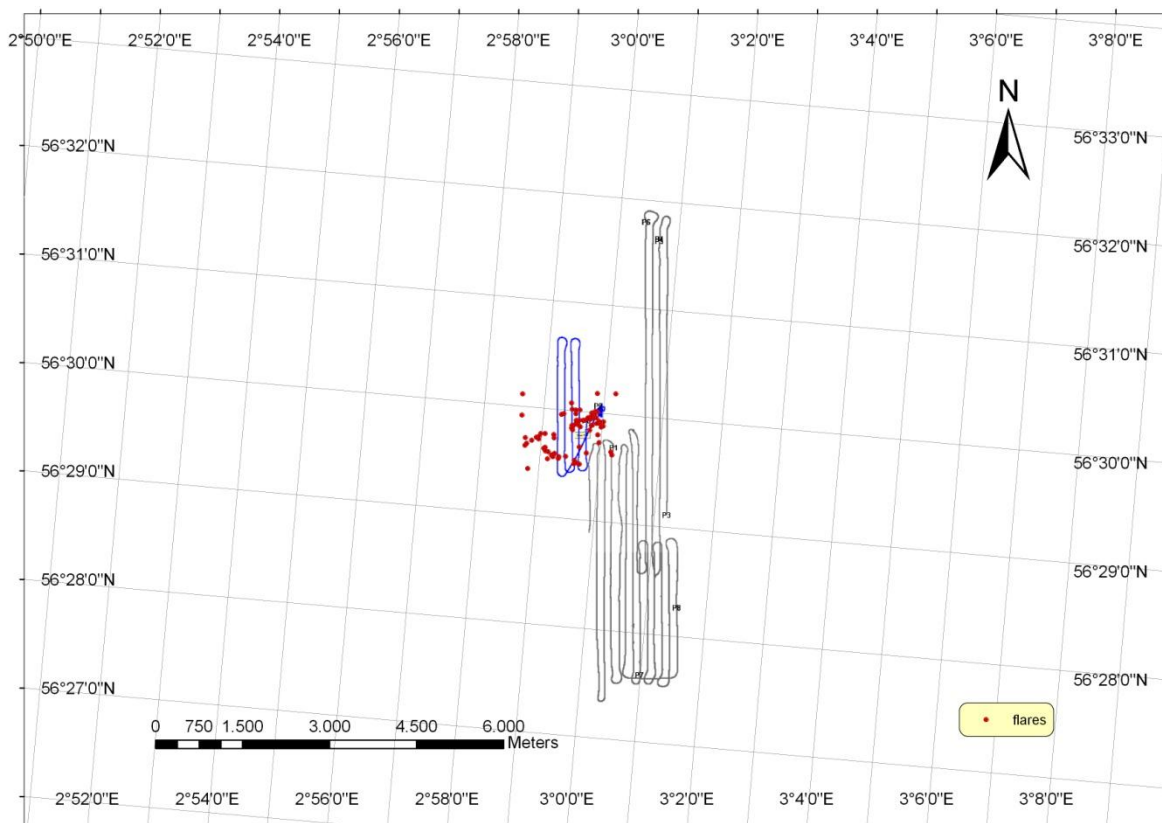


Fig. 6.1.1: Sub-bottom profiler survey lines at Tommeliten.

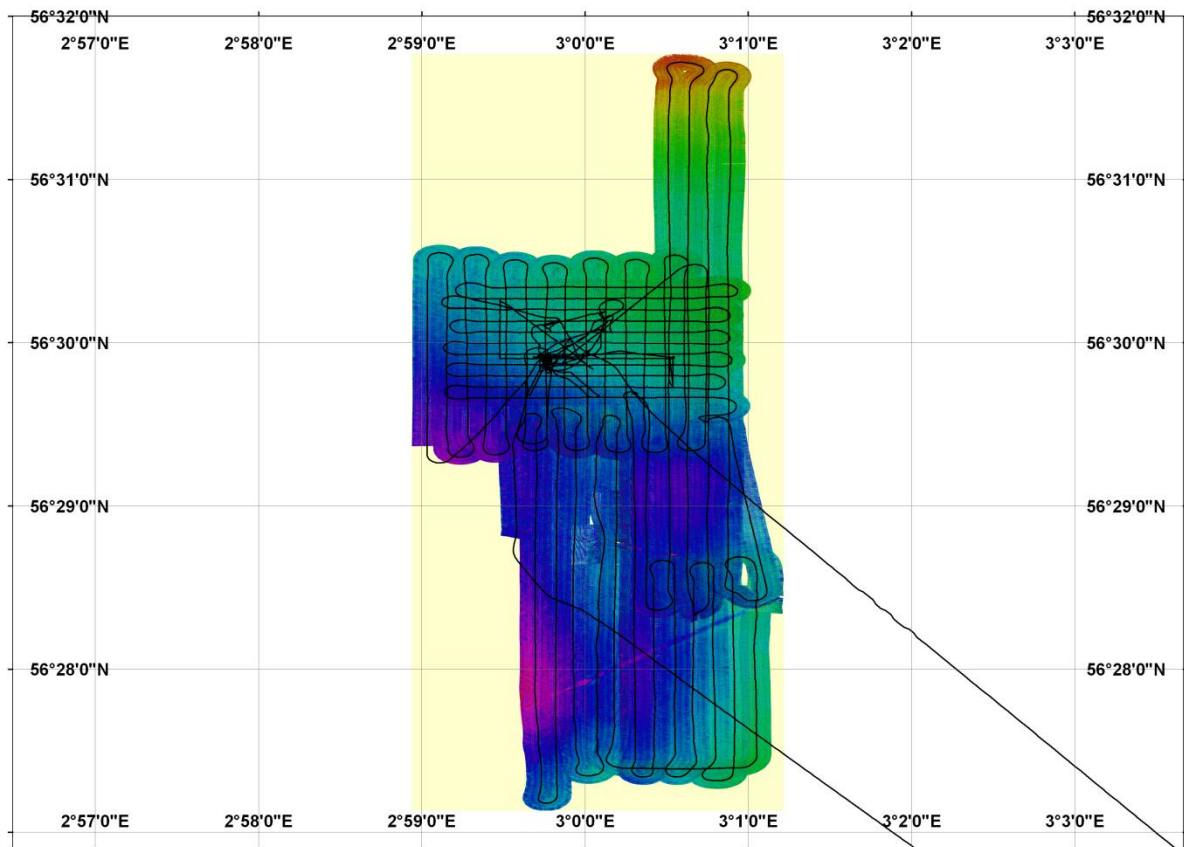


Fig. 6.1.2. Bathymetric map from Tommeliten. The difference between the shallow area (red colour) and the deep area (purple colour) is around 3 meters.

6.2. Preliminary results

Multibeam

To aid Lander deployments and ROV dives, bathymetric maps were already processed during the cruise, using data from the EM1002 multibeam. A first correlation of the bathymetry and backscattering reveal small depressions of around 40 cm compared to the surrounding area that match areas of high backscattering (Fig. 6.2.1, Fig. 6.2.2 and Fig. 6.2.3). These features can be interpreted as “carbonate features”, which have already been found on previous cruises in this area (e.g. Niemann et al., 2005).

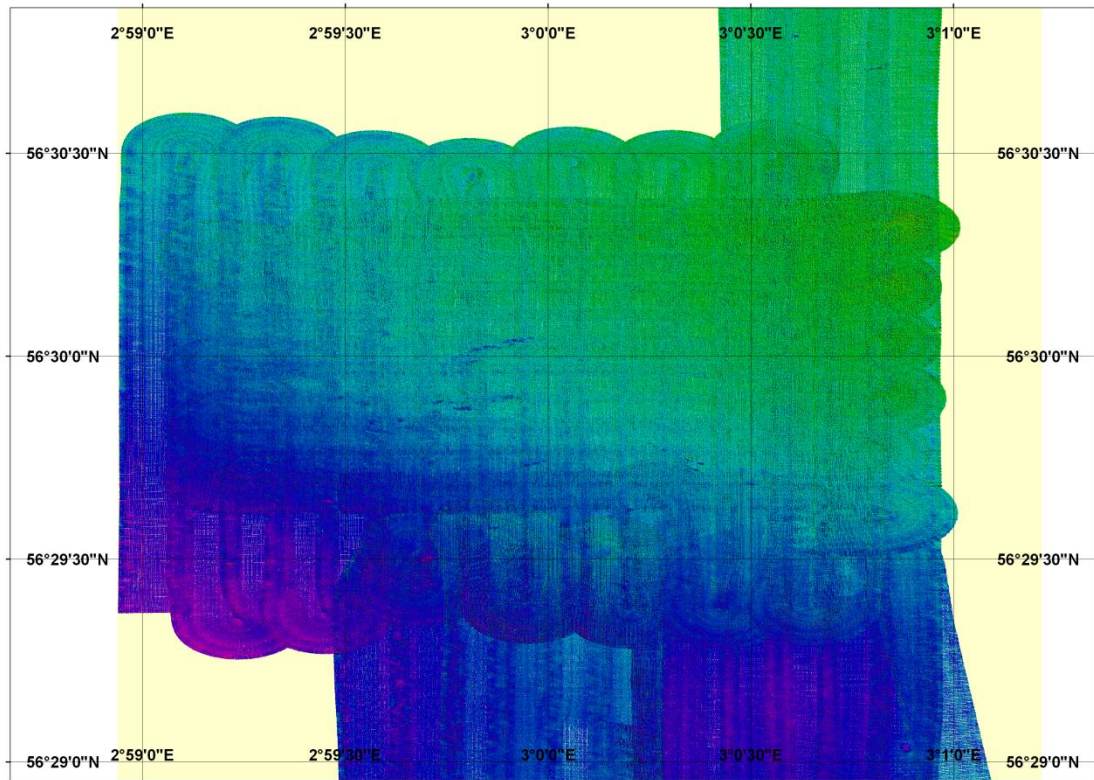


Fig. 6.2.1: Bathymetry map of Tommeliten. The blue spots represent small depressions, around 40 cm compared to the surrounding area.

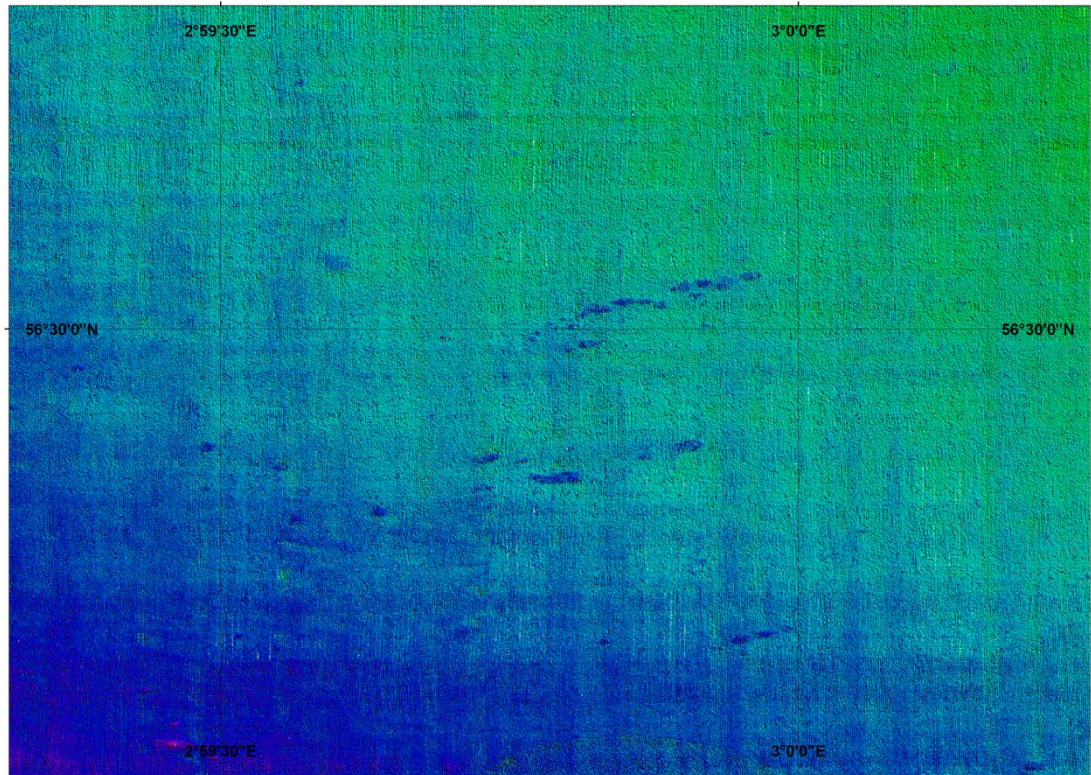


Fig. 6.2.2.: Detailed bathymetric map of the depressions at Tommeliten.

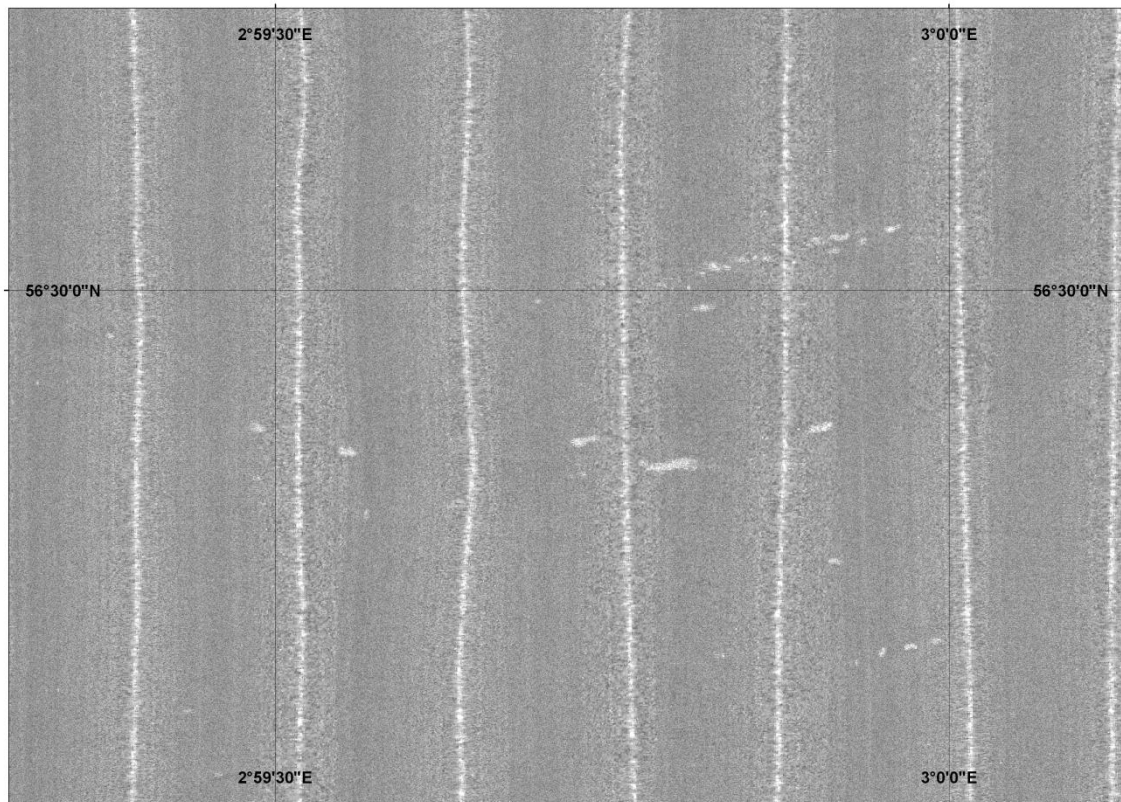


Fig. 6.2.3. Detailed map of backscatter at Tommeliten. The white dots represents a strong backscattering.

Sub-bottom profiler

The post processing and interpretation of the sub-bottom profiles surveyed with the SES Probe 5000 system is still ongoing. First results and interpretations are available for Tommeliten, showing a close correlation of flare activities in the water column with the level of the “gas-front” (i.e. the blanking of the acoustic signal caused by gas bubbles) in the sediment (Fig. 6.2.4).

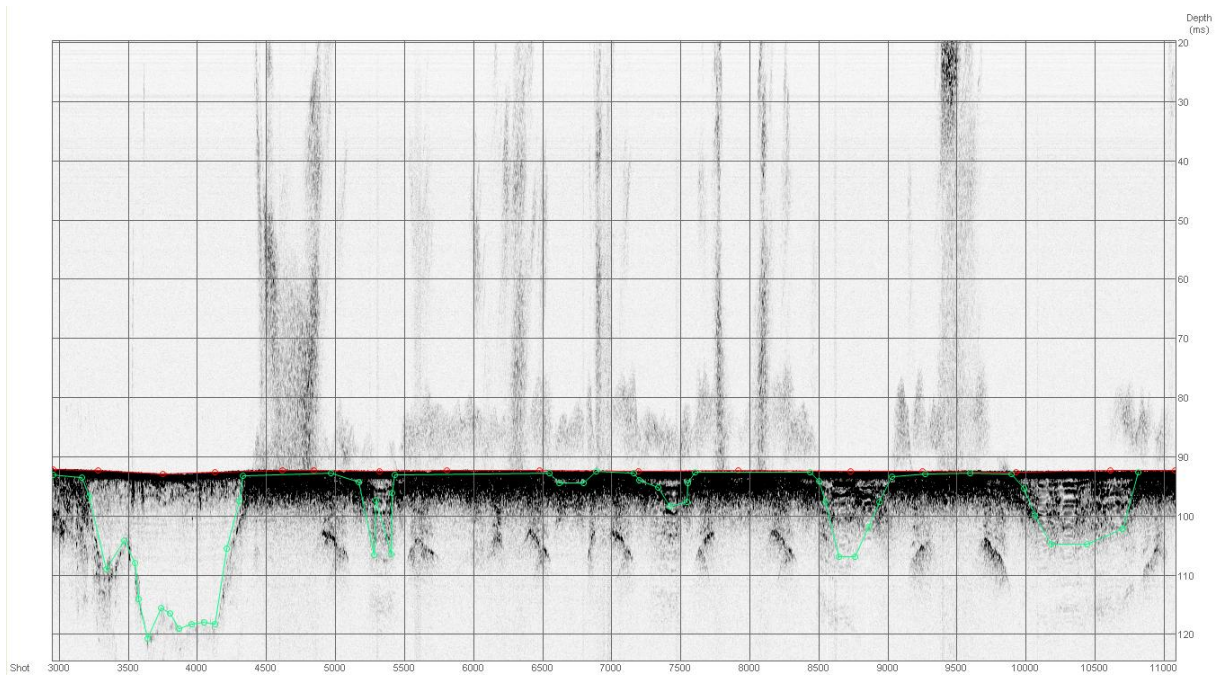
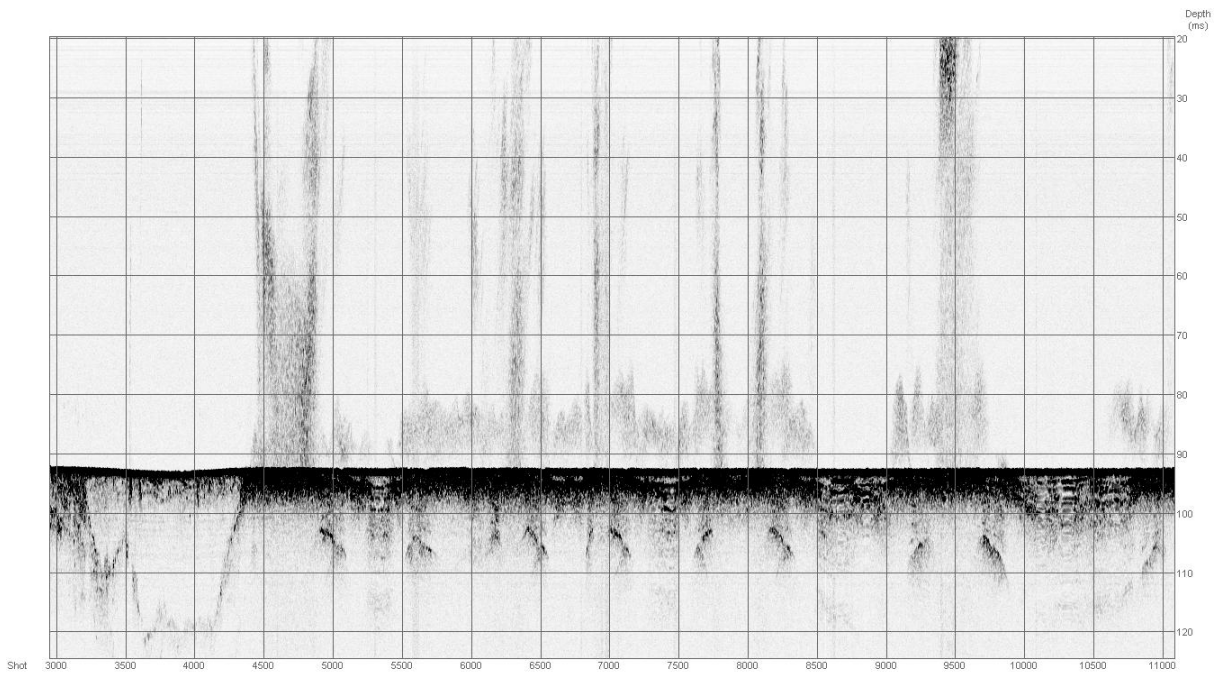


Fig. 6.2.4: Preliminary interpretation of a sub-bottom profile in the area of Tommeliten. The level of the gas front (green line) is clearly correlated to flare activities in the water column. The origin of flares is located in areas, where the gas front reaches the seafloor.

Single-beam echosounder

The single-beam echosounder was used for detecting and locating flares in the water column, already during the cruise. Further processing and interpretation of the single-beam echosounder profiles is still ongoing. Figure 6.2.5 shows an example of strong flare activities at Tommeliten.

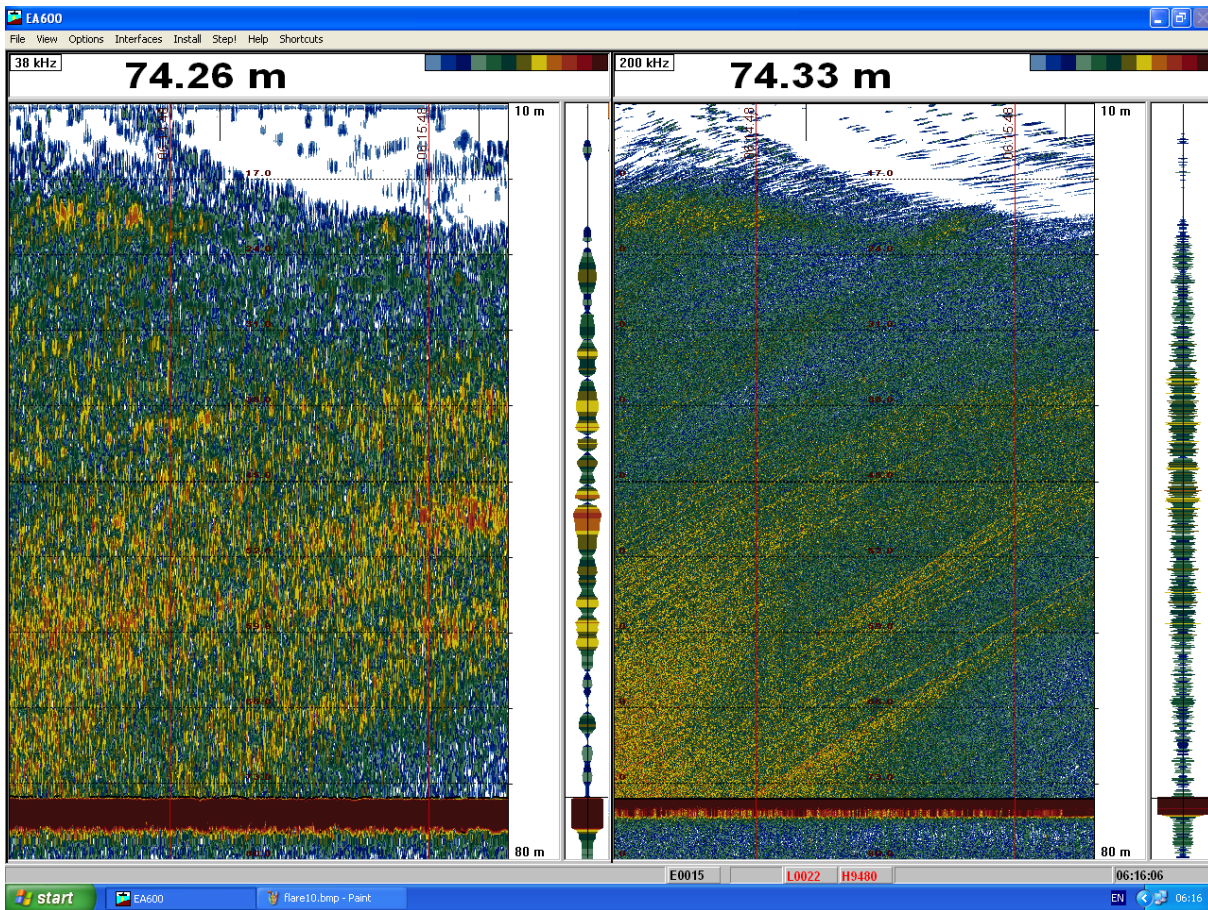


Fig. 6.2.5: Gas flare at Tommeliten covering the whole water column.

Reference

Niemann, H., Elvert, M., Hovland, M., Orcutt, B., Judd, A., Suck, I., Gutt, J., Joye, S., Damm, E., Finster, K., and Boetius, A. (2005) Methane emission and consumption at a North Sea gas seep (Tommeliten area). *Biogeosciences* 2, 335-351.

7. Sedimentology

(K. Schwarzer, M. Schmidt, S. Themann, A. Doennebrink, R. Ludwig, R. Schwarz)

7.1. Methodology

For sediment stratigraphy and geochemical analysis in total 14 sediment cores have been taken during the cruise with two comparable vibro corer systems (Geo-Corer 6000 from BSH Hamburg and from Geological Survey of Ireland, respectively). The Geo-Corer 6000 is a high frequency, electrically driven, vibrocorer system capable of fast penetration of all common seabed sediments, ranging from compact sands to stiff clays. Both configurations (BSH and GSI) used on board of the Celtic Explorer take cores in PVC liners of 6 m length and 106 mm inner diameter.



Fig. 7.1.1: Vibrocorer GEO 6000 operated from RV Celtic Explorer during CE0913.

7.2. First results

A first sedimentological description of the sediment cores has already been performed during the cruise. Preliminary results are given in Table 7.2.1. Pictures of the sediment cores are given in the Appendix. Detailed analyses for particle size distributions and C-14 age will be performed soon.

Table 7.2.1: Sedimentological description of the sediment cores.

Station ID CE0913	VC ID	Area	Depth TGS, cm	Color	Lithology	Description
2	1	Borkum Reef				
			-26		Middle sand	1-6 cm rounded pebbles, shell fragments
			-31	Moderate yellowish brown	Fine sand	
			-580	Medium light gray	Fine sand	33-36 mussel fragments; 31-580 mm-sized black dots (pyrite?); 527-531 silty clay lens; 31-580 few mm-sized silty clay lenses
7	2	Salt Dome Juist				
			-20			missing
			-80	Light olive gray	Fine sand	Reworked sediment (Bioturbation)
			-204	Olive gray	Silty sand	Mixed with mm-sized slightly rounded pebbles; mixed with black brownish mm-sized peat(?) fragments; clayey sand lenses at base
			-354	Light olive gray	Fine sand	Mixed with peat(?) particles; 230-240 consolidated peat clast
			-466	Olive gray	Fine sand	Mixed with peat(?) particles
			-520	Light olive gray	Fine sand	470 dark olive gray clay lens; mixed with mm-sized slightly rounded pebbles; mixed with clay lenses at base
10	3	Salt Dome Juist				
			-16	Olive gray	Fine sand	Reworked (Bioturbation), few shell fragments
			-46	Olive gray	Fine sand	Abundant shell fragments
			-246	Olive gray	Silty clay	Mixed with few peat fragments
			-263	Light olive gray	Fine sand	Shell fragments at base
			-400	Olive gray	Silty clay	Mixed with peat fragments; graded bedding at base
			-503	Olive gray	Silty clay	Thin sand lenses/layers of fine sand at 440, 465, 472-503 cm
			-560	Olive gray	Fine sand	Mixed with silty clay layers

Station ID	VC ID	Area	Depth TGS, cm	Color	Lithology	Description
CE0913						
17	4	Salt Dome Juist				
			-64	Olive gray	Fine sand	Mixed with cm-sized pebbles (10cm sized rock); peat particles at 28-30
			-93	Brownish black	Fine sand	Peat layer mixed with fine sand
			-99	Dark olive gray	Silty clay	
			-109	Olive gray	Fine sand	
			-123	Dark olive gray	Sandy clay	Graded bedding; erosive contact at base
			-500	Light olive gray	Fine sand	Mixed with few mm-sized peat particles
21	5	Salt Dome Juist				
			-135	Olive gray	Fine sand	Mixed with shell fragments; thin peat layer at 35 cm
			-400	Light brownish gray	Fine sand	Thin silty clay layers at 154-157, 184-187, 226-227, 384-387 cm 167-173 peat lens
			-502	Olive gray	Fine sand	Mixed with peat and silty clay lenses; clay layers at 428-432, 497-502
24	6	Salt Dome Juist				
			-38	Dark yellowish brown	Fine sand	Mixed with shell fragments
			-43	Brownish black	Fine sand	Peat layer mixed with fine sand and shell fragments
			-54	Dark yellowish brown	Fine sand	Mixed with few shell fragments
			-390	Olive gray	Fine sand	Mixed with shell fragments; 54-167 massive shell layer (cm-sized shell fragments)
			-500	Olive gray	Silty clay	Mixed with chalk, flint stone fragments

Station ID CE0913	VC ID	Area	Depth TGS, cm	Color	Lithology	Description
35	8	Salt Dome Juist				
			-38	light olive grey (5 Y 5/2)	Fine sand	well sorted, shell fragments
			-42		Fine sand	same sediment but clasts of silty sand, approximately 1 cm in diameter
			-53	light olive grey (5 Y 5/2)	Fine sand	fine sand, well sorted, small amount of shell fragments;
			-60	brown	Fine sand	small amount of peat fragments, 2 – 3 mm in diameter, seemed to be washed in
			-115	light olive grey (5 Y 5/2)	Fine sand	fine sand, well sorted, small amount of shell fragments
			-217	light olive grey (5 Y 5/2)	Fine sand	fine sand, well sorted, amount of shells is increasing, some complete shells (Astarte, Mya, ...); maximum size up to 3 cm
			-280	light olive grey (5 Y 5/2)	Fine sand	fine sand, well sorted, amount of shell fragments are decreasing strongly; at 260 cm and 270 cm flint stones, 1 cm in diameter, at 280 cm one shell up to 4 cm in diameter
			-318	light olive grey (5 Y 5/2)	Fine sand	fine sand, well sorted, no shell fragments, in-between are clasts of silty clay up to 5 cm in diameter, orientation vertical in the core, seem to be washed in from somewhere, colour: dusky brown (5 YR 2/2)
			-350	light olive grey (5 Y 5/2)	Fine sand	fine sand, well sorted, no shells or shell fragments
			-353	dark brown		another clast like before, 3 cm in diameter, no plant remnants inside the clast
			-412	light olive grey (5Y 5/2)	Fine sand	fine sand, well sorted, no structures, no shell fragments
			-422	light olive grey (5 Y 5/2)	Fine sand	as before, but slight increase in grain size
			-432	yellowish grey (5 Y 7/2)	Medium sand	no structures, no shell fragments
			-440	olive grey (5 Y 3/2)	Clay layer	some internal structure in a mm scale inside (old tidal flat sediments?)
			-456	light olive grey (5 Y 5/2)	Fine sand	fine sand, well sorted, no shell fragments
			-476	light olive grey (5 Y 5/2)	Fine sand / Medium sand	alteration of layers of fine sand and medium sand, thickness of layers of up to 1 cm, layers seem to be a little bit tilted by the coring process
			-486	dusky brown (5 YR 2/2)	Clasts of clay	including some very fragile shell fragments
			-511		Medium sand	well sorted, no shell fragments
			-518		Fine Sand	including some pieces of wood up to 1 cm in size

	-536	light olive grey (5 Y 5/2)	Fine Sand	well sorted, no shells,
	-540	Upper layer dark yellowish brownish (10 YR 4/2), lower layer yellowish brown (10 YR 2/2)	2 layers of clay	each 2 cm thick, upper one a little bit more brownish, clear unconformity to the upper sand layer
	-547	grey	Fine Sand	well sorted, no structures, becomes a little bit finer at the base

Station ID	VC ID	Area	Depth TGS, cm	Color	Lithology	Description
CE0913	9	Salt Dome Juist				
39	9	Salt Dome Juist				
			-25	light olive grey (5 Y 5/2)	Fine sand	well sorted, some shell fragments, at the base elongated clasts, 5 cm in length, dark grey, silty to clay material, orientation parallel to the layering
			-28	light brown olive (5 Y 5/6)	Fine sand	shells and shell fragments, cm-size, in-between peat fragments, diameter up to 5 mm, in-between a small amount of medium to coarse sand
			-34	moderate olive brown (5Y 4/4)	Fine sand	some shell fragments
			-393	light olive grey (5 Y 5/2)	Fine sand	some shell fragments, well sorted, from 130 – 131 and 171 – 172 layer of silty clay, no shell fragments inside, colour: olive grey (5 Y 3/2)
			-394		Boulder clay	transition to boulder clay, shell fragment horizon (transgression conglomerate)
			-554	olive grey (5 y 3/2)	Boulder clay	a lot of chalk fragments inside, material was never exposed to atmospheric conditions. The upper part of the boulder clay must have been eroded during the North Sea transgression

Station ID CE0913	VC ID	Area	Depth TGS, cm	Color	Lithology	Description
43	10	Salt Dome Juist				
			-11	light olive grey (5 Y 5/6)	Fine sand	Matrix fine sand, components: complete shell fragments, up to 2 cm in size
			-18	olive grey (5 Y 4/3)	Fine sand	shell fragments are becoming finer
			-75	light olive grey (5 Y 6/1)	Very fine sand	some horizontal layers, slightly visible
			-105	olive grey (5 Y 6/1)	Fine sand	a little bit darker due to some more fine components, from 098 – 105 some layers of a little bit more coarse grained material
			-144	olive grey (5 Y 4/1)	Fine sand	no structures
			-147	light olive brown (5 Y 5/6)	Fine sand	some silt content
			-148	greyish olive (10 Y 4/2)	Fine silt	
			-159		Fine sand	some layers in mm scale may indicate some moving water (transport structures?)
			-356	light olive grey (5 Y 6/1)	Fine sand	from 243 – 255 cm some fine gravel, poorly rounded, in general no structure
			-372		Fine sand	in-between some vertical structures seem to have some slight increase in water content
			-553	light olive grey (5Y 6/1)	Fine sand	slight increase in grain size towards the bottom
		Remark	From 18 cm it seems to be all melt-water deposits or glacial lake deposits as only very few transport structures can be seen. NO shell fragments in parts deeper than 18 cm.			

Station ID CE0913	VC ID	Area	Depth TGS, cm	Color	Lithology	Description
46	11	Tommeliten				
			-10	greyish olive grey (5 6Y 3/2)	Silty fine sand	cohesive, some small shell fragments
			-12		Shell	1 big shell, 8 cm in size, lying horizontal in the sediment
			-20	greyish olive grey (5 6Y 3/2)	Silty fine sand	same sediment than 000 – 010, partly shell accumulation
			-33	olive grey (5 Y 3/2)	Fine sand	amount of silt is decreasing, colour: traces of bioturbation;
			-40	light olive grey (5Y 3/2)	Fine sand	well sorted, no silt components, some shell fragments, they finish at 40 cm;
			-154	yellowish grey to light olive grey (5Y 7/2 – 5Y 5/2)	Fine sand	layered in a mm to cm scale, slightly differences in grain sizes, colour:
			-160	olive grey (5Y 3/2)	Clay	layer of clay fragments, app. 1 cm in diameter, rounded (seem to be transported a short distance), sand in-between, small white carbonate particles in the sand, mm-size, it could not be distinguished whether it were shell fragments or from other origin
			-169	light olive grey (5Y 5/2)	Fine sand	layers in a mm-scale, some dark flitters of organic material (peat), some mica particles
			-173	close to olive grey (5Y 5/2)	Silty clay	a bended layer of silty clay
			-278	light olive grey (5Y 5/2)	Silt	well sorted silt, no layers visible, sediment is oversaturated with water, slight shaking causes water to pour out at the sediment surface
			-299	light olive grey (5Y 5/2)	Clay	a vertical clay wedge exists in half of the core, no change in colour
			-357	light olive grey (5Y 5/2)	Silt	same sediment than before (well sorted silt)
			-365	light olive grey (5Y 5/2)	Silt	some bended layers visible by some organic content, same colour, sediment still oversaturated with water
			-375	light olive grey (5Y 5/2)	Fine silt	sediment like before

Station ID CE0913	VC ID	Area	Depth TGS, cm	Color	Lithology	Description
54	12	Tommeliten				
			-5	olive grey (5Y 3/2)	Fine Sand	Fine sand, well sorted, , no shell fragments
			-57	olive grey (5Y 3/2)	Fine Sand	fine sand, well sorted, a little bit darker than top layer, complete shells and shell fragments. At 27 cm one big shell, 11 cm in size, amount of shells is decreasing towards the bottom
			-187		Clay / sand	stiff clay, colour of these layers: olive grey (5Y 3/2), very fine structured in mm-scale and less; layers are horizontal but some microstructures are visible, thrusts (Verwerfungen) up to 1 cm. Bioturbation goes down to 101 cm, lenses of fine sand are transported to deeper layers. From 166 – 173 cm the amount of sand layers is increasing; colour of sandy layers: light olive grey (5Y 5/2)

Station ID CE0913	VC ID	Area	Depth TGS, cm	Color	Lithology	Description
61	13	Tommeliten				
			-36	olive grey (5Y 3/2) to greyish olive grey (5GY 3/2)	Fine sand	well sorted, slight silt content, complete shells and shell fragments, biggest shell (12 cm in size) taken as sample
			-100	light olive grey (5Y 6/1)	Fine sand	only a very small amount of shell fragments – very small in size, some organic material (plant remnants), layered
			-106			Concretions (the fine is fixed by some cement, layers are still visible)
			-123	olive grey (5Y 4/1)	Fine sand	a little bit finer than before, water content a little bit higher, some organic material in layers,
			-128			Concretion (taken as sample)
			-260	olive grey (5Y 4/1)	Clay	stiff, partly very fine layers, partly some organic material in-between, some layers have a lighter colour, layers are in a scale of less than 1 mm, strong H ₂ S smell

Station ID CE0913	VC ID	Area	Depth TGS, cm	Color	Lithology	Description
68	14	Tommeliten				
			-36	moderate olive brown (5Y 4/4)	Fine sand	well sorted, some bioturbation, some shell fragments
			-42		Shell layer	shell layer in a sandy matrix, complete shells (9 cm in diameter) and shell fragments
			-45	moderate olive brown (5Y 4/4)	Fine sand	like the top layer, a little bit more greyish
			-56	olive grey (5Y 3/2)	Clay	strongly bioturbated, seems to be an old hardground
			-100	medium dark grey (N 4)	Clay	stiff, very fine layered (mm-scale, even less), some microtectonics (trusts) in the scale of several mm
			-168	olive grey (5Y 3/2)	Clay	with some slight sand content, layers in a mm-scale but not that clear visible than before, some shell fragments are inside (No ice lake deposit), from 122 – 123 and from 141 – 142 a dark (black) layer, only change in colour, not in the sediment

Appendix

Core photography will be provided on request to the editors.

Videos, seafloor photography from ROV dives and video-guided CTD tracks are provided upon request to the editors.

I Station List

CTD: Water sampler rosette + CTD

POZ-L: Small lander system from paleoceanographic department

MB: Multibeam

VC: Vibro corer

ROV: Remotely operated vehicle ROV6000

MS-CTD: Micro-structure CTD

SP: Sparker seismic

PRF-L: Profiler lander

II Detailed station maps

III Gas concentration data measured by gas chromatography

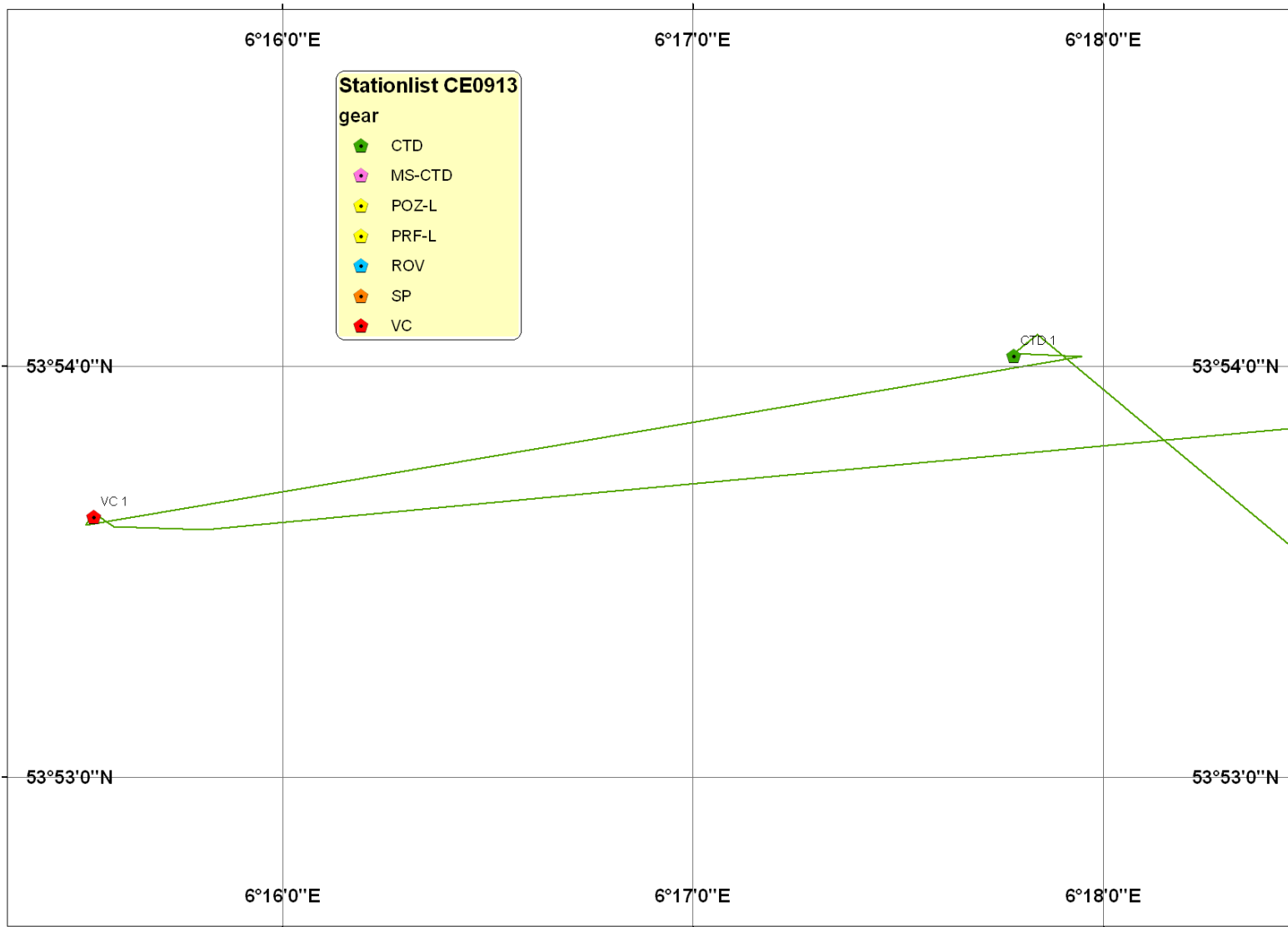
Station No.	Date	Gear	Gear No.	Area	Latitude N	Longitude E	UTC start	Water depth	UTC end	Added gear	Remarks
					<i>(Decimal degree)</i>			(mbsl)			
1	30.07.09	CTD	1	Borkum Reef	53.900433	6.296367	2:43		3:49	HydroC, PAH, pH, O.R.P, MIMS	tow CTD, ADCP 600 kHz
2	30.07.09	VC	1	Borkum Reef	53.893917	6.259000	4:37	30.0	5:15		
3	30.07.09	CTD	2	Salt Dome Juist	53.936050	6.759633	8:24	26.0	9:09	HydroC, PAH	tow CTD
4	30.07.09	CTD	3	Salt Dome Juist	53.935390	6.758153	11:15	26.0	12:00	HydroC, PAH, pH, O.R.P	tow CTD, ADCP 600 kHz
5	30.07.09	CTD	4	Salt Dome Juist	53.964730	6.972077	13:25	28.0	14:36	HydroC, PAH, pH, O.R.P	tow CTD, ADCP
6	30.07.09	SP	1	Salt Dome Juist	53.998117	6.732783	18:30	28.0	19:30		Failure due to rough sea
7	31.07.09	VC	2	Salt Dome Juist	53.936883	6.755220	6:46	23.7			1st try failure, 2nd ok
8	31.07.09	CTD	5	Salt Dome Juist	53.935367	6.758100	8:00	26.0	10:00	HydroC, PAH, pH, O.R.P, MIMS	tow CTD, MIMS modified, ADCP transect #1
9	31.07.09	ROV	1	Salt Dome Juist	53.935367	6.758150	12:15		16:32	pH/O.R.P, KIPS, 2 Niskin, 3 Push Core	
10	31.07.09	VC	3	Salt Dome Juist	53.995585	6.882578	19:15	29.5	19:25		
11	31.07.09	SP	2	Salt Dome Juist	54.002800	6.982283	20:08	28.0	21:50		still problems with the capacitors
12	31.07.09	CTD	6	Salt Dome Juist	53.976500	6.968967	22:00	28.0	0:50	HydroC, PAH, pH, O.R.P	tow CTD, ADCP 600 kHz, OFOS 2, ADCP new transect, EA600 7 000 5 file #
13	01.08.09	CTD	7	Salt Dome Juist	53.969233	6.971033	5:00	28.0	6:56	HydroC, PAH, pH, O.R.P	tow CTD, ADCP 600 kHz, pH drop, 53 58,037 Lat 6 58,140 Long
14	01.08.09	VC	4	Salt Dome Juist	53.966000	6.971667	7:38	25.3			failure, VC 4-1
15	01.08.09	CTD	8	Salt Dome Juist	53.965017	6.972717	9:00	27.0	11:18	pH, O.R.P.	ADCP new transect
16	01.08.09	ROV	2	Salt Dome Juist	53.956100	6.974867	12:00	24.0	17:30	PAH, pH, 3 KIPS, 2 Niskin, Push Core	Happy Birthday
17	01.08.09	VC	4	Salt Dome Juist	53.966028	6.971697	17:54	24.8	18:30		6m recovery, VC 4-2
18	01.08.09	SP	3	Salt Dome Juist	53.988800	6.955733	19:25	29.0	11:30	at 128 ms, 2 PPS	2,8-3 knots, Powersupply down

Station No.	Date	Gear	Gear No.	Area	Latitude N	Longitude E	UTC start	Water depth	UTC end	Added gear	Remarks
					(Decimal degree)			(mbsl)			
											again
19	02.08.09	CTD	9	Salt Dome Juist	53.924982	6.726162	2:29	24.0	5:03	pH, O.R.P.	no tow
20	02.08.09	CTD		Salt Dome Juist	53.931842	6.749468	6:30			Pump-Test, no data	Pump-Test, no data
21	02.08.09	VC	5	Salt Dome Juist	53.927697	6.747760	7:30	21.8	7:50		
22	02.08.09	CTD	10	Salt Dome Juist	53.935390	6.758135	8:20	26.9	9:59	pH, O.R.P.	ADCP new transect, pH drop 53 56,227 Lat 6 45,287 Long, 09:15 on SBE
23	02.08.09	ROV	3	Salt Dome Juist	53.937003	6.756167	11:15		16:55	KIPS, 1 Niskin, 3 Push Core	PWS, 1 Niskin, 1 Push Core
24	02.08.09	VC	6	Salt Dome Juist	53.924848	6.726510	17:45	21.7	18:00		
25	02.08.09	POZ-L	1	Salt Dome Juist	53.936883	6.755217	20:00	23.6		ADCP: WH300, RBR with P digiquartz	
26	02.08.09	SP	4	Salt Dome Juist	53.967133	6.733867	20:30	26.0	23:30		many remarks from Soeren
27	03.08.09	CTD	11	Salt Dome Juist	53.937608	6.756152	0:50	26.0	4:00	pH, O.R.P., MIMS	tow CTD, ADCP 600 kHz, Multibeam
28	03.08.09	CTD	12	Salt Dome Juist	53.931667	6.742333	4:20	24.0	7:40	pH, O.R.P.	tow CTD
29	03.08.09	VC	7	Salt Dome Juist	53.924345	6.725443	8:00	21.8	9:15		failure, "banana"
30	03.08.09	ROV	4	Salt Dome Juist	53.937067	6.756250				PAH, pH, KIPS, 2 Niskin, 3 Push Core	
31	03.08.09	POZ-L	1	Salt Dome Juist	53.936883	6.755217	14:40				recovery
32	03.08.09	CTD	13	Salt Dome Juist	53.936817	6.755283	15:30	25.5	18:00	pH, O.R.P.	ADCP new transect, 13 clear water on ADCP Backscatter, ENS 7860, ENS 7840, Backscatter 70-85
33	03.08.09	CTD	14	Salt Dome Juist	53.936687	6.754925	19:24	28.0	21:04	pH, O.R.P.	low pH bottle 3
34	04.08.09	CTD	15	Salt Dome Juist	53.936782	6.755143	23:30	26.0	8:00	pH, O.R.P., MIMS	new ADCP transect
35	05.08.09	VC	8	Salt Dome Juist	53.926863	6.742665	10:15	21.5	10:30		full penetration, 5,46m recovery
36	05.08.09	ROV	5	Salt Dome Juist	53.937500	6.754300	11:00			PWS at 12:20	Deployment of PWS@PM2, Water@PM1

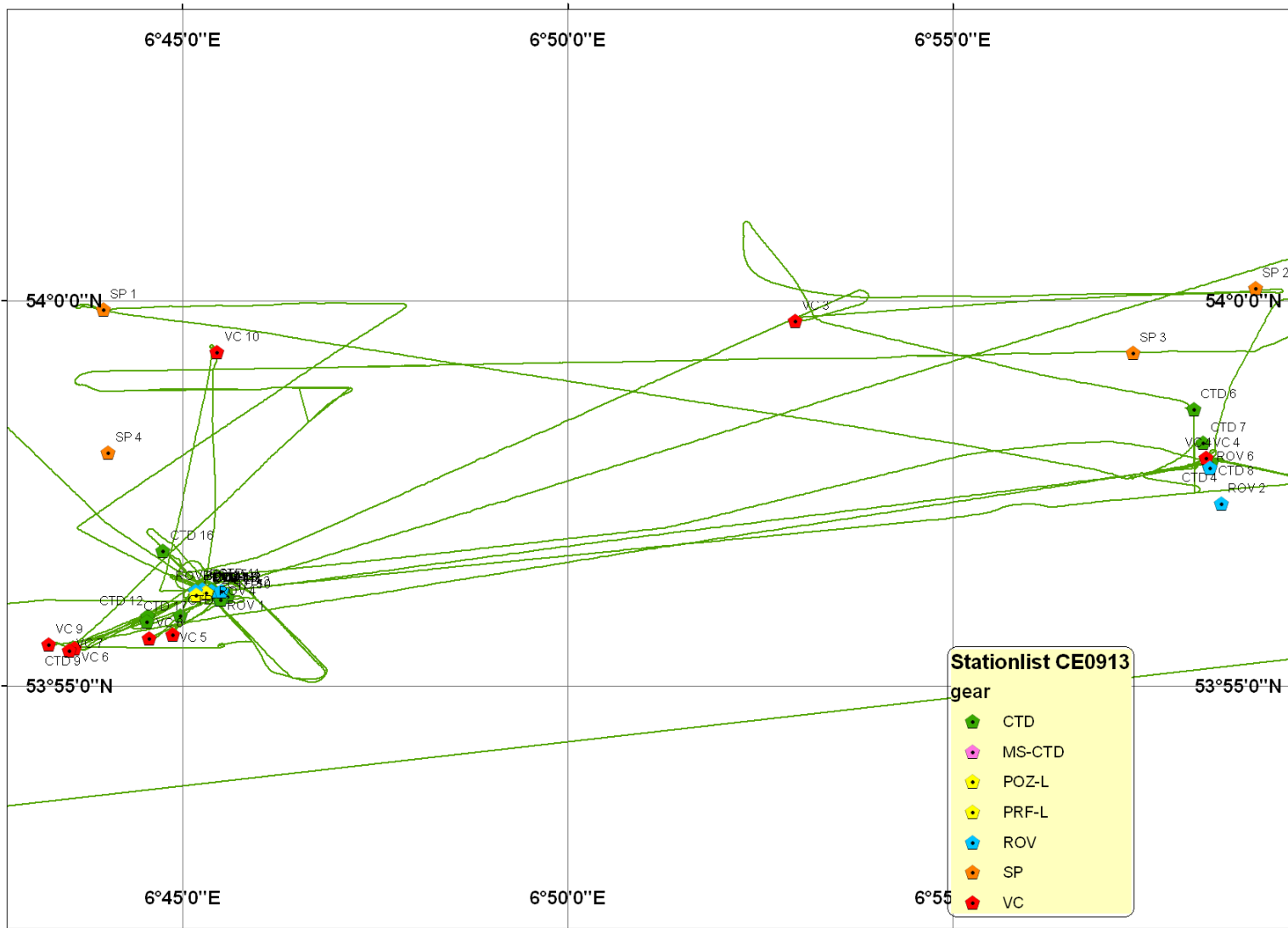
Station No.	Date	Gear	Gear No.	Area	Latitude N	Longitude E	UTC start	Water depth	UTC end	Added gear	Remarks
					(Decimal degree)			(mbsl)			
37-1	05.08.09	POZ-L	2	Salt Dome Juist	53.936817	6.755117	12:50			37-1	
37-2	05.08.09	POZ-L	2	Salt Dome Juist	53.936817	6.754863	18:22		18:45	37-2	
37-3	05.08.09	POZ-L	2	Salt Dome Juist	53.936795	6.755067	19:06		19:10	37-3	
38	05.08.09	CTD	16	Salt Dome Juist	53.945820	6.745720	21:12	28.0	6:06		
39	06.08.09	VC	9	Salt Dome Juist	53.925592	6.720870	6:15	21.5	6:45		5,54m core lenght
40	06.08.09	ROV	6	Salt Dome Juist	53.963883	6.972433	8:25	26.1			
41	06.08.09	ROV	7	Salt Dome Juist	53.937150	6.752750	15:30	25.0		HydroC, PAH, pH, O.R.P, KIPS, 3 Push Core, 1 BC	
42	06.08.09	CTD	17	Salt Dome Juist	53.930493	6.742118	19:55	25.0	5:40	pH, O.R.P.	transect
43	07.08.09	VC	10	Salt Dome Juist	53.988840	6.757380	6:15	24.7	6:40		5,53 recovery
44	07.08.09	ROV	8	Salt Dome Juist	53.937150	6.758333	8:07	26.0			
45	07.08.09	POZ-L	2	Salt Dome Juist	53.936250	6.752950	11:50	24.0	12:05		recovery
46	08.08.09	VC	11	Tommeliten	56.501817	2.995950	5:20	70.3	9:45		3,75m recovery
47	08.08.09	POZ-L	3	Tommeliten	56.501817	2.995600	10:14	70.0			
48	08.08.09	CTD	18	Tommeliten	56.498683	2.995245	11:25	73.0	11:33	pH, O.R.P.	sound velocity profile
49	08.08.09	ROV	9	Tommeliten	56.498583	2.995250	12:16	70.0		HydroC, PAH, pH, O.R.P, KIPS, Push Core, Gas Sampler, BC 1	
50	08.08.09	CTD	19	Tommeliten	56.498593	2.996320	19:30	73.0	20:00	pH, O.R.P.	
51-1	08.08.09	MS-CTD	2-6	Tommeliten	56.498617	2.996367	20:20	74.0	21:00	Shear 1+2, Accelometer, fC, fT, O2	cast 1 as test
51-2	08.08.09	MS-CTD	7-9	Tommeliten	56.498617	2.996367	22:10	74.0	22:40	Shear 1+2, Accelometer, fC, fT, O2	check power!
52	08.08.09	CTD	20	Tommeliten	56.498415	3.009113	23:13		2:00	HydroC CH4, pH, O.R.P, MIMS	new ADCP, no bottles!
53-1	09.08.09	MS-CTD	10	Tommeliten	56.498415	3.009113	2:30	74.0	3:10	Shear 1+2, Accelometer, fC, fT, O2	
53-2	09.08.09	MS-CTD	11-14	Tommeliten	56.498617	2.996367	4:00	74.0	4:35	Shear 1+2, Accelometer, fC, fT, O2	

Station No.	Date	Gear	Gear No.	Area	Latitude N	Longitude E	UTC start	Water depth	UTC end	Added gear	Remarks
					(Decimal degree)			(mbsl)			
53-3	09.08.09	MS-CTD	15-17	Tommeliten	56.498617	2.996367	5:30	74.0	6:10	Shear 1+2, Accelometer, fC, fT, O2	
54	09.08.09	VC	12	Tommeliten	56.497883	2.996633	6:15	70.9	6:40		187cm recovery
55	09.08.09	MS-CTD	18-26	Tommeliten	56.498617	2.996367	7:00	72.0	9:00	Shear 1+2, Accelometer, fC, fT, O2	
56	09.08.09	PRF-L	1	Tommeliten	56.502117	3.002212	11:40	70.0	12:01	ADCP: WH300/Aquadopp Profiler, Microprofiler	camera: 13:35 (LT) + 1h/10min
57	09.08.09	ROV	10	Tommeliten	56.502133	3.002233	15:00			ECS 1	16:18 ECS-1 deployed
58	09.08.09	ROV	11	Tommeliten	56.501400	3.001367	19:15			ECS 2	20:28 ECS-2 deployed
59-1	09.08.09	MS-CTD	27-29	Tommeliten	56.498617	2.996367	22:15	73.0	23:00	Shear 1+2, Accelometer, fC, fT, O2	Cast 28-29 with 1 shear sensor in disagreement
59-2	10.08.09	MS-CTD	30-33	Tommeliten	56.498617	2.996367	1:30	73.0	2:45	Shear 1+2, Accelometer, fC, fT, O2	
59-3	10.08.09	MS-CTD	34-36	Tommeliten	56.498617	2.996367	3:50	74.0	4:50	Shear 1+2, Accelometer, fC, fT, O2	
60-1	09.08.09	MB	1	Tommeliten	56.506283	2.987983	23:10	72.0	1:45	Multibeam, Singlebeam, Sound Bottom Profiler	
60-2	10.08.09	MB	2	Tommeliten	56.491345	2.993925	2:20	71.0	3:50	Multibeam, Singlebeam, Sound Bottom Profiler	
60-3	10.08.09	MB	3	Tommeliten	56.497087	2.995453				Multibeam, Singlebeam, Sound Bottom Profiler	Looking for flares
61	10.08.09	VC	13	Tommeliten	56.498625	2.995835	6:15	71.0	6:40		2,60m recovery
62	10.08.09	CTD	21	Tommeliten	56.498583	2.995740	8:00	74.0	11:15	HydroC, pH, O.R.P, MIMS	Gas?
63	10.08.09	ROV	12	Tommeliten	56.498617	2.995900	11:27			56 29,846 - 2 59,778 - Gas Flares	
64	10.08.09	PRF-L	1	Tommeliten	56.502783	3.002427					recovery
65	10.08.09	MS-CTD	37-40	Tommeliten	56.498617	2.996400	18:40	74.0	19:40	Shear 1+2, Accelometer, fC, fT, O2	
66	10.08.09	CTD	22	Tommeliten	56.498617	2.996367	20:18	74.0	3:00	HydroC, pH, O.R.P, MIMS, MIMS, full boat	new ADCP transect, MIMS w/ deep capacity
67	11.08.09	CTD	23	Tommeliten	56.498517	2.995800	3:25	74.0	5:22	HydroC, PAH, pH,	new ADCP

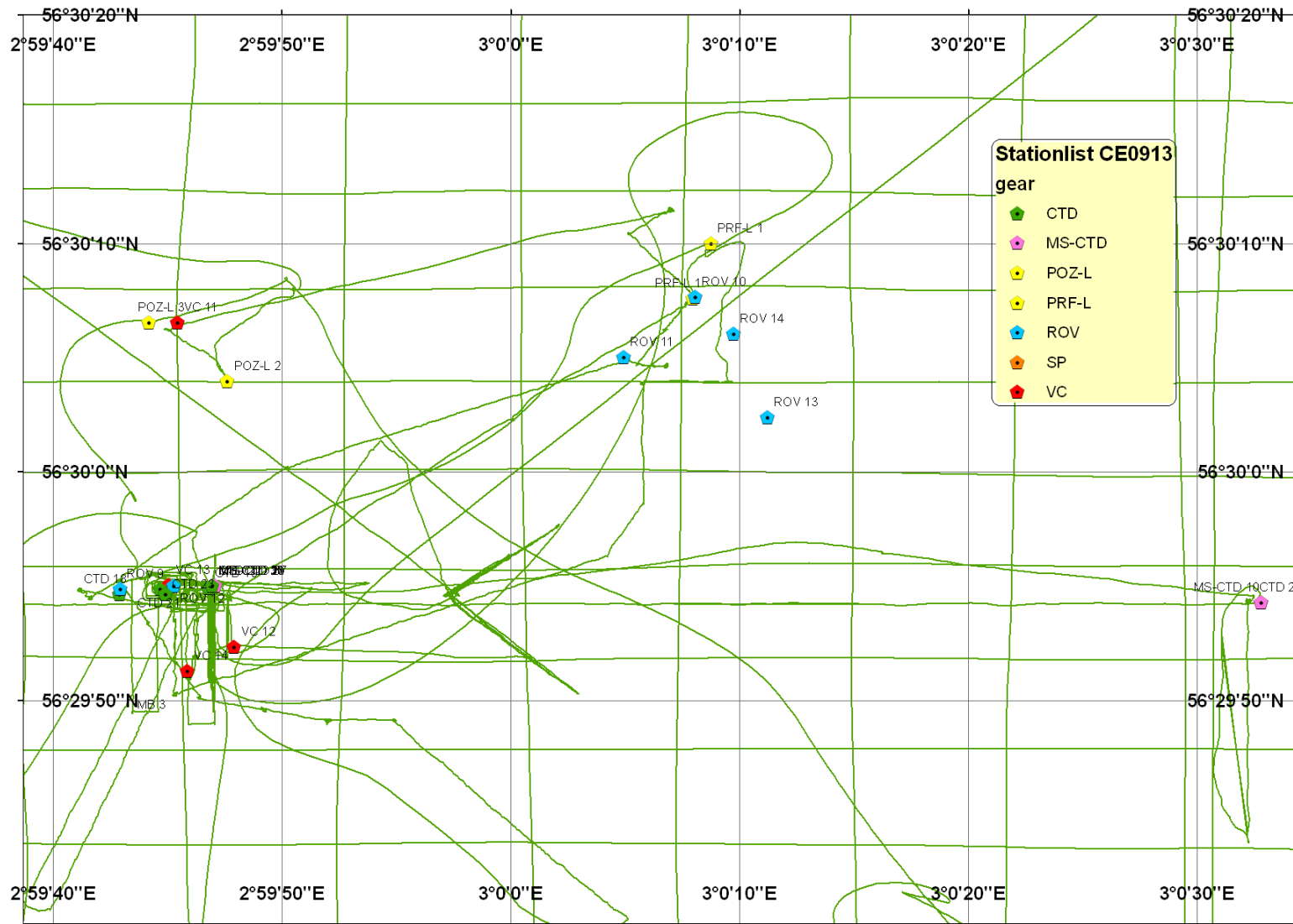
Station No.	Date	Gear	Gear No.	Area	Latitude N	Longitude E	UTC start	Water depth	UTC end	Added gear	Remarks
					<i>(Decimal degree)</i>			(mbsl)			
										O.R.P	
68	11.08.09	VC	14	Tommeliten	56.497592	2.996063	8:00	73.0	8:35		1,68m recovery
69	11.08.09	ROV	13	Tommeliten	56.500667	3.003117	7:15		8:35	ECS 1 recovery	EDC 1 an Beacon 52
70	11.08.09	ROV	14	Tommeliten	56.501683	3.002700	9:20	70.0	9:35	ECS 2 recovery	
71	11.08.09	POZ-L	2	Tommeliten	56.501112	2.996548	11:03	70.0	11:17		11:04 released
72	11.08.09	MB	4	Tommeliten	56.505618	2.993167	11:22	70.7	13:40	Multibeam, Singlebeam, Sound Bottom Profiler	
73	11.08.09	MB	5	Tommeliten	56.474863	3.014287	14:05	69.4	22:03	Multibeam, Singlebeam, Sound Bottom Profiler	



II.1 Borkum Reef ("Background") stations.



II.2 Salt Dome Juiſt ("Diffusive venting") stations.



II.3 Tommeliten ("Gas bubble seepage") stations.

III Gas concentration data measured by gas chromatography

Station No.	CTD No.	Bottle No.	Date UTM	Time UTM	Latitude N	Longitude E	Depth m	CO2 μ M/l	O2 μ M/l	N2 μ M/l	CH4 nM/l	CH4 ppmV	C2H6 ppmV	C3H8 ppmV
1	1	1	30.07.2009	02:56:53	53.9005	6.29654	0.339							
1	1	3	30.07.2009	02:58:56	53.9005	6.29652	9.88							
1	1	5	30.07.2009	02:59:49	53.9005	6.29652	14.3							
1	1	7	30.07.2009	03:02:15	53.9005	6.29652	27.049							
1	1	9	30.07.2009	03:04:34	53.9005	6.29652	29.949							
1	1	11	30.07.2009	03:30:01	53.9005	6.2965	30.176							
1	1	13	30.07.2009	03:38:51	53.9005	6.29756	29.837							
1	1	15	30.07.2009	03:42:30	53.9005	6.29842	29.799							
1	1	17	30.07.2009	03:45:55	53.9005	6.29922	29.818							
1	1	19	30.07.2009	03:47:04	53.90048	6.29926	23.887							
1	1	21	30.07.2009	03:48:01	53.9005	6.29924	16.868							
1	1	23	30.07.2009	03:48:27	53.9005	6.29926	11.821							
3	2	1	30.07.2009	08:26:24	53.93542	6.75799	23.29				2.9			
3	2	3	30.07.2009	08:29:27	53.93572	6.75746	23.216				2.8			
3	2	5	30.07.2009	08:31:41	53.93592	6.75724	23.162				1.9			
3	2	7	30.07.2009	08:35:51	53.93628	6.75634	23.534				2.5			
3	2	9	30.07.2009	08:43:52	53.93704	6.75498	23.403							
3	2	11	30.07.2009	08:49:35	53.93758	6.75401	23.452							
3	2	13	30.07.2009	08:54:54	53.93802	6.75314	23.588				2.4			
3	2	15	30.07.2009	08:57:06	53.93822	6.75273	23.573				1.5			
3	2	17	30.07.2009	09:00:22	53.93844	6.75242	23.694				2.2			
4	3	1	30.07.2009	11:32:33	53.93548	6.75776	20.05				3.6			
4	3	3	30.07.2009	11:40:01	53.93652	6.75592	22.34				4.6			
4	3	5	30.07.2009	11:46:50	53.9373	6.7545	19.215				3.6			
4	3	7	30.07.2009	11:54:54	53.9384	6.75245	23.102				4.7			
5	4	1	30.07.2009	13:37:17	53.96434	6.96987	19.158							
5	4	3	30.07.2009	13:53:13	53.96332	6.96455	24.292				1.7			
5	4	5	30.07.2009	13:55:52	53.96322	6.96402	24.914							
5	4	7	30.07.2009	13:58:39	53.9631	6.96319	22.894				1.9			
5	4	9	30.07.2009	14:12:56	53.96248	6.95992	23.904							

Station No.	CTD No.	Bottle No.	Date UTM	Time UTM	Latitude N	Longitude E	Depth m	CO2 μ M/l	O2 μ M/l	N2 μ M/l	CH4 nM/l	CH4 ppmV	C2H6 ppmV	C3H8 ppmV
5	4	11	30.07.2009	14:19:27	53.96218	6.95836	23.65				2.0			
5	4	13	30.07.2009	14:23:56	53.96198	6.95734	22.841				1.7			
5	4	15	30.07.2009	14:32:09	53.96164	6.95548	24.191							
8	5	1	31.07.2009	08:28:36	53.93558	6.75758	21.705	5.8	21.2	47.4	3.7			
8	5	3	31.07.2009	09:08:38	53.93788	6.75336	20.964	6.2	185.3	366.8	3.7			
8	5	5	31.07.2009	09:10:50	53.93798	6.7531	21.456	5.5	170.7	359.9	2.9			
8	5	7	31.07.2009	09:22:29	53.93856	6.75198	21.819	5.9	197.1	387.6	3.2			
8	5	9	31.07.2009	09:32:58	53.9391	6.75084	21.852	6.0	195.2	386.3	3.0			
8	5	11	31.07.2009	09:33:05	53.9391	6.75083	23.034	5.3	196.3	391.3	3.0			
8	5	13	31.07.2009	09:41:13	53.9395	6.74986	21.796	5.4	231.3	538.1	3.8			
8	5	15	31.07.2009	09:49:48	53.93998	6.74896	21.86	4.9	239.0	560.2	3.2			
8	5	17	31.07.2009	09:49:55	53.93998	6.74894	21.299	5.9	290.8	749.9	4.0			
8	5	19	31.07.2009	09:51:31	53.94006	6.74877	21.19	4.9	258.7	661.0	2.8			
8	5	21	31.07.2009	09:58:45	53.94048	6.74802	22.188	6.4	197.0	394.1	2.9			
8	5	23	31.07.2009	10:02:01	53.94064	6.74768	21.164	5.2	188.3	372.0	2.9			
12	6	1	31.07.2009	22:50:19	53.97654	6.9688	22.488	6.8	185.9	372.2	2.6			
12	6	3	31.07.2009	23:07:54	53.97408	6.96882	25.734	5.8	209.5	481.5	2.8			
12	6	5	31.07.2009	22:58:45	53.97372	6.9688	25.538	5.4	173.6	349.1	2.6			
12	6	7	31.07.2009	23:05:10	53.97284	6.96882	25.867	6.6	178.4	354.9	2.6			
12	6	9	31.07.2009	23:18:57	53.97254	6.96882	25.4	7.1	192.7	383.3	2.7			
12	6	11	31.07.2009	23:19:27	53.97248	6.96882	25.308	7.3	186.0	371.6	2.8			
12	6	13	31.07.2009	23:45:08	53.96892	6.96884	25.176	6.2	191.0	413.8	2.5			
12	6	15	31.07.2009	23:55:38	53.96744	6.96884	25.114							
12	6	17	01.08.2009	00:32:22	53.96236	6.96894	24.213	6.4	183.6	367.7	2.2			
12	6	19	01.08.2009	00:53:17	53.95948	6.96894	22.907	7.3	186.5	371.8	2.6			
13	7	1	01.08.2009	05:18:12	53.96875	6.969	22.809	6.9	185.5	373.9	2.5			
13	7	3	01.08.2009	05:18:43	53.96874	6.969	24.318	6.6	165.5	330.2	3.0			
13	7	5	01.08.2009	05:44:05	53.96744	6.969	26.971	6.4	174.3	346.9	2.5			
13	7	7	01.08.2009	05:49:45	53.96712	6.969	26.788	6.3	179.9	359.6	2.8			
13	7	9	01.08.2009	06:24:29	53.9652	6.96902	26.806	6.7	184.7	367.7	3.2			
13	7	11	01.08.2009	06:24:37	53.96518	6.96902	26.781	5.9	175.7	350.2	3.2			

Station No.	CTD No.	Bottle No.	Date UTM	Time UTM	Latitude N	Longitude E	Depth m	CO2 μ M/l	O2 μ M/l	N2 μ M/l	CH4 nM/l	CH4 ppmV	C2H6 ppmV	C3H8 ppmV
13	7	13	01.08.2009	06:35:21	53.9646	6.969	26.582							
13	7	15	01.08.2009	06:39:15	53.96438	6.96902	26.66	5.9	176.7	366.0	2.3			
13	7	17	01.08.2009	06:39:20	53.96438	6.96902	26.65	7.1	192.7	385.0	3.0			
13	7	19	01.08.2009	06:42:54	53.96416	6.96902	26.658	6.7	189.4	379.2	2.5			
13	7	21	01.08.2009	06:52:23	53.96364	6.96902	26.638	6.7	222.4	490.6	2.6			
13	7	23	01.08.2009	06:52:30	53.96364	6.96902	26.526	6.9	183.7	368.8	2.7			
15	8	1	01.08.2009	09:28:13	53.96484	6.97148	25.45	6.2	192.0	423.0	2.4			
15	8	3	01.08.2009	10:16:34	53.96409	6.96706	25.423							
15	8	5	01.08.2009	10:16:51	53.96408	6.96704	25.406							
15	8	7	01.08.2009	10:31:52	53.96386	6.96568	24.79	6.4	180.0	367.1	3.1			
15	8	9	01.08.2009	10:32:23	53.96386	6.96562	24.814							
15	8	11	01.08.2009	10:50:47	53.96358	6.96394	24.899	6.2	175.6	353.9	3.2			
15	8	13	01.08.2009	10:55:09	53.96352	6.96356	24.698	6.7	176.5	355.4	2.5			
19	9	1	02.08.2009	02:37:12	53.925	6.72614	22.025	4.0	181.4	373.2	2.7	4.6	0.4	0.7
19	9	3	02.08.2009	03:07:33	53.92484	6.72644	21.91	6.0	212.3	462.5	3.1	4.4	0.6	0.7
19	9	5	02.08.2009	03:28:03	53.92478	6.7264	21.93	3.6	401.5	1236	4.8	2.8	0.7	0.5
19	9	7	02.08.2009	03:47:05	53.9248	6.72644	21.787	6.5	206.6	416.4	3.3	5.0	1.0	0.7
19	9	9	02.08.2009	04:39:00	53.92496	6.72616	21.499	6.0	188.4	365.5	3.2	5.4	0.9	0.7
19	9	11	02.08.2009	05:03:21	53.925	6.72622	21.609	6.3	196.6	382.9	3.0	4.9	0.8	0.8
22	10	1	02.08.2009	08:29:07	53.93538	6.75808	24.649	5.1	211.2	498.0	3.5	4.6	0.7	0.0
22	10	3	02.08.2009	08:32:05	53.93548	6.75788	24.692	6.0	185.9	360.7	3.3	5.7	0.5	0.6
22	10	5	02.08.2009	09:14:45	53.93708	6.75488	24.684	5.9	198.7	388.7	3.8	6.0	1.0	0.8
22	10	7	02.08.2009	09:14:58	53.93708	6.75486	24.703	6.2	193.1	378.9	4.0	6.5	1.3	1.2
22	10	9	02.08.2009	09:15:50	53.9371	6.75481	24.658	6.0	188.6	367.1	3.2	5.4	0.5	0.8
22	10	11	02.08.2009	09:52:38	53.93838	6.75238	24.712	6.5	268.1	391.5	3.0	4.7	0.6	0.8
27	11	1	03.08.2009	00:51:42	53.93758	6.75608	11.822							
27	11	3	03.08.2009	01:36:50	53.9361	6.75266	11.795							
27	11	5	03.08.2009	01:39:20	53.936	6.75246	11.756							
27	11	7	03.08.2009	02:12:17	53.93492	6.74996	11.846							
27	11	9	03.08.2009	02:42:30	53.93394	6.74768	11.869							
28	12	1	03.08.2009	04:25:24	53.93166	6.74236	22.593	5.6	159.4	311.1	2.6	5.1	0.4	0.3

Station No.	CTD No.	Bottle No.	Date UTM	Time UTM	Latitude N	Longitude E	Depth m	CO2 μ M/l	O2 μ M/l	N2 μ M/l	CH4 nM/l	CH4 ppmV	C2H6 ppmV	C3H8 ppmV
28	12	3	03.08.2009	04:52:19	53.93078	6.7403	22.607	6.7	189.0	372.5	3.1	5.2	1.1	0.7
28	12	5	03.08.2009	05:17:10	53.92994	6.73844	22.575	6.5	179.3	350.0	3.0	5.3	0.6	0.5
28	12	7	03.08.2009	05:30:51	53.9295	6.73732	22.364	6.3	183.1	358.2	2.9	5.1	0.9	0.8
28	12	9	03.08.2009	06:03:13	53.92844	6.7349	22.249	5.5	168.5	334.1	3.4	6.4	1.2	0.5
28	12	11	03.08.2009	07:01:43	53.92652	6.73048	22.492	5.8	163.4	326.0	3.5	6.7	0.6	0.5
28	12	13	03.08.2009	07:25:28	53.92522	6.72747	22.615	6.2	179.0	355.3	3.6	6.4	0.9	0.7
28	12	15	03.08.2009	07:41:09	53.92432	6.7254	23.189	5.6	166.5	331.5	2.9	5.4	0.5	0.6
32	13	1	03.08.2009	15:32:28	53.93682	6.75536	23.673	5.6	164.4	320.8	3.2	6.1	1.2	0.7
32	13	3	03.08.2009	15:42:28	53.9368	6.75514	23.699							
32	13	5	03.08.2009	15:53:55	53.9369	6.75522	23.656	6.1	180.5	351.4	3.0	5.3	0.5	0.9
32	13	7	03.08.2009	16:02:29	53.93692	6.75526	23.632	5.7	168.1	325.1	2.7	5.1	0.5	0.6
32	13	9	03.08.2009	17:00:52	53.93678	6.75488	24.314	5.7	230.2	540.2	3.1	3.8	0.7	0.7
32	13	11	03.08.2009	17:05:36	53.93668	6.75504	24.318				3.4	4.9	1.0	0.8
32	13	13	03.08.2009	17:15:01	53.93682	6.75496	24.435	5.1	255.6	630.7	3.5	3.8	0.3	0.6
32	13	15	03.08.2009	17:23:18	53.9367	6.75492	24.24	5.9	206.6	452.3	2.9	4.2	0.6	0.9
32	13	17	03.08.2009	17:23:45	53.9367	6.75492	24.365	5.7	177.9	348.4	2.7	4.8	0.5	0.7
32	13	19	03.08.2009	17:26:12	53.9367	6.75492	24.39	6.4	169.7	330.5	3.0	5.6	0.5	1.1
33	14	1	03.08.2009	19:19:06	53.93664	6.75482	19.915	5.6	177.6	346.4	3.0	5.4	0.8	0.7
33	14	3	03.08.2009	19:20:45	53.93664	6.75482	25.08	6.6	187.6	370.3	3.0	5.0	0.5	0.5
33	14	5	03.08.2009	20:34:29	53.93664	6.75522	9.629	6.4	196.0	381.1	3.2	5.3	0.3	0.5
33	14	7	03.08.2009	21:00:08	53.93674	6.7554	9.516	6.4	197.3	382.4	3.3	5.4	0.5	0.8
34	15	1	04.08.2009	23:31:29	53.93678	6.75486	11.891							
34	15	3	05.08.2009	01:04:07	53.93678	6.75488	15.302							
34	15	5	05.08.2009	02:34:05	53.93676	6.75484	15.085							
34	15	7	05.08.2009	02:35:43	53.93682	6.75484	14.95							
34	15	9	05.08.2009	02:36:31	53.93682	6.75492	14.636							
34	15	11	05.08.2009	02:37:01	53.93682	6.75496	14.633							
34	15	13	05.08.2009	02:38:38	53.93674	6.75498	14.954	5.0	185.6	366.7	3.4	5.8	0.4	0.8
34	15	15	05.08.2009	02:40:46	53.93672	6.7548	15.316	6.9	196.3	393.5	3.2	5.1	0.5	0.7
34	15	17	05.08.2009	02:40:52	53.93672	6.7548	15.281	6.5	177.6	348.6	3.0	5.4	0.5	0.6
34	15	19	05.08.2009	02:41:15	53.93672	6.75478	15.273							

Station No.	CTD No.	Bottle No.	Date UTM	Time UTM	Latitude N	Longitude E	Depth m	CO2 μ M/l	O2 μ M/l	N2 μ M/l	CH4 nM/l	CH4 ppmV	C2H6 ppmV	C3H8 ppmV
34	15	21	05.08.2009	04:03:13	53.93674	6.75492	15.391							
34	15	23	05.08.2009	07:54:07	53.93682	6.75514	14.574	6.7	198.0	394.9	3.4	5.4	0.5	0.8
38	16	1	05.08.2009	23:25:44	53.94142	6.75038	25.311	7.2	202.0	403.0	0.4	0.7	0.0	0.0
38	16	3	06.08.2009	00:48:43	53.93828	6.75359	24.603							
38	16	5	06.08.2009	01:24:44	53.93654	6.75534	23.644							
38	16	7	06.08.2009	01:46:34	53.93546	6.75632	23.503	6.4	174.5	347.4	1.2	2.2	0.0	0.0
38	16	9	06.08.2009	02:43:32	53.93268	6.75897	22.369							
38	16	11	06.08.2009	02:53:08	53.93221	6.7594	22.487							
38	16	13	06.08.2009	03:49:24	53.92948	6.76196	21.784							
38	16	15	06.08.2009	03:59:09	53.92902	6.76236	21.814	6.0	197.6	424.5	3.6	5.4	0.9	0.6
38	16	17	06.08.2009	04:11:11	53.92846	6.76292	21.643							
38	16	19	06.08.2009	05:08:52	53.92608	6.76512	21.762	4.0	156.4	314.7	2.9	5.9	0.7	0.5
42	17	1	06.08.2009	20:10:21	53.93056	6.74228	22.697	7.7	183.4	374.5	4.0	6.8	0.7	0.8
42	17	3	06.08.2009	21:16:59	53.93318	6.74674	22.612	8.2	202.4	419.4	4.1	6.1	0.7	0.8
42	17	5	06.08.2009	22:12:14	53.93532	6.75048	24.239	6.9	178.4	366.6	4.1	7.1	0.7	1.0
42	17	7	06.08.2009	23:10:53	53.93758	6.75442	24.309	7.6	209.4	440.5	4.0	5.8	1.0	0.7
42	17	9	06.08.2009	23:18:29	53.93787	6.75492	24.269	7.3	218.0	480.9	4.0	5.3	1.1	1.3
42	17	11	06.08.2009	23:21:44	53.93799	6.75514	24.276	7.5	202.1	411.2	3.8	5.9	0.6	0.4
42	17	13	06.08.2009	23:24:33	53.9381	6.75536	24.211	6.3	180.5	361.9	3.5	6.1	0.8	1.9
42	17	15	06.08.2009	23:30:55	53.93836	6.75576	24.159	7.0	209.2	470.0	3.8	5.3	1.2	0.8
42	17	17	07.08.2009	03:42:38	53.93664	6.75428	21.369	6.7	207.9	456.2	3.1	4.5	0.0	0.0
42	17	19	07.08.2009	04:21:05	53.93672	6.75474	23.084	7.5	182.0	366.0	3.1	5.4	0.8	0.7
42	17	21	07.08.2009	05:12:04	53.9366	6.7553	22.345	8.7	233.5	512.1	4.8	6.0	1.1	0.0
42	17	23	07.08.2009	05:33:37	53.93718	6.75034	3.927	7.5	178.3	366.3	0.1	0.1	0.0	0.0
48	18	1	08.08.2009	11:21:16	56.49866	2.99526	3.636	5.5	187.5	358.7	1.7			
48	18	3	08.08.2009	11:27:25	56.49866	2.99526	69.919	8.0	184.0	413.3	144.2			
48	18	5	08.08.2009	11:27:38	56.49866	2.99526	69.966	8.9	196.8	441.6	152.9			
48	18	7	08.08.2009	11:31:53	56.49866	2.99524	4.376	6.0	190.1	362.9	2.3			
50	19	1	08.08.2009	19:46:28	56.49858	2.99632	70.973	7.3	196.2	450.6	160.4	236.1	0.9	0.4
50	19	3	08.08.2009	19:48:29	56.49858	2.99632	63.041							
50	19	5	08.08.2009	19:50:22	56.49858	2.99632	43.458	8.4	199.2	463.5	44.6	63.8	0.5	0.0

Station No.	CTD No.	Bottle No.	Date UTM	Time UTM	Latitude N	Longitude E	Depth m	CO2 μ M/l	O2 μ M/l	N2 μ M/l	CH4 nM/l	CH4 ppmV	C2H6 ppmV	C3H8 ppmV
50	19	7	08.08.2009	19:51:09	56.4986	2.99632	39.901	8.3	219.8	513.5	57.4	74.7	0.8	0.6
50	19	9	08.08.2009	19:51:54	56.49858	2.9963	37.853	7.7	206.6	430.9	40.0	59.3	0.7	0.0
50	19	11	08.08.2009	19:52:31	56.49858	2.99632	35.051							
50	19	13	08.08.2009	19:52:57	56.49858	2.99632	25.594	6.9	257.6	514.8	2.1	2.5	0.0	0.0
50	19	15	08.08.2009	19:53:13	56.49858	2.99632	19.537	6.9	216.3	415.7				
50	19	17	08.08.2009	19:53:51	56.49858	2.99632	6.186	6.5	196.9	374.0	2.6	4.3	0.1	0.0
50	19	19	08.08.2009	19:54:47	56.49858	2.99634	0.876	6.1	191.5	365.0	5.3	24.4	1.3	0.7
66	22	1	11.08.2009	00:03:57	56.49856	2.9963	70.755							
66	22	3	11.08.2009	00:46:07	56.49844	2.99624	70.738							
66	22	5	11.08.2009	02:23:33	56.49844	2.99658	70.713							
67	23	1	11.08.2009	03:27	56.49858	2.99578	70.983	8.1	193.4	459.5	48.5	64.3	0.9	0.0
67	23	3	11.08.2009	03:30	56.49856	2.9958	71.054	7.8	183.8	433.7	39.8	56.5	0.6	0.0
67	23	5	11.08.2009	03:38	56.49852	2.99592	71.173	8.4	194.4	461.0	53.2	70.6	0.8	0.0
67	23	7	11.08.2009	03:39	56.4985	2.9958	71.199	8.6	191.4	442.2	67.0	98.3	0.8	0.0
67	23	9	11.08.2009	03:43	56.49866	2.99564	71.005	7.6	178.3	415.9	32.6	46.5	0.7	0.7
67	23	11	11.08.2009	03:48	56.49852	2.996	71.269	8.3	174.4	402.2	32.1	47.2	0.8	0.0
67	23	13	11.08.2009	03:50	56.49848	2.99582	71.156	10.8	189.5	431.0	346.5	515.7	1.0	0.0
67	23	15	11.08.2009	03:54	56.49856	2.99556	71.018	6.1	153.5	372.4	40.7	59.9	0.3	0.0
67	23	17	11.08.2009	03:55	56.49858	2.99556	71.046	6.4	208.5	541.4	35.1	40.6	0.8	0.8
67	23	19	11.08.2009	04:12	56.4985	2.99591	71.22	8.2	187.8	439.5	59.9	88.5	0.5	0.0
67	23	21	11.08.2009	04:13	56.49854	2.9958	71.16	8.9	198.8	456.8	208.8	293.4	1.0	0.0
67	23	23	11.08.2009	04:15	56.49858	2.99568	71.167	8.5	186.5	428.9	47.8	71.4	0.0	0.0

IFM-GEOMAR Reports

- | No. | Title |
|-----|---|
| 1 | RV Sonne Fahrtbericht / Cruise Report SO 176 & 179 MERAMEX I & II (Merapi Amphibious Experiment) 18.05.-01.06.04 & 16.09.-07.10.04. Ed. by Heidrun Kopp & Ernst R. Flueh, 2004, 206 pp.
In English |
| 2 | RV Sonne Fahrtbericht / Cruise Report SO 181 TIPTEQ (from The Incoming Plate to mega Thrust EarthQuakes) 06.12.2004.-26.02.2005. Ed. by Ernst R. Flueh & Ingo Grevemeyer, 2005, 533 pp.
In English |
| 3 | RV Poseidon Fahrtbericht / Cruise Report POS 316 Carbonate Mounds and Aphotic Corals in the NE-Atlantic 03.08.-17.08.2004. Ed. by Olaf Pfannkuche & Christine Utecht, 2005, 64 pp.
In English |
| 4 | RV Sonne Fahrtbericht / Cruise Report SO 177 - (Sino-German Cooperative Project, South China Sea: Distribution, Formation and Effect of Methane & Gas Hydrate on the Environment) 02.06.-20.07.2004. Ed. by Erwin Suess, Yongyang Huang, Nengyou Wu, Xiqu Han & Xin Su, 2005, 154 pp.
In English and Chinese |
| 5 | RV Sonne Fahrtbericht / Cruise Report SO 186 – GITEWS (German Indonesian Tsunami Early Warning System 28.10.-13.1.2005 & 15.11.-28.11.2005 & 07.01.-20.01.2006. Ed. by Ernst R. Flueh, Tilo Schoene & Wilhelm Weinrebe, 2006, 169 pp.
In English |
| 6 | RV Sonne Fahrtbericht / Cruise Report SO 186 -3 – SeaCause II, 26.02.-16.03.2006. Ed. by Heidrun Kopp & Ernst R. Flueh, 2006, 174 pp.
In English |
| 7 | RV Meteor, Fahrtbericht / Cruise Report M67/1 CHILE-MARGIN-SURVEY 20.02.-13.03.2006. Ed. by Wilhelm Weinrebe und Silke Schenk, 2006, 112 pp.
In English |
| 8 | RV Sonne Fahrtbericht / Cruise Report SO 190 - SINDBAD (Seismic and Geoacoustic Investigations Along The Sunda-Banda Arc Transition) 10.11.2006 - 24.12.2006. Ed. by Heidrun Kopp & Ernst R. Flueh, 2006, 193 pp.
In English |
| 9 | RV Sonne Fahrtbericht / Cruise Report SO 191 - New Vents "Puaretanga Hou" 11.01. - 23.03.2007. Ed. by Jörg Bialas, Jens Greinert, Peter Linke, Olaf Pfannkuche, 2007, 190 pp.
In English |
| 10 | FS ALKOR Fahrtbericht / Cruise Report AL 275 - Geobiological investigations and sampling of aphotic coral reef ecosystems in the NE-Skagerrak, 24.03. - 30.03.2006, Eds.: Andres Rüggeberg & Armin Form, 39 pp. In English |

No.	Title
11	FS Sonne / Fahrtbericht / Cruise Report SO 192-1: MANGO: Marine Geoscientific Investigations on the Input and Output of the Kermadec Subduction Zone, 24.03. - 22.04.2007, Ernst Flüh & Heidrun Kopp, 127 pp. In English
12	FS Maria S. Merian / Fahrtbericht / Cruise Report MSM 04-2: Seismic Wide-Angle Profiles, Fort-de-France – Fort-de-France, 03.01. - 19.01.2007, Ed.: Ernst Flüh, 45 pp. In English
13	FS Sonne / Fahrtbericht / Cruise Report SO 193: MANIHIKI Temporal, Spatial, and Tectonic Evolution of Oceanic Plateaus, Suva/Fiji – Apia/Samoa 19.05. - 30.06.2007, Eds.: Reinhard Werner and Folkmar Hauff, 201 pp. In English
14	FS Sonne / Fahrtbericht / Cruise Report SO195: TOTAL TONGA Thrust earthquake Asperity at Louisville Ridge, Suva/Fiji – Suva/Fiji 07.01. - 16.02.2008, Eds.: Ingo Grevemeyer & Ernst R. Flüh, 106 pp. In English
15	RV Poseidon Fahrtbericht / Cruise Report P362-2: West Nile Delta Mud Volcanoes, Piräus – Heraklion 09.02. - 25.02.2008, Ed.: Thomas Feseker, 63 pp. In English
16	RV Poseidon Fahrtbericht / Cruise Report P347: Mauritanian Upwelling and Mixing Process Study (MUMP), Las-Palmas - Las Palmas, 18.01. - 05.02.2007, Ed.: Marcus Dengler et al., 34 pp. In English
17	FS Maria S. Merian Fahrtbericht / Cruise Report MSM 04-1: Meridional Overturning Variability Experiment (MOVE 2006), Fort de France – Fort de France, 02.12. – 21.12.2006, Ed.: Thomas J. Müller, 41 pp. In English
18	FS Poseidon Fahrtbericht /Cruise Report P348: SOPRAN: Mauritanian Upwelling Study 2007, Las Palmas - Las Palmas, 08.02. - 26.02.2007, Ed.: Hermann W. Bange, 42 pp. In English
19	R/V L'ATALANTE Fahrtbericht / Cruise Report IFM-GEOMAR-4: Circulation and Oxygen Distribution in the Tropical Atlantic, Mindelo/Cape Verde - Mindelo/Cape Verde, 23.02. - 15. 03.2008, Ed.: Peter Brandt, 65 pp. In English
20	RRS JAMES COOK Fahrtbericht / Cruise Report JC23-A & B: CHILE-MARGIN-SURVEY, OFEG Barter Cruise with SFB 574, 03.03.-25.03. 2008 Valparaiso – Valparaiso, 26.03.-18.04.2008 Valparaiso - Valparaiso, Eds.: Ernst Flüh & Jörg Bialas, 242 pp. In English
21	FS Poseidon Fahrtbericht / Cruise Report P340 – TYMAS "Tyrrhenische Massivsulfide", Messina – Messina, 06.07.-17.07.2006, Eds.: Sven Petersen and Thomas Monecke, 77 pp. In English

No.	Title
22	RV Atalante Fahrtbericht / Cruise Report HYDROMAR V (replacement of cruise MSM06/2), Toulon, France - Recife, Brazil, 04.12.2007 - 02.01.2008, Ed.: Sven Petersen, 103 pp. In English
23	RV Atalante Fahrtbericht / Cruise Report MARSUED IV (replacement of MSM06/3), Recife, Brazil - Dakar, Senegal, 07.01. - 31.01.2008, Ed.: Colin Devey, 126 pp. In English
24	RV Poseidon Fahrtbericht / Cruise Report P376 ABYSS Test, Las Palmas - Las Palmas, 10.11. - 03.12.2008, Eds.: Colin Devey and Sven Petersen, 36 pp, In English
25	RV SONNE Fahrtbericht / Cruise Report SO 199 CHRISP Christmas Island Seamount Province and the Investigator Ridge: Age and Causes of Intraplate Volcanism and Geodynamic Evolution of the south-eastern Indian Ocean, Merak/Indonesia – Singapore, 02.08.2008 - 22.09.2008, Eds.: Reinhard Werner, Folkmar Hauff and Kaj Hoernle, 210 pp. In English
26	RV POSEIDON Fahrtbericht / Cruise Report P350: Internal wave and mixing processes studied by contemporaneous hydrographic, current, and seismic measurements, Funchal – Lissabon, 26.04.-10.05.2007 Ed.: Gerd Krahnemann, 32 pp. In English
27	RV PELAGIA Fahrtbericht / Cruise Report Cruise 64PE298: West Nile Delta Project Cruise - WND-3, Heraklion - Port Said, 07.11.-25.11.2008, Eds.: Jörg Bialas & Warner Brueckmann, 64 pp. In English
28	FS POSEIDON Fahrtbericht / Cruise Report P379/1: Vulkanismus im Karibik-Kanaren-Korridor (ViKKi), Las Palmas – Mindelo, 25.01.-12.02.2009, Ed.: Svend Duggen, 74 pp. In English
29	FS POSEIDON Fahrtbericht / Cruise Report P379/2: Mid-Atlantic-Researcher Ridge Volcanism (MARRVi), Mindelo- Fort-de-France, 15.02.-08.03.2009, Ed.: Svend Duggen, 80 pp. In English
30	FS METEOR Fahrtbericht / Cruise Report M73/2: Shallow drilling of hydrothermal sites in the Tyrrhenian Sea (PALINDRILL), Genoa – Heraklion, 14.08.2007 – 30.08.2007, Eds.: Sven Petersen & Thomas Monecke, 235 pp. In English
31	FS POSEIDON Fahrtbericht / Cruise Report P388: West Nile Delta Project - WND-4, Valetta – Valetta, 13.07. - 04.08.2009, Eds.: Jörg Bialas & Warner Brückmann, 65 pp. In English
32	FS SONNE Fahrtbericht / Cruise Report SO201-1b: KALMAR (Kurile-Kamchatka and ALeutian MARGinal Sea-Island Arc Systems): Geodynamic and Climate Interaction in Space and Time, Yokohama, Japan - Tomakomai, Japan, 10.06. - 06.07.2009, Eds.: Reinhard Werner & Folkmar Hauff, 105 pp. In English
33	FS SONNE Fahrtbericht / Cruise Report SO203: WOODLARK Magma genesis, tectonics and hydrothermalism in the Woodlark Basin, Townsville, Australia - Auckland, New Zealand 27.10. - 06.12.2009, Ed.: Colin Devey, 177 pp. In English

- | No. | Title |
|------------|---|
| 34 | FS Maria S. Merian Fahrtbericht / Cruise Report MSM 03-2: HYDROMAR IV: The 3rd dimension of the Logatchev hydrothermal field, Fort-de-France - Fort-de-France, 08.11. - 30.11.2006, Ed.: Sven Petersen, 98 pp. In English |
| 35 | FS Sonne Fahrtbericht / Cruise Report SO201-2 KALMAR: Kurile-Kamchatka and ALEutian MARGinal Sea-Island Arc Systems: Geodynamic and Climate Interaction in Space and Time Busan/Korea – Tomakomai/Japan, 30.08. - 08.10.2009, Ed.: Wolf-Christian Dullo, Boris Baranov, and Christel van den Bogaard, 233 pp. In English |



IFM-GEOMAR

Leibniz-Institut für Meereswissenschaften
an der Universität Kiel

Das Leibniz-Institut für Meereswissenschaften
ist ein Institut der Wissenschaftsgemeinschaft
Gottfried Wilhelm Leibniz (WGL)

The Leibniz-Institute of Marine Sciences is a
member of the Leibniz Association
(Wissenschaftsgemeinschaft Gottfried
Wilhelm Leibniz).

Leibniz-Institut für Meereswissenschaften / Leibniz-Institute of Marine Sciences

IFM-GEOMAR
Dienstgebäude Westufer / West Shore Building
Düsternbrooker Weg 20
D-24105 Kiel
Germany

Leibniz-Institut für Meereswissenschaften / Leibniz-Institute of Marine Sciences

IFM-GEOMAR
Dienstgebäude Ostufer / East Shore Building
Wischhofstr. 1-3
D-24148 Kiel
Germany

Tel.: ++49 431 600-0
Fax: ++49 431 600-2805
www.ifm-geomar.de